Design and Implementation of Feedback Linearization based Adaptive Stabilizing Controller Coupled with Fuzzy Logic Swing-up for Pendulum on a Cart

By:- Daniel Abebe Beyene

Submitted to School of Electrical and Computer Engineering
In Partial Fulfillment of Masters of Science in Electrical Control Engineering
at

Thesis Supervisor Dr. Dereje Shiferaw

November 19, 2019

Declaration

I,Daniel Abebe Beyene,hereby declare that no part of the work referred to, in this dissertation has been submitted in support of an application for another degree or qualification of this or any other university or other institute of learning.

.....
Signed: Daniel Abebe Beyene.

Approval

ADDIS ABABA INSTITUTE OF TECHNOLOGY

The undersigned Thesis committee approves the Thesis titled by

FEEDBACK LINEARIZATION BASED ADAPTIVE STABILIZING CONTROLLER DESIGN COUPLED WITH FUZZY LOGIC SWING-UP FOR PENDULUM ON A CART

By:- Daniel Abebe Beyene

APPROVED FOR THE SCHOOL OF ELECTRICAL AND COMPUTER ENGINEERING

.....

Dr.Dereje Shiferaw School of ECE Thesis Supervisor Date

.....

Dr.Lebsework Negash School of ECE Internal Examiner Date

.....

Mr.Mihreteab Negash School of ECE External examiner Date

APPROVED FOR THE UNIVERSITY

.....

Dr.Yalemzewd Negash SECE Dean Date

Abstract

This thesis address an adaptive stabilizing controller for inverted pendulum on a cart based on feedback linearization coupled with an adaptive fuzzy logic based swing up controller. First feedback linearizing control signal is derived by decomposing the system into cart subsystem and pendulum subsystem. Then adaptive inverse control technique is applied to each feedback linearizing control signals. An adaptive inverse control method is used for compensation of unknown parameters of an inverted pendulum on a cart, while feedback linearization is used to cancel non-linearity in the system. The pendulum is driven from it's pendant position to inverted position using an adaptive fuzzy logic based swing up controller. When the pendulum reaches near it's inverted position, the stabilizing controller takes over the swing up controller. The MATLAB/SIMULINK simulation shows that the proposed controllers adapt to unknown mass of a cart between $0.1kg$ - $4kg$ and mass of a pendulum between $0.01kg$ - $4kg$. The performance of the stabilizing controller on hardware experimentation under unknown mass of a cart and mass of a pendulum shows that the proposed controller is a solution to inverted pendulum stabilization problem.

Keywords:- Feedback Linearization, Fuzzy Logic, Adaptive Inverse Control, Inverted Pendulum on a Cart, Swing up

Dedication

To my father Abebe Beyene, my mother Zenebech Degefu, my brothers Eshetu Abebe, Negash Abebe and Habtamu Abebe and my friends.

Family is the beginning and the end.
Daneil Abebe

Acknowledgment

First of all, my hearty gratitude goes to the almighty God. Then I am highly grateful to my advisor Dr.Dereje Shiferaw as without his encouragement, insight and guidance the completion of this work would not have been possible. Next my honorable gratitude goes to staffs of School of Electrical and Computer Engineering

1. Mr. Solomon Zegeye and
2. Mr. Teshome Hambisa

and staffs of School of Mechanical and Industrial Engineering

1. Mrs. Belayinesh Gebrehiwot
2. Mr. Anteneh Tadiwos and
3. Mr. Masresha Wendimu

for their support during hardware development and Mrs. Kibrework Alemayehu for her cooperation when I asked for support letter to use School of Mechanical and industrial Engineering Laboratory. Finally I want to acknowledge Abibual Abate, Addisalem Hailegnaw, Alemie Assefa, Amanuel Tesfaye, Awel Hussein, Eyob Dagne, Getsh Fekadie and Wondimagegn Minda for their ideas and support during hardware setup development and experimentation.

Daniel Abebe

Addis Ababa University
Addis Ababa Institute of Technology
School of Electrical and Computer Engineering
Addis Ababa, Ethiopia
November 19, 2019

Contents

List of Figures

List of Tables

Acronym's (Abbreviation)

Abbreviation	Description
DC	Direct Current
2D	2 Dimensional
IPC	Inverted Pendulum on Cart
AFLSC	Adaptive Feedback Linearization based Stabilizing Controller
AFLSUC	Adaptive Fuzzy Logic based Swing up Controller
T-S	Takagi–Sugeno
SMC	Sliding Mode Controller
LQR	Linear Quadratic Regulator
MATLAB	Matrix Laboratory
MIMO	Multiple Inputs and Multiple Outputs
PID	Proportional-Integral-Derivative
PWM	Pulse Width Modulation
SIMO	Single Input and Multiple Outputs
FL	Feedback Linearization

Chapter 1

Introduction

1.1 Theoretical Background

The inverted pendulum on a cart indicated on figure 1.1 is a popular benchmark problem for researchers in control systems and automation. It is also a very good platform to verify and apply different control logic's in the field of control theory. The $2D$ inverted pendulum on a cart has one input, the force applied to the cart and two outputs, position of the cart and the angle of the pendulum [1]. This makes an inverted pendulum on a cart a SIMO system. The pendulum is stable while hanging downwards, but the inverted pendulum is inherently unstable nonlinear system and needs to be balanced. The control of an inverted pendulum is analogous to balancing a broomstick on the index finger with the control motion constrained to a single dimension of space. The control of an inverted pendulum is difficult due to certain properties it possesses.

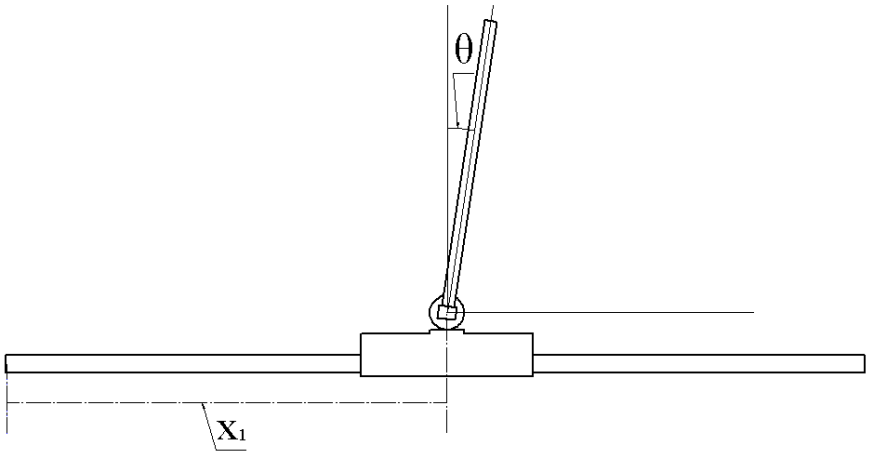

Figure 1.1: Inverted pendulum on a cart

An inverted pendulum on a cart is an under-actuated mechanical system due to the lack of direct control over some direction it needs to be steered. The control techniques for such under-actuated mechanical systems find ready applications in modern automation, robotics and fault tolerant control as indicated on figure 1.2.

These application areas include altitude control of space satellites and rockets, the landing of aircraft, balancing of a ship against tide and Seismographer [2] (which monitors the motion of the ground due to an earthquake and nuclear explosions).

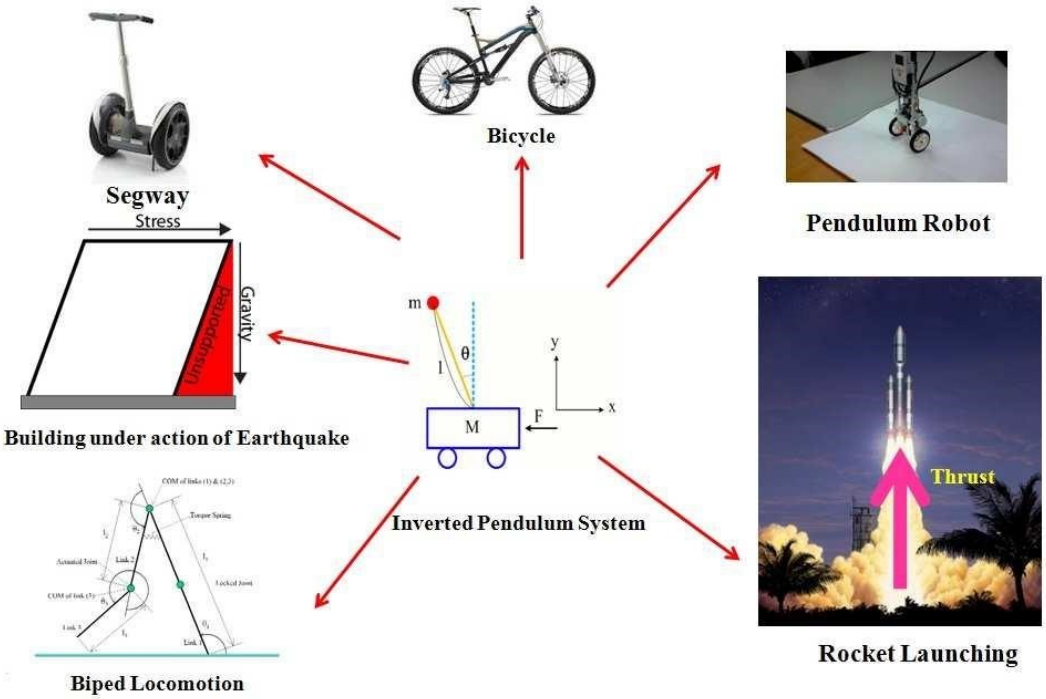

Figure 1.2: Applications of Inverted Pendulum Control [2]

The physical system consists of a cart driven by a DC motor or stepper motor and a pendulum attached to a cart. The cart can move along a horizontal track and the pendulum is able to rotate freely about the pivot. There is no direct control applied to the pendulum. Both the position of the cart x and the angle of the pendulum θ are measurable through linear position sensor and angular position sensor respectively. The dynamics of the system is described by the state of the system, which consists of the position of a cart x, velocity of a cart $\dot{x}$, angular position of a pendulum θ and angular velocity of a pendulum $\dot{\theta}$. The physical system has state and control constraints. Specifically, the cart position and the maximum speed of the cart is restricted.

From a control theoretic viewpoint, the inverted pendulum is a non-minimum phase system as it has unstable zeroes. This implies the system initially steers in an opposite direction relative to the control sense. The non-minimum phase of the system makes it possess an unstable zero dynamics and therefore difficult to use input-output feedback linearization techniques. Furthermore, as is stated in [3], the pendulum is not globally controllable, especially when moving from pendant position to inverted position. Because, the controllability matrix losses rank when it crosses the horizontal axis (ı.e when angular position of a pendulum is equal to ± 90 degree). This makes a swing up of a pendulum using active control from any single controller difficult task.

In this thesis an adaptive feedback linearization based controller is used for the stabilization of a pendulum at inverted position. While swinging-up of the pendulum from it's pendant position is achieved by using an adaptive fuzzy logic based swing-up controller.

Feedback linearization is a control strategy that uses change of coordinates to simplify complex non linear systems into their simpler form. The change of coordinate is achieved by selecting relevant diffeomorphism[1] function [4],[5]. Because feedback linearization is model based, the system has to be modeled precisely to capture significant details about the dynamics of the system. Depending on control target, feedback linearization of any dynamic system is divided into two, input-state feedback linearization and input-output feedback linearization. Input-state feedback linearization is applied to system that satisfy sufficient condition and necessary condition(which will be explained later on chapter 3 section 3.5). While input-output feedback linearization can be applied to system that fulfill necessary condition only [6]. Many dynamic systems can be input-output feedback linearized, if there exist appropriate diffeomorphism function. Input-state feedback linearization is only applied to few dynamic systems even if a diffeomorphism function exists.

An inverted pendulum on a cart is one of such dynamic systems that doesn't fulfill involutivity condition. This makes input-state feedback linearization an impossible task. Due to this, researchers propose approximate feedback linearization technique to design stabilizing controller for dynamics of inverted pendulum on a cart. An approximate feedback linearization is achieved by neglecting the effect of dynamics which are function of control signal that makes relative order of feedback linearized system less than the order of original nonlinear system, which will be explained later in chapter 3 section 3.5.

If the dynamics of an inverted pendulum on a cart is divided into two subsystems; namely cart subsystem and pendulum subsystem, the two subsystem satisfy involutivity condition independently. Thus input-state feedback linearization is possible for the two subsystems. But combining the two subsystem after applying feedback linearization is difficult, because feedback linearizing input for one subsystem makes the other subsystem nonlinear.

In this thesis the two subsystems are considered to be parallel, thus the overall system feedback linearizing input is the superposition of the two subsystems feedback linearizing inputs. The effect caused by parallel combination of the two subsystems is handled by proper selection of design signal(explained later in chapter 3 section 3.6). After deriving the two subsystems feedback linearizing inputs signals, an adaptive inverse control technique is applied to each of them. An adaptive inverse control is suitable for nonlinear systems with zero dynamics as explained in [7].

Adaptive feedback linearization based stabilizing controller is applied to the system after the pendulum reaches near it's inverted position. To drive the pendulum from it's pendant position to inverted position a feedforward controller is required.

[1] A diffeomorphism is a map between manifolds which is differentiable and has a differentiable inverse

This feedforward controller is called swing-up controller. The swing up controller is mainly designed based on energy of the pendulum and/or energy of overall system. The approaches to design swing-up controller are derived from this energy methods and the nature of the dynamic system.

In this thesis an adaptive fuzzy logic based swing up controller is designed using impulse-momentum approach,as the method suits the nature of a pendulum on a cart. Because it uses fast back and forth movement of a cart to swing-up the pendulum. Still it is energy based method, since the controller inject energy to the dynamic system to drive the system away from it's stable position. This approach can move the pendulum to a vicinity of unstable equilibrium point in less than 5 seconds.

When the pendulum reach near it's inverted position adaptive feedback linearization based stabilizing controller will take over the adaptive fuzzy logic based swing-up controller. The switching mechanism can be designed in many different ways. But in this thesis simple switching mechanism is employed.

1.2 Statement of the Problem

The challenge of this thesis is to balance pendulum on a cart about it's inverted position by swinging up the pendulum from it's pendant position under model imperfection and unknown plant parameters. The effect of non-linearity is handled by feedback linearization and the effect of unknown system parameters is tackled by using adaptive inverse control mechanism. This thesis shows that an adaptive feedback linearization based stabilizing controller (AFLSC) is a solution for stability problem of a inverted pendulum. While swing-up of the pendulum from it's pendant position is addressed by an adaptive fuzzy logic based swing-up controller(AFLSUC).

1.3 Objective of this Thesis

1.3.1 Main Objective

- Studying Mathematical model of IPC, designing and implementing an adaptive feedback linearization based stabilizing controller (AFLSC) and an adaptive fuzzy logic based swing up controller(AFLSUC).

1.3.2 Specific Objectives

- Study mathematical model of the system and design feedback linearizing input.
- Design an adaptive controller using adaptive inverse control.
- Design an adaptive fuzzy logic based swing-up controller.
- Test the performance of the controllers using simulation and hardware experimentation

1.4 Scope of the Thesis

This thesis focus on studying mathematical model of an inverted pendulum on a cart system along with it's electrical actuator. Then design and test of an adaptive feedback linearization based stabilizing controller and an adaptive fuzzy logic based swing-up controller for single inverted pendulum on a cart.

1.5 Organization of the Thesis

This thesis is organized into 8 chapters including appendix. The rest part of this thesis discuss, review of related and relevant previous research works in chapter 2. Modeling, analysis and controller design techniques for dynamics of the inverted pendulum on a cart along with its electrical actuator in Chapter 3. An adaptive swing up controller design in chapter 4 and an adaptive stabilizing controller design in chapter 5. Model verification, validation and performance test of the controllers using simulation in chapter 6 and hardware experimentation in chapter 7. Conclusion, recommendation and limitations will be presented in chapter 8. Finally codes and models used in simulation and hardware experimentation are stated on appendix.

Chapter 2

Literature Review

The objective of control is to regulate, direct and command systems to the desired behavior. Control is everywhere, it exists naturally or designed by human being [8]. Almost all naturally existing systems surrounding us don't respond proportionally or in a desired way to the stimulus or excitation applied to them. For a longtime control engineers try to solve this problem through different approaches. The first approaches were the design of linear controllers based on linear models developed for systems under various assumptions. Later on, advancements in field of control system leads to the formulation of nonlinear control theories like feedback linearization, sliding mode control, back-stepping, passivity-based control, high gain observers, intelligent controllers based on genetic algorithm, fuzzy logic, neural network, particle swarm optimization [9] and recently contracting system theory [10].
As indicated in chapter 1 an inverted pendulum on a cart is a popular benchmark in testing the performance of these control theories due to the following characteristics [2].

- It's nonlinear property and instability.
- It has relative degree less than order of the system.
- The constraints on the size of the control action and the states.
- It's Sensitivity to external disturbance.

An inverted pendulum problem is first tackled by Roberge (1960) who demonstrated a solution to the inverted pendulum system at M.I.T. in his aptly named bachelor's thesis, "The Mechanical Seal". Roberge's research was supervised by Leonard Gould. While swing-up control of an inverted-pendulum system was demonstrated by Mori et al. (1976) (which cites Schaefer and Cannon (1966) but nothing earlier) [11]. Then after many researcher have developed different methods to balance inverted pendulum on a cart.
Stabilizing controller for inverted pendulum can be linear model based classical linear controllers or non linear controllers. Designing controller using linear model is easier, but the assumptions made to approximate nonlinear system with it's linear model might degrade the performance of the controller. Nonlinear controller design methods take non-linearity in dynamic system into consideration during designing controller. There are many controllers designed using this method for stabilization of inverted pendulum on a cart. The authors of [12] design adaptive sliding mode

controller for inverted pendulum using fuzzy logic based reference model. On the other hand authors of [13] design coupled sliding-mode control (SMC) for inverted-pendulum systems.
There is also neural network based proposed controllers as on [14], which decouples the system into position control and angle control and uses neural network based PID controller to stabilize inverted pendulum on a cart. Fuzzy controllers [15],[16] and adaptive fuzzy controllers are also used in stabilizing of an inverted pendulum based on feedback linearization. The controllers approximate feedback linearizing control signal by fuzzy logic [17]. Additionally command governor control design method is also applied to inverted pendulum problem. Command governor approach is a method of forcing the system to operate in linear operation region [18].

Since the dynamics of an inverted pendulum on a cart in not involutive, input state feedback linearization is impossible as stated in chapter 1. Thus some researchers use approximated feedback linearization to design controller [19], [20], [21]. Computed feedback linearization based controller is also used as indicated on [22] for position tracking problem and regulation of inverted pendulum on a cart. While the authors of [2] used input-output feedback linearization in combination with sliding mode control and energy based swing up and authors of [23] has designed feedback linearization combined with back-stepping for stabilization of inverted pendulum on a cart.
Recently researchers applied feedback linearization to design controller for dynamic systems like magnetic levitation [24], induction machine control [25] and Magnetic Telemanipulation [26].

Swinging the pendulum from pendant position to an inverted position is an other interesting problem. Instead of driving it manually, researchers develop different methods to solve this particular problem. Almost all of this methods uses mechanical energy of the system. This methods can be designed based on the energy of the whole system or only the energy of the pendulum [27], [28]. Additionally this methods can be approximated by fuzzy logic [15], [29] or neural network [30]. There are many approaches used in designing energy based swing up controller. An impulse momentum approach is one of those approaches used in designing energy based method swing up controller [31]. Any energy based methods can be heuristic to swing up the pendulum in short period of time [32], [33]. The other method of designing swing up controller is to consider closed loop fundamentals of the system, like frequency and damping coefficient [34].
The design of swing-up controller is not a necessary part in design and test of stabilizing controller for a inverted pendulum on a cart. The design method used in developing stabilizing controller has nothing to do with the method used to design swing up controller and vice versa. They act in different operating region of the system. Since they do not operate simultaneously there must be switching mechanism that check some criteria to switch on either of the two controllers.
In this thesis, adaptive feedback linearization based controller is used for the stabilization of a pendulum on a cart at it's inverted position, by swinging the pendulum from it's pendant position using an adaptive fuzzy logic based swing up controller. The switching is performed using angle criteria.

Chapter 3

Mathematical Modeling and Controller Design Methods

3.1 System Parameters Considered in Modeling

An inverted pendulum on a cart is an under-actuated mechanical system driven by electrical actuator. Hence inverted pendulum modeling require both mechanical subsystem modeling and electrical subsystem modeling. The summary of inverted pendulum on a cart parameters considered in modeling are shown on table 3.1.

Table 3.1: System parameters considered in modeling

Parameters	Description	Unit
V_a	Armature Voltage	V
I_a	Armature Current	A
R_a	Armature Resistance	Ω
L_a	Armature Inductance	H
E_b	DC motor Back Emf	V
k_m	DC motor torque constant	Nm/A
k_t	DC motor back emf constant	Vs/rad
ω	DC motor rated speed	rad/s
η_m	DC motor efficiency	$-$
τ_m	DC motor output torque	Nm
k_g	gear box ratio	$-$
r_g	gear radius	m
η_g	gear efficiency	$-$
τ_g	gear output torque	Nm
v_{ref}	reference Voltage	V
β	servo feedback amplifier gain	$-$
A	servo amplifier gain	$-$
l	arm length of a pendulum	m
m_p	mass of pendulum	kg
m_c	mass of a cart	kg
g	acceleration due to gravity	m/s^2

3.2 Mathematical Modeling Requirements for the System

The modeling requirement for inverted pendulum parameters can be categorized into functional and additional requirements [33].

3.2.1 Functional Requirements

The functional requirements are the necessary capabilities that must be fulfilled in order to consider the scheme operational. Which include:

1. Able to autonomously stabilize the pendulum at it's upright position.
2. Able to keep the cart from colliding with the physical barriers of the system.

3.2.2 Additional Requirements

The additional requirements are features that are desirable, but not necessary.

1. Swing up the pendulum within ±20 degrees (0.34888 radians) of it's upright position. The torque responsible for falling of the pendulum increases proportional to the sine of deviation angle (ı.e $\tau_p = l \times m_p g = m_p l g sin\theta$). This implies that for large deviation angle the require counter acting force must be large (to generate higher acceleration of the cart) with require high energy. Which is one input constraint of inverted pendulum dynamics.
2. Swing up the pendulum in less than 2 seconds. The rise time is smaller for fast swing up and larger for slow swing up methods. Which implies that the motion of the cart if fast back forth withing the range of applied constraint on position of the cart.
3. Stabilise the pendulum with oscillations less than ±2 degrees (0.0349 radians).
4. Keep the cart within 40 centimeters of the reference position while stabilizing the pendulum (ı.e position constraint of inverted pendulum dynamics).

Preliminary concepts
Generalized momentum:-The generalized momentum of analytical (Lagrangian, Hamiltonian) formulations of classical mechanics is defined as the partial derivative of the Lagrangian with regards to the time derivative of generalized coordinates.
Collocated partial feedback linearization is a procedure of linearizing dynamics of actuated variable. Where as noncollocated partial feedback linearization is a procedure of linearizing uncatuated variable of a dynamic system.
Under actuated mechanical system are classified to over 16 *classes depending on possession or lack of Actuated shape variables, Non-interacting inputs (lack of input coupling), Integrable normalized momentum and additional requirements(different for different classes). For more detail see [3] PhD dissertation paper at MIT. This paper state many future research works that can be done on underactuated mechanical systems.*

3.3 Mathematical Modeling and State Space Representation of IPC

As inverted pendulum is third class[1] under-actuated mechanical system with unactuated shape variable[2] [3]. For such kind of systems the controller design technique used is called noncollocated partial feedback linearization. In noncollocated partial feedback linearization controller design, change of control is applied to partially linearized unactuated configuration variable. This change of control can be achieved by appropriate coordinate transformation, which require the concept of differential geometry. Hence feedback linearization of under-actuated mechanical system depends on the availability of such change of coordinate.

Consider under-actuated mechanical system,with the following Legendere transform,

$$L(q,\dot{q}) = \frac{1}{2}\begin{bmatrix}\dot{q}_1\\ \dot{q}_2\end{bmatrix}^T \begin{bmatrix}m_{11}(q) & m_{12}(q)\\ m_{21}(q) & m_{22}(q)\end{bmatrix}\begin{bmatrix}\dot{q}_1\\ \dot{q}_2\end{bmatrix} - V(q) \tag{3.1}$$

The generalized momentum conjugate to q_i can be obtained via partial Legendre transform.

$$p_i = \frac{\partial L}{\partial q_i} = m_{i1}(q)\dot{q}_1 + m_{i2}(q)\dot{q}_2 \tag{3.2}$$

For the system on equation 3.1, the generalized momentum is,

$$p_1 = \frac{\partial L}{\partial q_1} = m_{11}(q)\dot{q}_1 + m_{12}(q)\dot{q}_2 \tag{3.3}$$

$$p_2 = \frac{\partial L}{\partial q_2} = m_{i1}(q)\dot{q}_1 + m_{22}(q)\dot{q}_2 \tag{3.4}$$

Normalized momentum conjugate to q_1 and q_2 with respect to q_1 is defined as:

$$\pi_1 = m_{11}(q)P_1 = \dot{q}_1 + m_{11}(q)m_{12}(q)\dot{q}_2 \tag{3.5}$$

$$\pi_2 = m_{21}(q)P_2 = \dot{q}_1 + m_{21}(q)m_{22}(q)\dot{q}_2 \tag{3.6}$$

π_1 is well defined and π_2 is defined where ever m_{21} is invertable. $\pi = \pi(q,\dot{q})$ is integrable normalized momentum, if there exist generalized configuration function $h(q)$ such that $\dot{h}(q) = \pi$. If normalized momentum of a dynamic system is integrable the system can be expressed as cascaded nonlinear normal form or non-triangular quadratic normal form.

In the case of inverted pendulum on a cart the system dynamics can be expressed as strict non-triangular quadratic form with strict feed-forward controller design method [3].
Using generalized coordinate $(x,\theta) \mapsto (q_1,q_2)$, the dynamic equation of inverted pendulum on a cart on figure 3.1 is derived in the following sections.

[1]Third class under actuated mechanical systems are mechanical systems that has unactuated shape variable, lack input coupling, integrable normalized momentum, differentially symmetric rows and constant diagonal elements in inertia matrix and potential energy as function of shape variable only

[2]shape variables are configuration variables that appear in inertia matrix

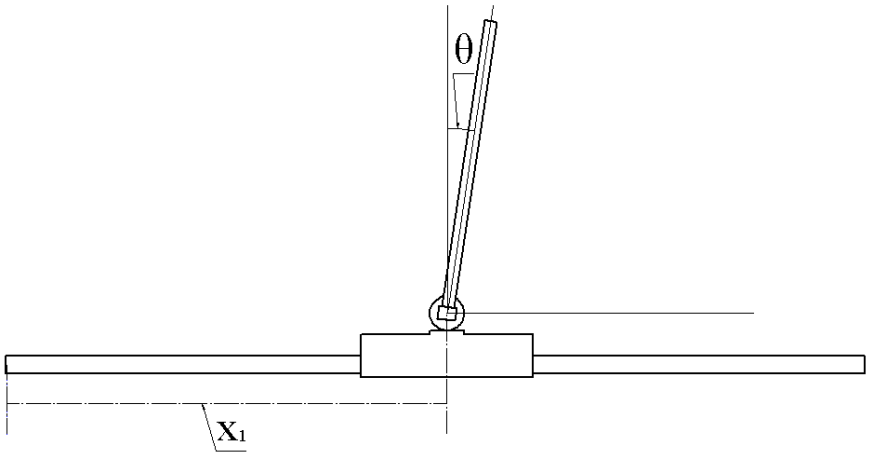

Figure 3.1: Inverted pendulum on a cart

The position of a cart and position of a pendulum using generalized coordinate are stated on equations 3.7 and 3.8 respectively.

$$\begin{bmatrix} x_c \\ y_c \end{bmatrix} = \begin{bmatrix} q_1 \\ 0 \end{bmatrix} \tag{3.7}$$

$$\begin{bmatrix} x_p \\ y_p \end{bmatrix} = \begin{bmatrix} q_1 + l \sin q_2 \\ l \cos(q_2) \end{bmatrix} \tag{3.8}$$

The linear velocity of a cart and angular velocity of the pendulum are stated on equations 3.9 and 3.10 respectively.

$$\begin{bmatrix} \dot{x}_c \\ \dot{y}_c \end{bmatrix} = \begin{bmatrix} \dot{q}_1 \\ 0 \end{bmatrix} \tag{3.9}$$

$$\begin{bmatrix} \dot{x}_p \\ \dot{y}_p \end{bmatrix} = \begin{bmatrix} \dot{q}_1 + \dot{q}_2 l \cos q_2 \\ -l\dot{q}_2 sinq_2 \end{bmatrix} \tag{3.10}$$

The kinetic energy of the system is equal to,

$$\begin{aligned} K_e(q) &= \frac{1}{2} m_c \dot{x}_c^2 + \frac{1}{2} m_p (\dot{x}_p^2 + \dot{y}_p^2) + \frac{1}{2} I \dot{\theta}^2 \\ &= \frac{1}{2}(m_c + m_p)\dot{q}_1^2 + m_p(\dot{q}_1, \dot{q}_2) l \cos q_2 + \frac{1}{2}(m_p l^2 + I)\dot{q}_2^2 \end{aligned} \tag{3.11}$$

The potential energy of the system is expressed as,

$$V(q) = m_p g l \cos q_2 \tag{3.12}$$

The Lagrangian equation governing dynamics of the system is expressed as:

$$L(q_1, q_2) = K_e(q) - V(q)$$

$$L(q_1, q_2) = \frac{1}{2}\begin{bmatrix}\dot{q}_1\\ \dot{q}_2\end{bmatrix}' \begin{bmatrix}m_c + m_p & m_p l\cos q_2\\ m_p l\cos q_2 & m_p l^2 + I\end{bmatrix}\begin{bmatrix}\dot{q}_1\\ \dot{q}_2\end{bmatrix} - m_p g l\cos q_2 \tag{3.13}$$

Relating equations 3.1 and 3.13, $m_{11} = m_c + m_p$, $m_{12} = m_{21} = m_p l\cos q_2$ and $m_{22} = m_p l^2 + I$. Replacing for m_{11}, m_{12}, m_{21} and m_{22}, the Euler-Lagrangian equation

$$\frac{dL}{dt}\begin{bmatrix}\frac{\partial L}{\partial \dot{q}}\end{bmatrix} - \frac{\partial L}{\partial q} = \begin{bmatrix}u\\ 0\end{bmatrix} \tag{3.14}$$

of the system becomes

$$m_{11}\ddot{q}_1 + m_{12}\ddot{q}_2 - m_p l\dot{q}_2^2\sin q_2 = u \tag{3.15}$$

$$m_{21}\ddot{q}_1 + m_{22}\ddot{q}_2 - m_p g l\sin q_2 = 0 \tag{3.16}$$

From this Euler-Lagrangian, the state space representation of inverted pendulum on a cart dynamics can be determined.
Let $q_1 = x_1$, $q_2 = x_3$, $\dot{q}_1 = x_2$ and $\dot{q}_2 = x_4$, then the state space representation will be:

$$\begin{bmatrix}\dot{x}_2\\ \dot{x}_4\end{bmatrix} = \begin{bmatrix}m_p + m_c & m_p l\cos x_3\\ m_p l\cos x_3 & m_p l^2 + I\end{bmatrix}^{-1}\begin{bmatrix}u + m_p l x_4\sin x_3\\ m_p l g\sin x_3\end{bmatrix} \tag{3.17}$$

$$\begin{aligned}
\dot{x}_1 &= x_2\\
\dot{x}_2 &= \frac{(m_p l^2 + I)m_p l x_4^2\sin x_3 - (m_p l)^2 g\sin x_3\cos x_3 + (m_p l^2 + I)u}{(m_p + m_c)(m_p l^2 + I) - (m_p l\cos x_3)^2}\\
\dot{x}_3 &= x_4\\
\dot{x}_4 &= \frac{-(m_p l)^2(x_4)^2\sin x_3\cos x_3 + (m_p + m_c)m_p l g\sin x_3 - (m_p l\cos x_3)u}{(m_p + m_c)(m_p l^2 + I) - (m_p l\cos x_3)^2}
\end{aligned} \tag{3.18}$$

Letting

$$\begin{aligned}
a &= (m_p l^2 + I)m_p l x_4^2\sin x_3 - (m_p l)^2 g\sin x_3\cos x_3\\
b &= -(m_p l)^2(x_4)^2\sin x_3\cos x_3 + (m_p + m_c)m_p l g\sin x_3\\
c &= (m_p + m_c)(m_p l^2 + I) - (m_p l\cos x_3)^2\\
\xi &= m_p l^2 + I\\
\eta &= -m_p l\cos x_3
\end{aligned}$$

Then the state space equation will be:

$$\begin{bmatrix}\dot{x}_1\\ \dot{x}_2\\ \dot{x}_3\\ \dot{x}_4\end{bmatrix} = \begin{bmatrix}x_2\\ \frac{a}{c}\\ x_3\\ \frac{b}{c}\end{bmatrix} + \begin{bmatrix}0\\ \frac{\xi}{c}\\ 0\\ \frac{\eta}{c}\end{bmatrix} u \tag{3.19}$$

where u is the force applied to a cart.

3.4 Mathematical Modeling of Electrical Subsystem

3.4.1 Servo Amplifier and DC motor Modeling

A DC motor or a stepper motor is used to derive a cart proportional to control signal. The position of a cart is manipulated by controlling output torque of the motor or angular position of the motor. The torque of dc motor is controlled by either controlling armature current or armature voltage of DC motor. The first method require controllable current source that generate a current proportional to control signal. while the later require controllable voltage source that generate output voltage proportional to control signal. But using servo amplifier can simplify torque control of DC motor as servo amplifies can generate a signal that drive DC motor proportional to control signal. The relation between control signal from the controllers and the force required to drive the cart is derived in this sections.

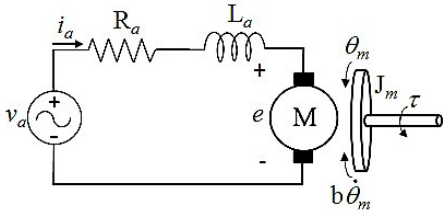

Figure 3.2: DC Motor Model [2]

The dynamics of DC motor is governed by two equations. From circuit diagram on figure 3.2, the equations are,

$$V_a = L_a \frac{dI_a}{dt} + R_a I_a + E_b \tag{3.20}$$

$$\tau_m = \eta_m k_t I_a \tag{3.21}$$

Neglecting the effect of armature inductance L_a, equation 3.20 is simplifies to,

$$V_a = R_a I_a + E_b \tag{3.22}$$

The velocity of the cart is equal to tangential velocity of a motor. From this, the relation between linear velocity and back emf of a DC motor can be established.

$$\omega = k_g \frac{\dot{x}}{r_g} \tag{3.23}$$

$$E_b = k_m \omega = k_m k_g \frac{\dot{x}_1}{r_g} \tag{3.24}$$

Replacing equation 3.24 for back emf E_b in equation 3.22 gives the relation ship between supplied voltage and linear velocity of a cart.

$$V_a = I_a R_a + k_m k_g \frac{\dot{x}_1}{r_g} \tag{3.25}$$

The relation between output torque of DC motor and supply voltage source can be derived from equation 3.21 by replacing for I_a, after solving for I_a from equation 3.25.

$$\tau_m = \eta_m k_t \left(\frac{V_a r_g - k_m k_g \dot{x}_1}{r_g R_a} \right) \tag{3.26}$$

Due to mechanical losses and gear efficiency this torque will not appear at input terminal. The actual torque at input terminal is a fraction of torque generated by DC motor.

$$\tau_g = \eta_g \tau_m \tag{3.27}$$

$$\tau_g = \eta_g \eta_m k_t \left(\frac{V_a r_g - k_m k_g \dot{x}_1}{r_g R_a} \right) \tag{3.28}$$

The linear force that drive's a cart is derived from equation 3.28.

$$u = \frac{\tau_g}{r_g} \tag{3.29}$$

$$u = \frac{\eta_g \eta_m k_t}{r_g} \left(\frac{V_a}{R_a} - \frac{k_m k_g \dot{x}_1}{r_g R_a} \right) \tag{3.30}$$

A block diagram representation of overall system is shown on figure 3.3.
If armature voltage control is used as shown on figure 3.3, the input to DC motor is the output of servo amplifier. The reference voltage v_{ref} can be zero or periodic

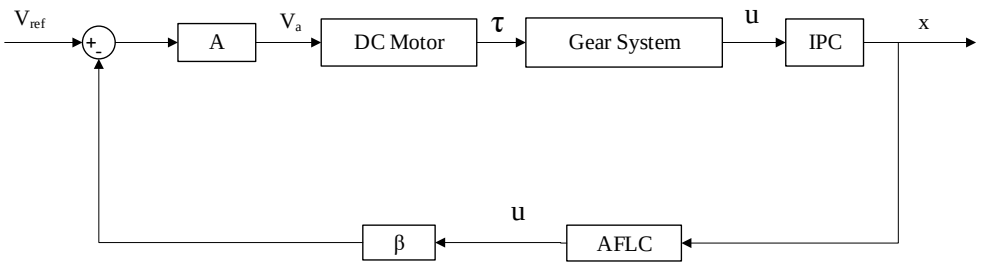

Figure 3.3: Integrated System Block Diagram

square voltage source. From block diagram on figure 3.3, the armature voltage at the terminal of DC motor is equal to the difference between the reference voltage and the control signal (which is added as voltage source) times a servo amplifier gain A. Servo amplifier is used to increase the intensity of the error signal.

$$V_a = A(v_{ref} - \beta u) \tag{3.31}$$

replacing for V_a in equation 3.30. The required force to derive a cart is expressed as function of reference signal, control signal and velocity of a cart.

$$\begin{aligned} u &= \frac{\eta_g \eta_m k_t}{r_g}\left(\frac{A(v_{ref} - \beta u)}{R_a} - \frac{k_m k_g \dot{x}_1}{r_g R_a}\right) \\ u &= \frac{\eta_g \eta_m k_t A}{R_a r_g} v_{ref} - \frac{\eta_g \eta_m k_t k_m k_g}{R_a r_g^2}\dot{x}_1 - \frac{\eta_g \eta_m k_t A \beta}{R_a r_g} u \\ u &= k_1 v_{ref} - k_2 \dot{x}_1 - k_3 u \\ u &= \frac{k_1 v_{ref} - k_2 \dot{x}_1}{1 + k_3} \end{aligned} \tag{3.32}$$

where

$$\begin{aligned} k_1 &= \frac{\eta_g \eta_m k_t A}{R_a r_g} \\ k_2 &= \frac{\eta_g \eta_m k_t k_m k_g}{R_a r_g^2} \ and \\ k_3 &= \frac{\eta_g \eta_m k_t A \beta}{R_a r_g} \end{aligned}$$

The analogy to current control is inferred from equation 3.25. Solving for armature current I_a, this equation shows that the armature current is altered by control signal.

$$\begin{aligned} I_a &= \frac{V_a r_g - k_g k_m \dot{x}_1}{R_a r_g} \\ I_a &= \frac{A(v_{ref} - \beta u) r_g - k_g k_m \dot{x}_1}{R_a r_g} \\ I_a &= \frac{A}{R_a} v_{ref} - \frac{k_g k_m}{R_a r_g}\dot{x}_1 - \frac{A\beta}{R_a} u \end{aligned} \tag{3.33}$$

If v_{ref} is zero, from equation 3.33 the value of armature current I_a, is dependent on $\dot{x}_1$ and u. As $\dot{x}$ is a system variable, it is affected by u. This implies that armature current depends entirely on u.

$$I_a = -\frac{k_g k_m}{R_a r_g}\dot{x}_1 - \frac{A\beta}{R_a} u \tag{3.34}$$

If there is no torque applied to the system (i.e. after disturbance is removed, rejected or compensated) the control signal is zero. As indicated on equation 3.35, the control signal will be zero, since the linear velocity of the cart is zero under this condition.

$$u = -\frac{k_g k_m}{A\beta r_g}\dot{x} \tag{3.35}$$

It is also possible to use voltage controlled voltage source to control the force applied to a cart via armature voltage control. The block diagram representation for this method is shown on figure 3.4. For armature current control, voltage controlled current source can be used. The block diagram representation is same as armature

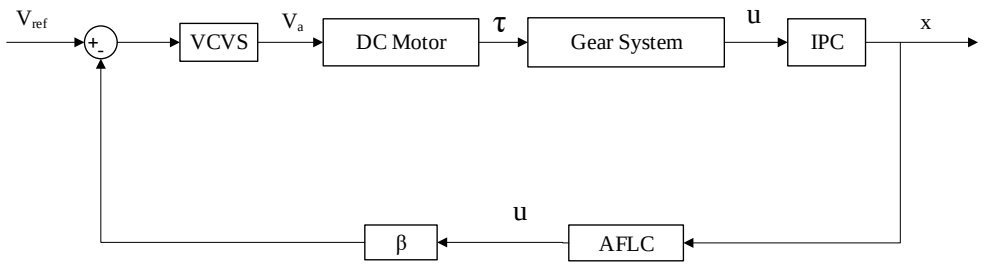

Figure 3.4: Controllable voltage source control method

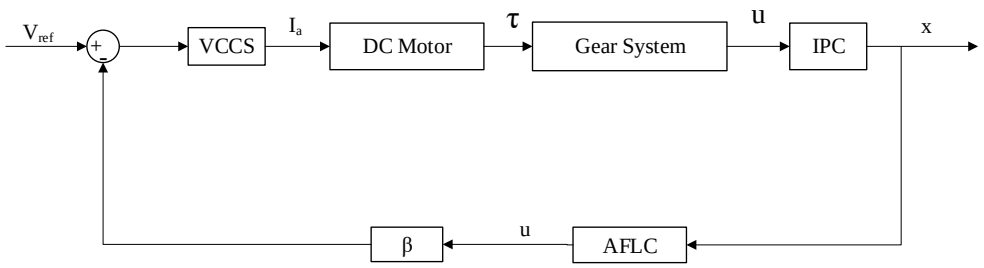

Figure 3.5: Controllable current source Control method

voltage control method on figure 3.3 if servo amplifier is used, the only difference is instead of V_a the input signal to DC motor is I_a and control signal u, is added as current source. The block diagram represention for this method is shown on figure 3.5.

If stepper motor is used to drive a cart, the above equations are applied to the system with simple modification to command signal fed to stepper motor driver. This modification is derived from the relation of required linear motion of a cart and angular position of a stepper motor θ_s.

$$u = m_c r_g \ddot{\theta}_s \tag{3.36}$$

solving for θ_s from equation 3.36,

$$\begin{aligned} \theta_s &= \frac{1}{r_g m_c} \int_{t=t_0}^{t} \int_{t=t_0}^{t} u(t)\ dt\ dt \\ \theta_s &= \frac{n_o\ step\ per\ revolution}{2\pi r_g m_c} \int_{t=t_0}^{t} \int_{t=t_0}^{t} u(t)\ dt\ dt \end{aligned} \tag{3.37}$$

Equation 3.37 shows the required angular position of the stepper motor. The block diagram representation using this method is shown on figure 3.6.

If there is no controllable voltage source, dc-dc converters can be used with constant DC voltage source. In this case V_a is equal duty cycle φ, times source voltage V_s. The duty cycle generated must be proportional to the controllers output control

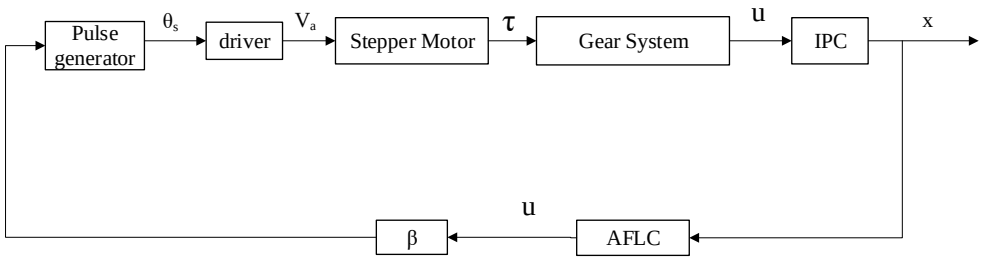

Figure 3.6: Controller application with stepper motor

signal. Which implies that duty cycle φ is

$$\begin{aligned} \varphi V_s &= I_a R_a + k_m k_g \frac{\dot{x}_1}{r_g} \\ &= \frac{\tau_m}{k_t \eta_m} R_a + k_m k_g \frac{\dot{x}_1}{r_g} \\ &= \frac{R_a r_g}{k_t \eta_m \eta_g} u + k_m k_g \frac{x_2}{r_g} \end{aligned} \tag{3.38}$$

From equation 3.38, the duty cycle required is

$$\varphi = \lambda_1 u + \lambda_2 x_2 \tag{3.39}$$

where $\lambda_1 = \dfrac{R_a r_g}{k_t \eta_m \eta_g V_s}$ and $\lambda_2 = \dfrac{k_m k_g}{r_g V_s}$.
The block diagram representation of this method is shown on figure 3.7 The linear

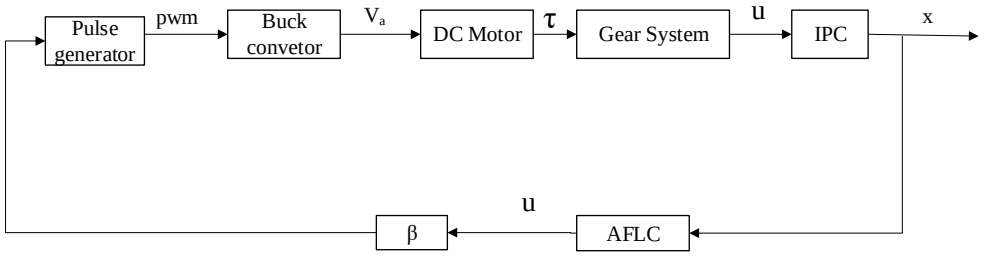

Figure 3.7: Controller application with dc dc converter

velocity of a cart is restricted by the rated speed of DC motor (this issues should be considered in hardware experimentation).

3.5 Feedback Linearization

For any nonlinear system which is linear in input and nonlinear in states of the form

$$\dot{x} = f(x) + g(x)u \tag{3.40}$$
$$y = h(x) \tag{3.41}$$

Where $x \in \mathbb{D} \subset \mathbb{R}_n, f : \mathbb{D} \mapsto \mathbb{R}_n, g : \mathbb{D} \mapsto \mathbb{R}_n$, and the domain $\mathbb{D}$ contains the origin.

To apply the notion of feedback linearization the following two cases should be identified correctly as explained on [35], [9], [10], [6].
Case 1:- Guarantee for nonlinear system (3.40) and (3.41) to be feedback linearizable, If there exist a nonlinear change of variable

$$z = T(x) = \begin{bmatrix} \mu_1 \\ \mu_2 \end{bmatrix} \tag{3.42}$$

and a control input

$$u = \alpha(x) + \beta(x)v \tag{3.43}$$

that would transform the system (3.40) and (3.41) into the following partially linear form

$$\dot{\Psi}_1 = f_0(\Psi, \mu) \tag{3.44}$$
$$\dot{\mu} = A\mu + Bv \tag{3.45}$$
$$y = C\mu \tag{3.46}$$

Case 2:- Guarantee for nonlinear system (3.40) and (3.41) to be input output linearizable if there exist a nonlinear change of variables

$$\mu = T(x) \tag{3.47}$$

and the same control input that would transform the system (3.40) into the following fully linear form.

$$\dot{\mu} = A\mu + Bv \tag{3.48}$$

To determine whether a nonlinear system is input-state feedback linearizable or input-output feedback linearizable, there are conditions to be checked. This conditions are called necessary condition and sufficient condition. The conditions are derived from concept of differential geometry which is beyond the scope of this thesis. But from this broad subject the overview on the concept of lie algebra and its application on design of feedback linearization is discussed in section 3.5.1. While, the conditions are stated in section 3.5.3.

Nonlinear control system problems that can be solved by using the concept of lie theory are called lie group problems. In such kind of problems the states of the system are modeled by the members of lie group and control signal are members of lie algebra.

3.5.1 Lie Algebra and Coordinate Transformation

Definition [36]: A Lie algebra is a vector space W over a field $\mathbb{G}$

1. It is bilinear.
2. It is skew symmetric: $[x, x] = 0$ which implies $[x, y] = -[y, x]$ for all $x, y \in W$.
3. It satisfies the Jacobi Identitiy: $[x, [y, z]] + [y, [z, x]] + [z, [x, y]] = 0$.

Consider any two vector fields V and U in lie group $\mathbb{G}$ mapping smooth continuous functions $f(x)$ and $g(x)$ from manifold[3] $\mathbb{M}$ to $\mathbb{N}$ respectively. The Lie derivative of $f(x)$ and $g(x)$ with respect to this vector field is given as:

$$L_u fg = (L_u f)g + f(L_u g) \tag{3.49}$$
$$L_v fg = (L_v f)g + f(L_v g) \tag{3.50}$$

and

$$\begin{aligned} U \circ V(fg) &= U(fV(g) + V(f)g) \\ U \circ V(fg) &= U(f)V(g) + fU(V(g)) + U(V(f))g + V(f)U(g) \end{aligned} \tag{3.51}$$

similarly

$$\begin{aligned} V \circ U(fg) &= V(fU(g) + U(f)g) \\ V \circ U(fg) &= V(f)U(g) + fV(U(g)) + V(U(f))g + U(f)V(g) \end{aligned} \tag{3.52}$$

Taking the difference of equation (3.51) and equation (3.52) result in the Lie commutator or lie bracket [4], [37], [5]. Which is defined as:

$$[U, V] = UV - VU \tag{3.53}$$

If V and U are differentiable, bijection[4] and there exist inverse V^{-1} and U^{-1} mapping from $\mathbb{N}$ to $\mathbb{M}$, they are called a diffeomorphism. If these functions are r times continuously differentiable, they are called a $\mathbb{C}^{\infty}$ diffeomorphism.

[3]Manifold is a topological space that locally resembles Euclidean space near each point
[4]bijection is a mapping that is both one-to-one (an injection) and onto (a surjection)

3.5.2 Application to Feedback Linearization

To apply the concept of lie commutator to feedback linearization, consider scalar function $h(x)$ and vector field $f(x)$, The lie derivative of $h(x)$ with respect to $f(x)$ is given as;

$$L_f h = \nabla h \cdot f = \frac{\partial h(x)}{\partial x} \cdot f \tag{3.54}$$

In control system $h(x)$ is taken to be the output of the system. where $f(x)$ is state mapping function. The n^{th} order lie derivative of $h(x)$ with respect to $f(x)$ is

$$\begin{aligned}
L_f^0 h &= h \\
L_f^1 h &= \nabla h \cdot f = \frac{\partial h(x)}{\partial x} \cdot f \\
L_f^2 h &= \nabla (L_f^1 h) \cdot f = \frac{\partial L_f^1 h(x)}{\partial x} \cdot f \\
&\vdots \\
L_f^n h &= \nabla (L_f^{n-1} h) \cdot f = \frac{\partial L_f^{n-1} h(x)}{\partial x} \cdot f
\end{aligned} \tag{3.55}$$

The number of times the lie derivative of an output is taken in order for the input explicitly appear in the equation is called the relative degree of the system [6]. If the relative degree of the system is less than the order of the system, there are dynamics that doesn't appear on the output. This dynamics are called zero dynamics of the system or left over dynamics of the system. Systems with left over dynamics can only feedback linearized if the left over dynamics is asymptotically stable. If the relative degree of the system is equal to the dimension of the system then the system can be input-state feedback linearizable as well as input output feedback linearizable, depending on the choice of $h(x)$.

For the system (3.40) and (3.41) with state mapping vector field or state mapping function $f(x)$ and input mapping vector field or input mapping function $g(x)$. The n^{th} order lie bracket of $f(x)$ and $g(x)$ which is also known as n^{th} order ad-joint of $f$and g is defined as

$$\begin{aligned}
adj_f g &= [f, g] = \nabla g \cdot f - \nabla f \cdot g = \frac{\partial g}{\partial x} \cdot f - \frac{\partial f}{\partial x} \cdot g \\
adj_f^2 g &= [f, adj_f g] = \nabla adj_f g \cdot f - \nabla f \cdot adj_f g = \frac{\partial adj_f}{\partial x} \cdot f - \frac{\partial f}{\partial x} \cdot adj_f g \\
&\vdots \\
adj_f^n g &= \left[f, adj_f^{n-1} g\right] = \nabla adj_f^{n-1} \cdot f - \nabla f \cdot adj_f^{n-1} = \frac{\partial adj_f^{n-1}}{\partial x} \cdot f - \frac{\partial f}{\partial x} \cdot adj_f^{n-1}
\end{aligned}$$

The n^{th} order lie derivative is used in deriving the necessary and sufficient conditions, which is discussed below.

3.5.3 Necessary and Sufficient Conditions

The system (3.40) and (3.41) is feedback linearizable i.e. there exist change of coordinate that will result in change of control, that linearize the dynamics of the system. So that, convectional linear control design technique can be applied to the system if the following condition are fulfilled.

1. Necessary condition

$$\left[g, ad_f g, ad_f^2 g, ad_f^3 g, \ldots, ad_f^{n-1} g\right] \tag{3.56}$$

2. Sufficient condition

$$\left[g, ad_f g, ad_f^2 g, ad_f^3 g, \ldots, ad_f^{n-2} g\right] \tag{3.57}$$

   this condition guarantees involutivity[5] or Integrability of the family.

The first condition stated on equation 3.56 states that there exist a linearly independent vector field that span n-dimensional space and the second condition stated on equation 3.57 state that the vector field is indeed a gradient (remark:- All vector field are not a gradient). Which means there exist

$$\nabla h(x) = \left[g, ad_f g, ad_f^2 g, ad_f^3 g, \ldots, ad_f^{n-2} g\right]^{-1} \cdot \begin{bmatrix} 0 \\ 0 \\ \vdots \\ 1 \end{bmatrix}$$

For more detail see [6] and [35].

3.6 Adaptive Inverse Control

Consider a plant with non linearity $N(\cdot)$ at the input of linear part $G(D)$

$$y(t) = G(D)u(t) \tag{3.58}$$

where the input is expressed as:

$$u(t) = N(v(t)) \tag{3.59}$$

$G(D)$ is rational transfer function, where D, represent Laplace transform in s-domain for continuous time systems and z-domain (advance operator) for discrete time systems.

The control objective is to cancel the effect of non-linearity and use the commonly used scheme for linear control technique to ensure the desired performance of the system [7],[34].
To achieve this objectives,

1. Clarification of such non-linearities for which such compensator can be used is required.

2. Adaptive law that can effectively update compensator parameter is required.

[5]Involutivity condition state that the lie bracket of any combination of a vector fields in the involutivity matrix result in an other vector in involutivity matrix

Clarification of non-linearities

Parameterized model for all non-linearities can be unified as,

$$u(t) = N(v(t)) = N(\theta^*; v(t)) \tag{3.60}$$

$$= -\theta^* \omega^{*T}(t) + a_s^*(t) \tag{3.61}$$

where $\theta^* \in R^{n\theta}$ unknown parameter vector of non-linearity. While $\omega^*(t)$ and $a_s^*(t)$ are unknown signals, whose components are determined by their flow in the non-linearity $N(\cdot)$.
The essence of adaptive inverse control is to cancel the effect of non-linearity,using the inverse characteristics $\widehat{NI}(\cdot)$ parametrized by $\theta(t)$ which is an estimate of θ^*. The system is drived by $u_d(t)$ a desired control signal from feedback law. The criteria to apply such inverse control law is

- The parameters should be adapted
- This parameters should stay in a pre-specified region to implement the inverse control law.

which is achieved by,

- The parametrized error model and
- parameter projection function(to ensure parameters are in range of predefined boundary).

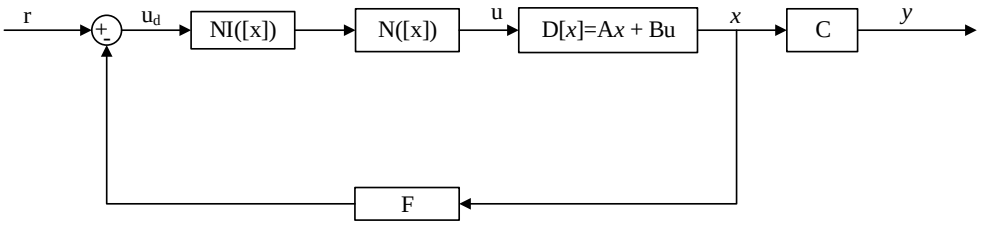

Figure 3.8: State feedback inverse control

As seen from figure 3.8 the control law is;

$$u_d(t) = -Fx(t) + r(t) \tag{3.62}$$

Theorem[7]:
Inverse model:- A desirable inverse $v(t) = \widehat{NI}(u_d(t))$ should be parametrized by $-\theta^T(t)\omega(t) + a_s(t)$, where $\omega(t) \in R^{n\theta}$ and $a_s(t) \in R$ are known signal. The components of $\omega(t)$ and $a_s(t)$ are determined by their flow through the non-linearity inverse model. If $u_d(t)$ is bounded then, $v(t)$, $\omega(t)$ and $a_s(t)$ are bounded.
Hence,

$$v(t) = \widehat{NI}(u_d(t)) \tag{3.63}$$

$$u_d(t) = -\theta^T(t)\omega(t) + a_s(t) \tag{3.64}$$

and from equation (3.61)

$$u(t) = -\theta^{*T}\omega^*(t) + a_s^*(t) \tag{3.65}$$

The feedback gain F on block diagram of figure 3.8 must be selected using state feedback controller design method like pole placement method or linear quadratic regulator(LQR) so that, $(A - BF)$ is stabilizable.

Using $u(t) = -Fx(t) + r(t)$ the response of closed loop system on figure 3.8 is

$$y(t) = C[DI - A - BF]^{-1}B([r](t) + [(\theta - \theta^*)\omega + d_N](t) + \epsilon_o(t) \tag{3.66}$$

where $\epsilon_o(t)$ exponentially decaying term due to initial conditions.
Let $W(D) = C[DI - A - BF]^{-1}B$, the expression on equation 3.66 reduces to

$$y(t) = W(D)([r](t) + [(\theta - \theta^*)\omega + d_N](t) + \epsilon_o(t) \tag{3.67}$$

If $d_N(t) = 0$ and the inverse cancels the non-linearity ($\theta = \theta^*$) the response will be

$$y(t) = W(D)[r](t) + \epsilon_o(t) \tag{3.68}$$

Th reference model of this system can be derived from equation 3.68 by ignoring the effect of $\epsilon_o(t)$. The reference model is then

$$y_m(t) = W_m(D)[r](t) \tag{3.69}$$

To quantify the disturbance signal $d_N(t)$, subtract equation(3.64) from equation (3.61) and rearrange

$$\begin{aligned} u(t) &= u_d(t) + (-\theta^{*T}\omega^*(t) + a_s^*(t)) - (-\theta^T(t)\omega(t) + a_s(t)) \\ &= u_d(t) + \theta^{*T}\omega^*(t) + (\tilde{\theta}^T(t) + \theta^{*T})\omega(t) + a_s^*(t) - a_s(t) \\ &= u_d(t) + \theta^{*T}\omega^*(t) + (\omega(t) - \omega^*(t))\theta^{*T} + a_s^*(t) - a_s(t) \\ &= u_d(t) + \theta^{*T}\omega^*(t) + d_N(t) \end{aligned} \tag{3.70}$$

Thus from equation 3.70, $d_N(t) = (\omega(t) - \omega^*(t))\theta^{*T} + a_s^*(t) - a_s(t)$. This implies $d_N(t) = 0$, iff $\omega(t) = \omega^*(t)$ and $a_s^*(t) = a_s(t)$. Going back to the block diagram on figure 3.8

$$\begin{aligned} y(t) &= W_m(D)[r](t) + W_m(D)[(\theta(t) + \theta^*)^T\omega](t) + W_m(D)[d_N](t) + \epsilon_o(t) \\ &= W_m(D)[r](t) + W_m(D)[\tilde{\theta}^T\omega](t) + W_m(D)[d_N](t) + \epsilon_o(t) \end{aligned} \tag{3.71}$$

Using reference model on equation (3.69) and assuming $W(D) = W_m(D)$ the output error is

$$\begin{aligned} y(t) - y_m(t) &= W_m(D)[(\theta(t) - \theta^*)^T\omega](t) + W_m(D)[d_N](t) \\ &= W_m(D)[\theta^T\omega](t) - \theta^{*T}W_m(D)[\omega](t) + W_m(D)[d_N](t) \end{aligned} \tag{3.72}$$

The estimation error is then,

$$\epsilon(t) = y(t) - y_m(t) + \varrho(t) \tag{3.73}$$

where

$$\varrho(t) = \theta^{*T}(t)\zeta(t) - W_m(D)[\theta^T\omega](t) \tag{3.74}$$

and

$$\zeta(t) = W_m(D)[\omega](t) \tag{3.75}$$

Substituting back for $\varrho(t)$ and $\zeta(t)$ in equation 3.73

$$\begin{aligned}\epsilon(t) &= y(t) - y_m(t) + \theta^T(t)W_m(D)[\omega](t) - W_m(D)[\theta^T\omega](t)\\ &= (\theta(t) - \theta^*)^T W_m(D)[\omega](t) + W_m(D)[d_N](t)\end{aligned} \tag{3.76}$$

In time domain,

$$\epsilon(t) = \tilde{\theta}^T\zeta(t) + d_N(t) \tag{3.77}$$

Which is linear in $\tilde{\theta}(t)$ with bounded error due to uncertainty of non-linearity $N(\cdot)$. if $d_N(t) = 0$ the estimation error is

$$\begin{aligned}\epsilon(t) &= (\theta(t) - \theta^*)^T W_m(D)[\omega](t)\\ &= \tilde{\theta}^T W_m(D)[\omega](t)\end{aligned} \tag{3.78}$$

Continuous Lyapunov Adaptive Law Design Method

The closed loop state space representation of the system on figure 3.8 is

$$\dot{x}(t) = Ax(t) + Br(t) + B(\tilde{\theta}^T\omega(t) + d_N(t)) \tag{3.79}$$

$$y(t) = Cx(t) \tag{3.80}$$

If $d_N(t) = 0$, which means $\theta(t) = \theta$ with control signal on equation 3.62, the system on equation 3.79 and 3.80 simplified to

$$\dot{x}(t) = (A - BF)x(t) + Br(t) \tag{3.81}$$

$$y(t) = Cx(t) \tag{3.82}$$

which imply reference model

$$\dot{x}_m(t) = (A - BF)x_m(t) + Br(t) \tag{3.83}$$

$$y_m(t) = Cx_m(t) \tag{3.84}$$

Let $\tilde{x}(t) = x(t) - x_m(t)$ and $e(t) = y(t) - y_m(t)$. The error dynamics is

$$\dot{\tilde{x}}(t) = (A - BF)\tilde{x}(t) + B(\tilde{\theta}^T\omega(t) + d_N(t)) \tag{3.85}$$

$$e(t) = C\tilde{x}(t) \tag{3.86}$$

To develop adaptive law for the system consider the following Lyapunov function

$$\nu(\tilde{x}, \tilde{\theta}) = \frac{1}{2}(\tilde{x}^T P_a\tilde{x} + \tilde{\theta}^T\Gamma^{-1}\tilde{\theta}) \tag{3.87}$$

where, $\Gamma = diag[\gamma_1, \gamma_2, ..., \gamma_{n\theta}]$, and γ_i's are any positive real number for continuous time systems and $0 < \gamma_i < 2$ for discrete time systems. While P_a is any positive definite matrix, $P_a = P_a^T > 0$ satisfying Lyapunov equation stated on equation 3.88.

$$P_a(A - BF) + (A - BF)^T P_a = -2Q_a \tag{3.88}$$

Q_a is any positive definite matrix, $Q_a = Q_a^T > 0$.
The derivative of Lyapunov function is

$$\begin{aligned}\dot{\nu} &= \frac{1}{2}[\frac{d}{dt}(\tilde{x}^T P_a \tilde{x} + \tilde{\theta}^T \Gamma^{-1} \tilde{\theta})] \\ &= \tilde{x}^T P_a \dot{\tilde{x}} + \tilde{\theta}^T \Gamma^{-1} \dot{\tilde{\theta}}\end{aligned} \tag{3.89}$$

replacing $\dot{\tilde{x}}(t)$ with $(A - BF)\tilde{x}(t) + B(\tilde{\theta}^T \omega(t) + d_N(t)$

$$\begin{aligned}\dot{\nu} &= \tilde{x}^T P_a((A - BF)\tilde{x} + B(\tilde{\theta}^T \omega + d_N) + \tilde{\theta}^T \Gamma^{-1} \dot{\tilde{\theta}} \\ &= \tilde{x}^T P_a(A - BF)\tilde{x} + \tilde{x}^T P_a B(\tilde{\theta}^T \omega + d_N) + \tilde{\theta}^T \Gamma^{-1} \dot{\tilde{\theta}} \\ &= -\tilde{x}^T Q_a \tilde{x} + \tilde{x}^T P_a B(\tilde{\theta}^T \omega + d_N) + \tilde{\theta}^T \Gamma^{-1} \dot{\tilde{\theta}}\end{aligned} \tag{3.90}$$

Selecting an adaptive law

$$\dot{\tilde{\theta}} = -\Gamma \omega(t) \tilde{x}^T(t) P_a B + f_\theta(t) \tag{3.91}$$

If $d_N(t) = 0$, select parameter projection function $f_\theta(t) = 0$ then,

$$\tilde{x}^T P_a B \tilde{\theta}^T \omega + \tilde{\theta}^T \Gamma^{-1} \dot{\tilde{\theta}} = 0 \tag{3.92}$$

Which imply that equation (3.96) becomes

$$\dot{\nu} = -\tilde{x}^T Q_a \tilde{x} \leq 0 \tag{3.93}$$

as required. This means that ν is bounded and $\tilde{y} = y - y_m \in L^2$ i.e $\tilde{y}$ and $\tilde{\theta}$ are bounded, so are y and θ.
If $d_N(t) \neq 0$, use parameter projection law $f_\theta(t)$,

$$f_\theta(t) = \begin{cases} 0 & if\ \theta_i \in [\theta_i^a, \theta_i^b]\ or \\ & if\ \theta_i = \theta_i^a\ and\ g_i(t) \geq 0\ or \\ & if\ \theta_i = \theta_i^b\ and\ g_i(t) \leq 0 \\ -g_i(t) & otherwise \end{cases} \tag{3.94}$$

where $g_i(t)$ is given as;

$$g_i(t) = -\Gamma \omega(t) \tilde{x}^T P_a B \tag{3.95}$$

and $[\theta_i^a, \theta_i^b]$ is reasonable span of parameters, with θ_i^a minimum value and θ_i^b maximum value. With same adaptive law on equation 3.91, the derivative of Lyapunov function becomes,

$$\begin{aligned}\dot{\nu} &= \tilde{x}^T P_a((A - BF)\tilde{x} + B(\tilde{\theta}^T \omega + d_N) + \tilde{\theta}^T \Gamma^{-1}(-\Gamma \omega \tilde{x}^T P_a B + f_\theta) \\ &= \tilde{x}^T P_a(A - BF)\tilde{x} + \tilde{x}^T P_a B(\tilde{\theta}^T \omega + d_N) + \tilde{\theta}^T \Gamma^{-1}(-\Gamma \omega \tilde{x}^T P_a B + f_\theta) \\ &= -\tilde{x}^T Q_a \tilde{x} + \tilde{x}^T P_a B(\tilde{\theta}^T \omega + d_N) + \tilde{\theta}^T \Gamma^{-1}(-\Gamma \omega \tilde{x}^T P_a B + f_\theta) \\ &= -\tilde{x}^T Q_a \tilde{x} + \tilde{x}^T P_a B \tilde{\theta}^T \omega + \tilde{x}^T P_a B d_N - \tilde{\theta}^T \Gamma \Gamma^{-1} \omega \tilde{x}^T P_a B + \tilde{\theta}^T \Gamma^{-1} f_\theta \\ &= -\tilde{x}^T Q_a \tilde{x} + \tilde{x}^T P_a B d_N + \tilde{\theta}^T \Gamma^{-1} f_\theta\end{aligned} \tag{3.96}$$

Which means Γ must fulfill additional condition $\tilde{\theta}^T\Gamma^{-1}f_\theta(t) \leq 0$. From projection function on equation 3.94, for each θ_i, $(\theta_i(t) - \theta_i^*)f_i(t) \leq 0$ for $i = 1, 2, 3, \cdots, n\theta$. Which means that $\tilde{\theta}^T\Gamma^{-1}f_\theta(t) \leq 0$ and $d_N(t)$ is bounded as well as $x(t)$. Equation 3.84 shows that $x_m(t)$ is bounded and equation 3.70 imply $u_d(t)$ is bounded. Finally from inverse control theorem, $\omega(t), a(t), v(t)$ are all bounded. Since all closed loop signals are bounded ,the output error $e(t) = y(t) - y_m(t)$ and $\dot{\theta}(t)$ are bounded, which means in square sense: $\int_{t_1}^{t_2} e^2(t)dt \leq \gamma_o + k_o \int_{t_1}^{t_2} d_N^2(t)dt$ for some constants $\gamma_o,\ k_o > 0$. The effect of $\tilde{x}^T P_a B d_N$ is handled by proper selection of design signal u_n. u_n ensure robustness with respect to the bounded error term $d_N(t)$.

3.6.1 Application to Feedback Linearization

Consider the following non-linear system of the form

$$\begin{aligned} \dot{x} &= f(x) + g(x)u \\ y &= h(x) \end{aligned} \tag{3.97}$$

if the control signal $u(t)$ is not available and if it can be replaced by $u_d(t)+\tilde{\theta}^T\omega+d_N$, state equation of nonlinear system on equation 3.97 is reformulated as,

$$\dot{x} = f(x) + g(x)(u_d(t) + \tilde{\theta}^T\omega + d_N) \tag{3.98}$$

$$y = h(x) \tag{3.99}$$

By considering non-linearities of the system on equation 3.97 as actuator non-linearity, it is possible to design feedback linearizing signal that linearize the system. After that classical feedback control can be applied to the system to achieve the desired performance.

To determine linear form of the system, apply the concept of lie-algebra and determine diffeomorphism coordinate transformation $T(x)$. Letting $y = h(x) = T(x)$ and substitute for $\dot{x}$ from equation 3.97, the diffeomorphism coordinate transformation is

$$\begin{aligned} \dot{y}_1 &= \frac{\partial T_1}{\partial x}\dot{x} = \frac{\partial T}{\partial x}(f(x) + g(x)(u_d(t) + \tilde{\theta}^T\omega + d_N)) \\ &= L_f T_1(x) + L_g T_1(x)(u_d(t) + \tilde{\theta}^T\omega + d_N) \\ \dot{y}_2 &= L_f T_2(x) + L_g T_2(x)(u_d(t) + \tilde{\theta}^T\omega + d_N) \\ &\vdots \\ \dot{y}_\rho &= L_f T_\rho(x) + L_g T_\rho(x)(u_d(t) + \tilde{\theta}^T\omega + d_N) \end{aligned} \tag{3.100}$$

Let $\beta(x) = L_f T_\rho(x)$ and $\alpha(x) = L_g T_\rho(x)$ the last expression on equation (3.100) becomes;

$$\dot{y}_\rho = \beta(x) + \alpha(x)u_d + \alpha(x)(\tilde{\theta}^T\omega + d_N) \tag{3.101}$$

With $w(t) = \beta(x) + \alpha(x)u_d(t)$, $u_d(t)$ is

$$u_d(t) = \frac{w(t) - \beta(x)}{\alpha(x)} + u_n \tag{3.102}$$

u_n is design signals that ensure robustness with respect to bounded error.
With control signal on equation (3.102) the state space representation of nonlinear system on 3.97 with output $y = h(x)$ is changed to linear linear form

$$\begin{aligned}
\dot{y}_1 &= y_2 \\
\dot{y}_2 &= y_3 \\
&\vdots \\
\dot{y}_{\rho-1} &= y_\rho \\
\dot{y}_\rho &= b(\mu, \Psi) + a(\mu, \Psi)u
\end{aligned} \tag{3.103}$$

For systems with relative degree ρ less than the order of the system the diffeomorphism coordinate transformation include feedback linearizable part and left over dynamics (zero dynamics), $T(x) = [T_c(x), T_z(x)]^T$ and similarly the output becomes $y = [\mu, \Psi]$. Where T_c and μ represent feedback linearized part which is controllable, T_z and Ψ represent uncontrollable zero dynamics respectively.

$$\begin{aligned}
\mu &= [y_1, y_2, ..., y_\rho]^T \\
\Psi &= [y_{\rho+1}, y_{\rho+2}, ..., y_n]^T
\end{aligned}$$

In state space representation

$$\dot{\mu} = A\mu + Bw + B\alpha(x)(\tilde{\theta}^T\omega + d_N) \tag{3.104}$$

$$y = \mu \tag{3.105}$$

where

$$A = \begin{bmatrix} 0 & 1 & 0 & . & . & . & 0 \\ 0 & 0 & 1 & . & . & . & 0 \\ . & . & . & . & . & . & . \\ . & . & . & . & . & . & . \\ . & . & . & . & . & . & . \\ 0 & 0 & 0 & . & . & . & 1 \\ 0 & 0 & 0 & . & . & . & 0 \end{bmatrix} \qquad B = \begin{bmatrix} 0 \\ 0 \\ . \\ . \\ . \\ 0 \\ 1 \end{bmatrix}$$

representing the linearized part of the the dynamics equation(3.100). For this part linear state feedback control technique with control signal $w = -Fy + r$ can be used. The reference model for system on equation 3.101 is

$$\dot{y}_m = (A - BF)y_m + Br \tag{3.106}$$

the tracking error $\tilde{y} = y - y_m$ is

$$\dot{\tilde{y}} = (A - BF)\tilde{y} + \alpha(x)(\tilde{\theta}^T\omega + d_N + u_n) \tag{3.107}$$

choosing an adaptive law

$$\dot{\tilde{\theta}} = -\Gamma\omega(t)\tilde{y}^T(t)P_aB + f_\theta(t) \tag{3.108}$$

and lyapunov function

$$\nu(\tilde{x},\tilde{\theta}) = \frac{1}{2}(\tilde{y}^T P_a \tilde{y} + \tilde{\theta}^T \Gamma^{-1} \tilde{\theta}) \tag{3.109}$$

The derivative of lyapunov function is

$$\begin{aligned}\dot{\nu} &= \frac{1}{2}[\frac{d}{dt}(\tilde{y}^T P_a \tilde{y} + \tilde{\theta}^T \Gamma^{-1} \tilde{\theta})] \\ &= \tilde{y}^T P_a \dot{\tilde{y}} + \tilde{\theta}^T \Gamma^{-1} \dot{\tilde{\theta}}\end{aligned} \tag{3.110}$$

replacing $\dot{\tilde{y}}(t)$ with $(A - BF)\tilde{y}(t) + B(\tilde{\theta}^T \omega(t) + d_N(t) + u_n)$

$$\begin{aligned}\dot{\nu} &= \tilde{y}^T P_a((A - BF)\tilde{y} + B(\tilde{\theta}^T \omega + d_N + u_n) + \tilde{\theta}^T \Gamma^{-1} \dot{\tilde{\theta}} \\ &= \tilde{y}^T P_a (A - BF)\tilde{y} + \tilde{y}^T P_a B(\tilde{\theta}^T \omega + d_N + u_n) + \tilde{\theta}^T \Gamma^{-1} \dot{\tilde{\theta}} \\ &= -\tilde{y}^T Q_a \tilde{y} + \tilde{y}^T P_a B(\tilde{\theta}^T \omega + d_N + u_n) + \tilde{\theta}^T \Gamma^{-1} \dot{\tilde{\theta}}\end{aligned} \tag{3.111}$$

If $d_N(t) = 0$, select design signal $u_n = 0$ and parameter projection function $f_\theta(t) = 0$. With an adaptive law on equation (3.108),

$$\tilde{y}^T P_a B \tilde{\theta}^T \omega + \tilde{\theta}^T \Gamma^{-1} \dot{\tilde{\theta}} = 0 \tag{3.112}$$

The derivative of lyapunov function is

$$\dot{\nu} = -\tilde{y}^T Q_a \tilde{y} \leq 0 \tag{3.113}$$

as desired. This means that ν is bounded and $\tilde{y} = y - y_m \in L^2$ ı.e $\tilde{y}$ and $\tilde{\theta}$ are bounded, so are y and θ. Since $\dot{y} = T(x)$ is diffeomorphism, $x(t)$ is also bounded and so are u_d and $\dot{\tilde{y}}$, which implies $\lim_{t \mapsto 0}(y(t) - y_m(t)) = 0$.
If $d_N(t) \neq 0$ choose design signal

$$u_n = -\gamma \alpha(x) \tilde{y}^T P_a B \tag{3.114}$$

where γ is any positive real number.
Under this condition the derivative of lyapunov function becomes,

$$\begin{aligned}\dot{\nu} &= -\tilde{y}^T Q_a \tilde{y} + \tilde{y}^T P_a B(\tilde{\theta}^T \omega + d_N + u_n) + \tilde{\theta}^T \Gamma^{-1} \dot{\tilde{\theta}} \\ &= -\tilde{y}^T Q_a \tilde{y} + \tilde{y}^T P_a B(\tilde{\theta}^T \omega + d_N - \gamma \alpha(x) \tilde{y}^T P_a B) + \tilde{\theta}^T \Gamma^{-1}(-\Gamma \omega \tilde{y}^T P_a B + f_\theta) \\ &= -\tilde{y}^T Q_a \tilde{y} + \tilde{y}^T B \alpha(x) d_N + \tilde{\theta}^T \Gamma^{-1} f_\theta - \gamma(\alpha(x) \tilde{y}^T P_a B)^2 \\ &= -\tilde{y}^T Q_a \tilde{y} + \tilde{\theta}^T \Gamma^{-1} f_\theta + \frac{1}{4\gamma} d_N^2\end{aligned} \tag{3.115}$$

Since $d_N(t)$ is bounded, $\tilde{y}$ is bounded so is $y(t)$. Then $x(t)$ is bounded, because $T(x)$ is diffeomorphism and $u_d(t)$ is also bounded[6].

[6]The stability analysis of robust adaptive control is explained in book on reference [7] in chapter three "Adaptive Parameter Estimation" section 3.8.

Chapter 4

Swing-up Controller Design

4.1 Mechanical Energy and Heteroclinic Orbits

Swing-up control strategy is mainly based on mechanical energy of the system. The potential energy reference u_{ref}, is placed where the pendulum is at rest, as depicted in figure 4.1. In order to avoid negative potential energy, this reference potential energy is set to

$$u_{ref} = m_p g l \tag{4.1}$$

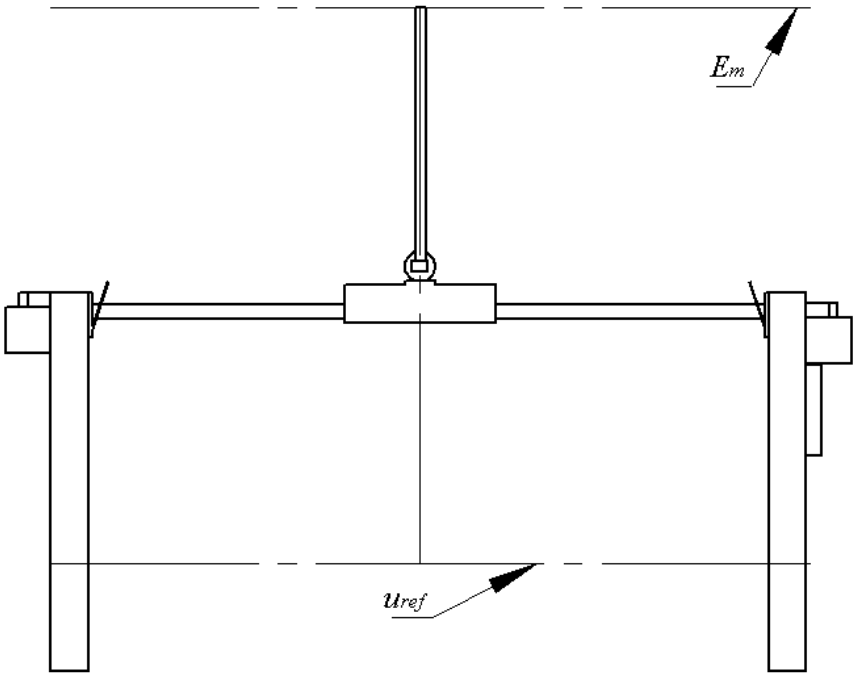

Figure 4.1: Potential energy reference (SOLIDWORKS)

While the potential energy of the pendulum at upright position E_m indicated on figure 4.1 corresponds to the energy reference

$$E_m = 2m_p g l \tag{4.2}$$

The energy of a pendulum at any point is given as

$$E_p = \frac{1}{2}(I + m_p l^2)\dot{\theta}^2 + m_p g l(1 + cos\theta). \tag{4.3}$$

Swinging up the pendulum will specifically concern with controlling the energy of the system, so that the pendulum reaches it's heteroclinic orbits. Heteroclinic orbits are trajectories that connect two stable equilibrium points of a system (i.e. there exist an equilibrium point on either side of heteroclinic orbits). Hetereoclinic orbits are found by investigating the case where the energy of the pendulum is equal to E_m, i.e.

$$\begin{aligned} E_m &= E_p \\ 2m_p g l &= \frac{1}{2}(I + m_p l^2)\dot{\theta}^2 + m_p g l(1 + cos\theta) \end{aligned} \tag{4.4}$$

Solving for $\dot{\theta}$ yields the expression for the heteroclinic orbits.

$$\dot{\theta} = \sqrt{\frac{2g}{l}(1 + cos\theta)} \tag{4.5}$$

The doted line on figure 4.2 represent heteroclinic orbit of a pendulum. Inside heteroclinic orbits the trajectory move away from unstable equilibrium point on one side and moves toward it on the other side. Outside Heteroclinic orbits the energy of the system is greater than reference energy, this shows that if there is no friction the system will continue on the path. But if there is friction it looses the energy and end up on the next stable equilibrium point. For Inverted pendulum on a cart for zero friction if the system energy is greater than reference energy the pendulum continues rotating or swing back and forth continuously and never stops. But if there is friction it will end up at one of its stable equilibrium point $(2n\pi, 0)$. The first

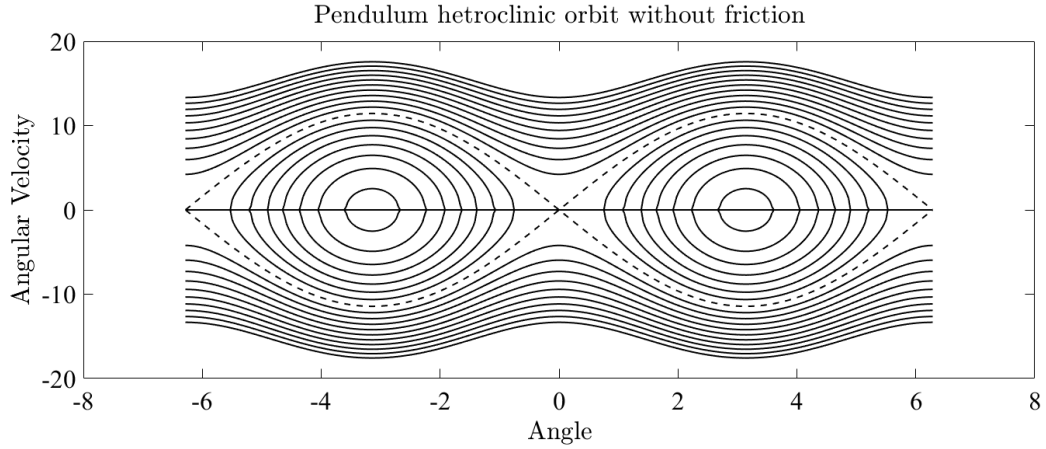

Figure 4.2: Heteroclinic orbits without friction (MATLAB)

heteroclinic orbit connect the two stable equilibrium points $(0, 0)$ and $(-2\pi, 0)$ of an inverted pendulum. Physically the two points exist on same location on vertical line of pendulum. The process of driving a pendulum from its pendant position, where the energy of the system is minimum to inverted position where the energy of the

system is maximum is called swing-up. The main objective of this process is to add energy to the system so that the system reach at it's unstable equilibrium point, for control purpose. There are different swing up controller design techniques available for inverted pendulum on a cart.

- Position-Velocity swing-up method [2]
- Energy based swing-up method [27],[28]
- Sign Based swing-up method [33]
- Optimal Swing up method [32]
- Using closed loop fundamental of the dynamics system [34]
- Impulse-Momentum approach [31]
- Fuzzy logic based swing-up method [29]

4.2 Adaptive Fuzzy Logic based Swing-up Controller (AFLSUC) Design

In this thesis among the listed methods, impulse-momentum swing up approach is approximated by fuzzy logic to swing the pendulum from pendant position to inverted position. Since the mass of a cart and the mass of a pendulum are unknown the swing up controller should adapt in order to achieve the desired objective.
The basic idea behind fuzzy logic based swing-up controller design in this thesis is, when the cart move back and forth as quickly as possible the pendulum will get the energy required to reach near its unstable equilibrium point which is the concept of impulse-momentum swing up approach.

Taking linear position error ex_1 and angular position error ex_3 as an input for fuzzy logic based swing-up controller with three membership functions (N-negative, Z-zero and P-positive) for both inputs. The output of the controller is swing-up control signal u with five membership functions (NB-negative big, NS-negative small, Z-zero, PS-positive small and PB-positive big). The rule base of fuzzy logic based swing up controller is shown on table 4.1. Membership functions of inputs (linear

Table 4.1: Fuzzy logic based swing-up controller Rule base

$ex_1 \setminus ex_3$	N	Z	P
N	PB	Z	PS
Z	NS	Z	PS
P	NB	Z	NS

position error and angular position error) to fuzzy logic based swing up controller are indicated on figure 4.3 and figure 4.4 respectively. The output control signal membership function of fuzzy logic based swing up controller along with surface plot of fuzzy inference system are shown below on figure 4.5 and figure 4.6 respectively.

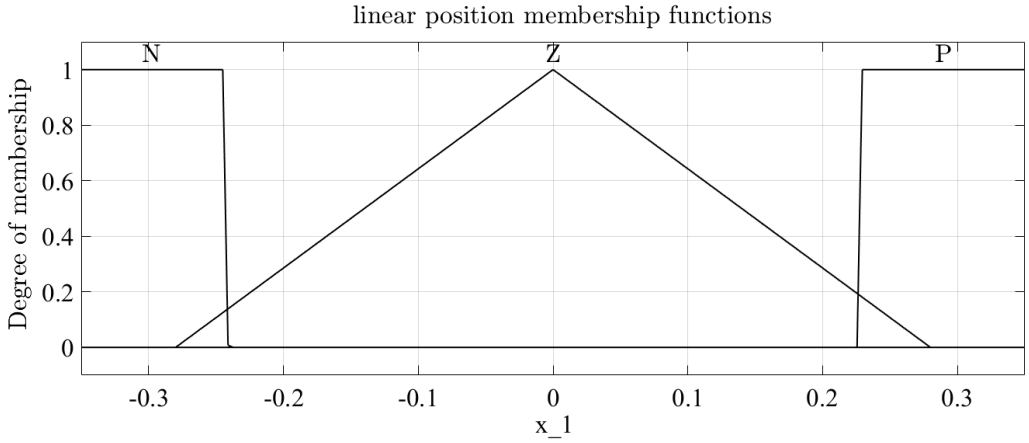

Figure 4.3: Cart linear position membership functions (MATLAB)

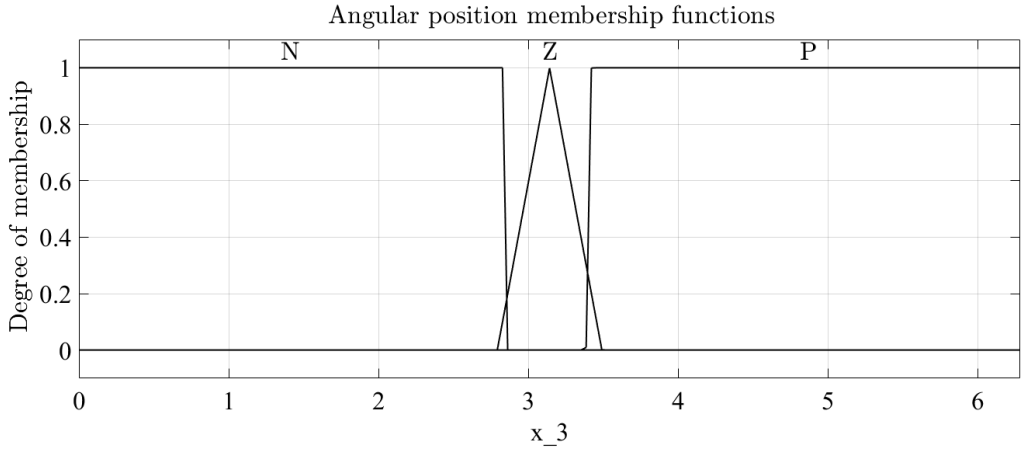

Figure 4.4: Pendulum angular position membership functions (MATLAB)

Since the parameter of the system is unknown the must learn to achieve desired angular position. Designing an adaptive fuzzy logic controller is achieved by changing the gain of input and/or output variables of fuzzy logic controller. As explained above in this thesis the input variables of fuzzy logic controller are angular position error and linear p osition error. The position of the cart is restricted within specified range since the cart position should be within reasonable range. These are shown on the graph of input variables membership functions. See figure 4.3 and figure 4.4. The only gain that can be adjusted is the gain of output variable (fuzzy logic based swing-up controller output control signal).
Consider the change in mechanical energy of the pendulum,

$$\begin{aligned} \dot{E}_p &= \frac{d}{dt}\left(0.5(m_p l^2 + I){x_4}^2 + m_p g l(1+\cos\theta)\right) \\ \dot{E}_p &= -m_p l \dot{x}_2 \dot{\theta}\cos\theta \end{aligned} \tag{4.6}$$

From equation 4.6 since the variables m_p and l are unknown the only way to alter the energy of the system is by changing acceleration of the cart, angular velocity $\dot{\theta}$

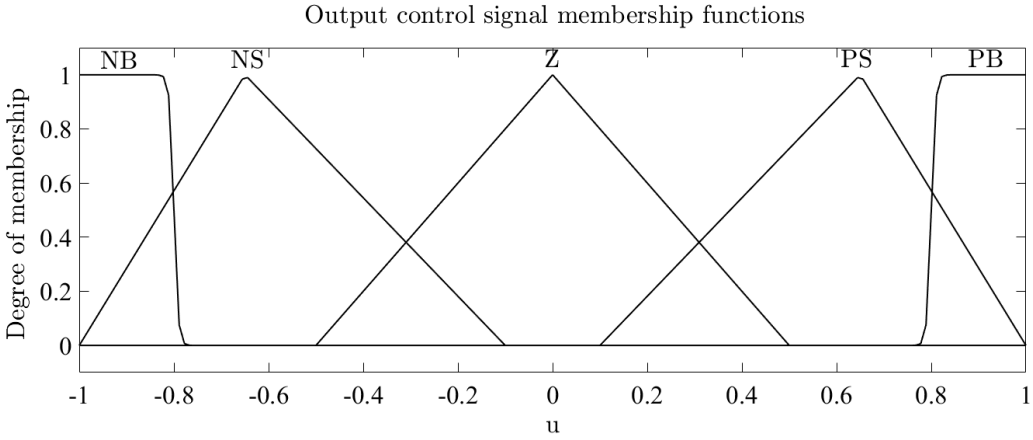

Figure 4.5: Control signal membership functions (MATLAB)

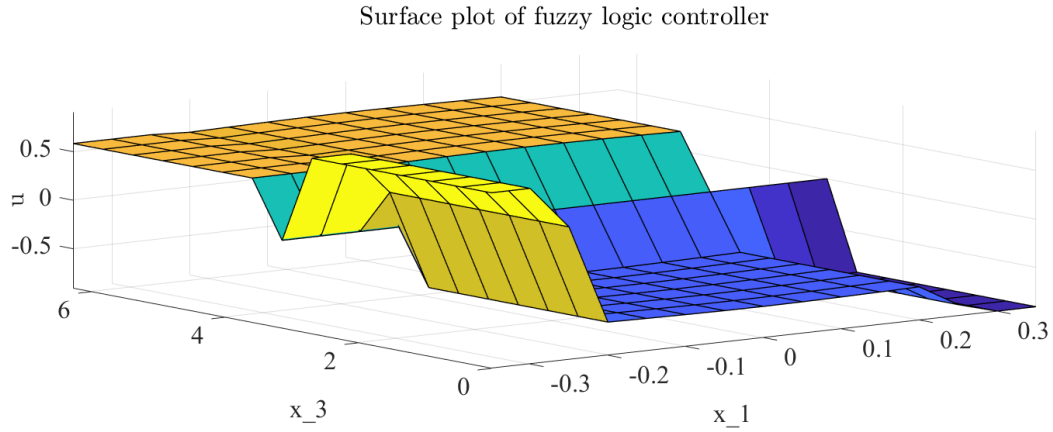

Figure 4.6: Surface plot of fuzzy logic based swing up controller rule base (MATLAB)

or angle θ. Maximum energy is injected to the system or removed from the system when its angular position is zero. Rather than injecting high amount of energy at first, injecting small amount of energy is advisable due the constraint in cart position. Relatively high energy is injected when the pendulum passes its stable equilibrium point after first energy injection. Measuring the amount of change in angular velocity of the pendulum can tell the amount of energy injected to the system or removed from the system. Thus this can be used to adjust the amount of energy injected to the system. By applying this method the pendulum can be driven from pendant position to upright or inverted position in less than 2 seconds. The mass of the cart has significant effect on the amount of energy injected to the system. In this thesis, scalar multiplier of adaptive fuzzy logic based swing-up controller output signal is selected by trial end error for particular initial mass of a cart.

4.3 Switching Conditions

After the pendulum reaches near its unstable equilibrium point the stabilizing controller must take over the swing up controller. Hence there must be switching mechanism. The requirements to switch from swing up controller to stabilizing controller are

- Change in energy of the pendulum must be in range $E_m - E_p \leq 0.5|E^*|$.
- The angle of the pendulum must be in range $|\theta| \leq \frac{\pi}{9}$.

For known system parameter, if none,or only one of these two criteria's are met, the output of the swing-up controller will be applied to the system. When both are satisfied, the output from the stabilizing controller is applied to the system. But the parameter of the inverted pendulum are unknown, checking the energy criteria is difficult. Hence in this thesis only angle criteria will be checked. If this criteria is met the stabilizing controller will be switched on.
Note that when one controller is active, the other remains passive. In terms of implementation, it is beneficial to completely skip computing the output of the passive controller.

Chapter 5

Stablizing Controller Design

5.1 Checking Feedback Linearizability of the System

Applying test for feedback linearizability stated in section 3.5.3 to dynamics of inverted pendulum.

1. Check for necessary condition:

$$f = \begin{bmatrix} x_2 \\ \frac{a}{c} \\ x_4 \\ \frac{b}{c} \end{bmatrix} \quad g = \begin{bmatrix} 0 \\ \frac{\xi}{c} \\ 0 \\ \frac{\eta}{c} \end{bmatrix} \tag{5.1}$$

$$\begin{aligned} ad_f^1 g &= [f, g] = \nabla g \cdot f - \nabla f \cdot g \\ ad_f^2 g &= [f, ad_f^1 g] = \nabla ad_f^1 g \cdot f - \nabla f \cdot ad_f^1 g \\ ad_f^3 g &= [f, ad_f^2 g] = \nabla ad_f^2 g \cdot f - \nabla f \cdot ad_f^2 g \end{aligned} \tag{5.2}$$

   The rank of controlability matrix is 4, as checked by MATLAB script on appendix A.

2. Check for sufficient condition
   Intregrability matrix must be involutive,ı.e the adjoint of any two vectors in controlability matrix should produce and other vector in controlability matrix. For the case of inverted pendulum dynamic equation, this criteria is not satisfied as checked by MATLAB script on appendix A.

Hence an inverted pendulum on a cart dynamics can be input output feedback linearized if the left over dynamics are stable. But it cannot be input-state feedback linearized since the relative degree of the system is less than the order of the system. The next step is determining output expression $h(x)$ that yield minimum number of zero dynamics after input-output feedback linearization. Taking the output $h(x) = x_1$, $h(x) = x_3$ or $h(x) = k_1 x_1 + k_2 x_3$ will result in relative degree of $\rho = 2$ for the

system as seen below

$$\begin{aligned} h(x) &= k_1 x_1 + k_2 x_3 \\ L_f h(x) &= T_1(x) = k_1 x_1 + k_2 x_3 \\ L_f^1 h(x) &= T_2(x) = k_1 \dot{x}_1 + k_2 \dot{x}_3 = k_1 x_2 + k_2 x_4 \\ L_f^2 h(x) &= T_3(x) = k_1 \dot{x}_2 + k_2 \dot{x}_4 \\ &= k_1 \left(\frac{a}{c} + \frac{\xi}{c} u \right) + k_2 \left(\frac{b}{c} - \frac{\eta}{c} u \right) \end{aligned}$$

The selection of this output function result with order two left over dynamics. In this case one should have to solve partial differential equation in order to perform input-state feedback linearization. The two linearly independent solutions are used to compensate for the second order left-over dynamics. The partial differential equation is derived from dynamics of the system. The solution to this partial differential equation is used to construct diffeomorphism function that has relative degree equal to order of the system. For system with relative degree r the diffeomorphism function is

$$T(x) = [\mu_1, \mu_2, \cdots, \mu_r, \Psi_1, \Psi_2, \cdots, \Psi_{n-r}]^T$$

where $\mu_1, \mu_2, \cdots, \mu_r$ represent controllable part and $\Psi_1, \Psi_2, \cdots, \Psi_{n-r}$ represent zero dynamics of the system. These are vectors that form normal coordinate or normal state of the new system, if they are linearly independent. If the relative degree of the system is r then $\mu_1, \mu_2, \cdots, \mu_r$ are linearly independent from partial differential equation 5.5. The other vector fields are determined so that they are linearly independent. Since the control signal must not appear on r^{th} lie derivative of each Ψ_j's for $r < n$. i.e

$$L_g^r \Psi_j(x_i) = 0 \tag{5.3}$$

which means that

$$\nabla \Psi_j g = 0 \tag{5.4}$$

For the case of inverted pendulum on a cart dynamics, equation 5.4 becomes

$$\begin{aligned} &\left[\frac{\partial \Psi}{\partial x_1}, \frac{\partial \Psi}{\partial x_2}, \frac{\partial \Psi}{\partial x_3}, \frac{\partial \Psi}{\partial x_4} \right] g = 0 \\ &\left[\frac{\partial \Psi}{\partial x_1}, \frac{\partial \Psi}{\partial x_2}, \frac{\partial \Psi}{\partial x_3}, \frac{\partial \Psi}{\partial x_4} \right] \left[0, \frac{\xi}{c}, 0, \frac{\eta}{c} \right]^T = 0 \\ &\frac{\partial \Psi}{\partial x_2} \xi - \frac{\partial \Psi}{\partial x_4} \eta = 0 \end{aligned} \tag{5.5}$$

But it is difficult to find two linearly independent solution for partial differential equation on 5.5. Hence trying partial feedback linearization using an other form of $h(x)$ that yield higher relative degree is the best choice. This can be derived from normalized moment of inertia of the system. To do this start with stating the dynamic equation of inverted pendulum in standard form of $M(q)\ddot{q} + C(q, \dot{q})\dot{q} + G(q) = \tau$. The equation will be

$$\begin{bmatrix} m_c + m_p & m_p l \cos q_2 \\ m_p l \cos q_2 & m_p l^2 + I \end{bmatrix} \begin{bmatrix} \ddot{q}_1 \\ \ddot{q}_2 \end{bmatrix} + \begin{bmatrix} \dot{q}_1 \\ \dot{q}_2 \end{bmatrix}' \begin{bmatrix} 0 & 0 \\ 0 & -m_p l \sin q_2 \end{bmatrix} \begin{bmatrix} \dot{q}_1 \\ \dot{q}_2 \end{bmatrix} + \begin{bmatrix} -m_p g l \sin q_2 \\ 0 \end{bmatrix} = \begin{bmatrix} u \\ 0 \end{bmatrix} \tag{5.6}$$

Inertia matrix is not a function of q_1 hence q_1 is an external variable and q_2 is shape variable. This dynamic equation can be considered as second order under actuated mechanical system with second order constraint.
i.e.

$$m_{11}\ddot{q}_1 + m_p l\cos q_2\ddot{q}_2 - m_p l\sin q_2 = u \tag{5.7}$$

with constraint

$$\varphi(q,\dot{q},\ddot{q}) = m_p l\cos q_2\ddot{q}_1 + (m_p l^2 + I)\ddot{q}_2 - m_p gl\sin q_2 = 0 \tag{5.8}$$

To solve the problem the constraint should be holonomic i.e. there exist

$$h(q,\dot{q}) = \int \varphi(q,\dot{q},\ddot{q})\ dt \tag{5.9}$$

But there is no such $h(q,\dot{q})$, so the constraint is nonholonomic constraint which implies that the system is non-flat under actuated mechanical system. For non-flat under actuated mechanical system there is no control design technique proposed until now (It is an open research idea). Which will not be a solution to inverted pendulum on a cart stabilization problem.

The next step is to check whether dynamics of inverted pendulum on a cart has integrable normalized momentum. Using equation(3.3) and equation (3.4), the normalized momentum with respect to q_1 and q_2 is

$$\pi_1 = \dot{q}_1 + \frac{m_p l\cos q_2}{m_c + m_p}\dot{q}_2 \tag{5.10}$$

$$\pi_2 = \dot{q}_1 + \frac{m_p l^2 + I}{m_p l cos q_2}\dot{q}_2 \tag{5.11}$$

respectively. Then try to find $h(q)$ such that $\dot{h}(q) = \pi$ i.e $\nabla h(q)\dot{q} = \pi$

$$\begin{bmatrix} \frac{\partial h_1}{\partial q_1} & \frac{\partial h_1}{\partial q_2} \\ \frac{\partial h_2}{\partial q_1} & \frac{\partial h_2}{\partial q_2} \end{bmatrix} = \begin{bmatrix} 1 & \frac{m_p l\cos q_2}{m_c+m_p} \\ 1 & \frac{m_p l^2+I}{m_p l\cos(q_2)} \end{bmatrix} \begin{bmatrix} \dot{q}_1 \\ \dot{q}_2 \end{bmatrix} = \begin{bmatrix} \pi_1 \\ \pi_2 \end{bmatrix} \tag{5.12}$$

solving for$h_(q)$ and $h_2(q)$:

$$\begin{aligned} \frac{\partial h_1(q_1,q_2)}{\partial q_1} &= 1 \\ \int \partial h(q_1,q_2) &= \int \partial q_1 \\ h_1(q_1,q_2) &= q_1 + h_1(q_2) \\ \frac{\partial h_1(q_1,q_2)}{\partial q_2} &= \frac{\partial(q_1 + h_1(q_2))}{\partial q_2} \\ \frac{\partial h_1(q_1,q_2)}{\partial q_2} &= \frac{\partial h_1(q_2)}{\partial q_2} \end{aligned}$$

but;

$$\frac{\partial h_1(q_2)}{\partial q_2} = \frac{\partial h_1(q_1,q_2)}{\partial q_2} = \frac{m_p l\cos q_2}{m_c + m_p}$$

$$h_1(q_2) = \frac{1}{m_p + m_c} \int m_p l \cos q_2 \; dq_2$$
$$h_1(q_2) = \frac{-m_p l \sin q_2}{m_p + m_c}$$
$$\therefore h_1(q_1, q_2) = q_1 - \frac{m_p l \sin q_2}{m_c + m_p} \tag{5.13}$$

Using similar way,

$$h_2(q_1, q_2) = q_2 + \frac{m_p l^2 + I}{m_p l} \ln \mid \sec q_2 + \tan q_2 \mid \tag{5.14}$$

Since normalized momentum of inverted pendulum is integrable, it is possible to find coordinate transformation that result in change of control that partially linearize unactuated system. This change of coordinate is derived by solving for $\ddot{q}_1$ from (3.16) and replacing in equation (3.15) as follows:

$$\ddot{q}_1 = \frac{m_p g l \sin q_2 - (m_p l^2 + I)}{m_p l \cos q_2} \ddot{q}_2$$
$$m_{11} \left(\frac{m_p g l \sin q_2 - (m_p l^2 + I)}{m_p l \cos q_2} \ddot{q}_2 \right) + m_{12}(q_2)\ddot{q}_2 - m_p l \sin q_2 = u$$
$$\left[m_{12}(q_2) - \frac{m_{11} m_{22}}{m_{21}} \right] + m_{11} g \tan q_2 - m_p l \sin q_2 \dot{q}_2^2 = u \tag{5.15}$$

Thus selecting feedback control law

$$u = \left[m_{12}(q_2) - \frac{m_{11} m_{22}}{m_{21}} \right] + m_{11} g \tan q_2 - m_p l \sin q_2 \dot{q}_2^2 \tag{5.16}$$

will result in linear unactuated dyanmics

$$\dot{q} = p \tag{5.17}$$
$$\dot{p} = u \tag{5.18}$$

which is called nested saturation controller design technique. From this it can be understood that there exist

$$u = \alpha(q_2)u + \beta(q, \dot{q}) \tag{5.19}$$

noncollocated partial linearizing change of coordinate over domain of control signal ı.e.

$$U \in \{q_2 \in (Q_s) : \det m_{21}(q_2) \neq 0\}$$

As indicated on [3] change of coordinate

$$q_r = q_1 + \gamma(q_2) \tag{5.20}$$
$$p_r = m_{21}(q)\dot{q}_1 + m_{22}(q_2)\dot{q}_2 = \frac{\partial L}{\partial \dot{q}_2} \tag{5.21}$$

guarantee that strict feed-foward controller form can stabilize an inverted pendulum on a cart in the upper half plane. where

$$d\gamma(q_2) = m_{21}^{-1}(q_2) m_{22}(q_2) dq_2 \tag{5.22}$$

replacing for m_{21} and m_{22} with $m_p l \cos q_2$ and $m_{22} = m_p l^2 + I$ respectively in equation 5.22 and integrate the equation to solve for $\gamma(q_2)$

$$\gamma(q_2) = \frac{m_p l^2 + I}{m_p l} \ln \mid \sec q_2 + \tan q_2 \mid \tag{5.23}$$

Applying to inverted pendulum on a cart dynamics, the output $h(x)$ that yield minimum left over dynamics will be,

$$h(x) = x_1 + \frac{m_p l^2 + I}{m_p l} \ln \mid \sec x_3 + \tan x_3 \mid \tag{5.24}$$

the coordinate transform expression derived using this output is

$$T(x) = \begin{bmatrix} L_f^0 h(x) \\ L_f^1 h(x) \\ L_f^2 h(x) \\ L_f^3 h(x) \end{bmatrix} = \begin{bmatrix} \mu_1 \\ \mu_2 \\ \mu_3 \\ \mu_4 \end{bmatrix} \tag{5.25}$$

where

$$\begin{aligned} \mu_1 &= x_1 + \frac{m_p l^2 + I}{m_p l} \ln \mid \sec x_3 + \tan x_3 \mid \\ \mu_2 &= x_2 + l x_4^2 \sec x_3 \\ \mu_3 &= \tan x_3 (g + l x_4^2 \sec x_3) \\ \mu_4 &= (2 \sec^s x_3 - \sec x_3) l x_4^3 + (3g \sec^2 x_3 - 2g) x_4 - 2 x_4 \tan x_3 u \end{aligned} \tag{5.26}$$

By ignoring the term $-2x_4 \tan x_3 u$ in the last expression, the system can be partially input-state feedback linearized, with relative degree of $\rho = 4$. After applying this coordinate transformation the dynamics of inverted pendulum is transformed into

$$\begin{aligned} \dot{\mu}_1 &= \mu_2 \\ \dot{\mu}_2 &= \mu_3 \\ \dot{\mu}_3 &= \mu_4 \\ \dot{\mu}_4 &= f_e(x) + g_e(x) u \end{aligned} \tag{5.27}$$

where

$$\begin{aligned} f_e(x) = {} & (6 \sin x_3 \sec^4 x_3 - \sin x_3 sec^2 x_3) l^4 x_4 + 6g \sec^3 x_3 \sin x_3 x_4^2 + \\ & 3(2g \sin x_3 \sec^3 x_3 - g \sin x_3 \sec x_3) x_4 + (3g \sec^2 x_3 - 2g) g \frac{\sin x_3}{l} \\ g_e(x) = {} & -6 x_4^2 \sec^2 x_3 + 3 x_4^2 - 3g \frac{\sec x_3}{l} \end{aligned}$$

But this expression is complex to design adaptive law. Using known system parameter approximate feedback linearization coupled with sliding mode controller performance is reasonable as explained on references [2] and [38].

5.2 Adaptive Feedback Linearization based Stabilizing Controller (AFLSC) Design

Considering dynamics of inverted pendulum as two parallel separate subsystems, namely cart subsystem and pendulum subsystem, then applying the concept on 3.6. For cart subsystem,

$$\dot{x}_1 = x_2 \tag{5.28}$$

$$\dot{x}_2 = \frac{a}{c} + \frac{\xi}{c}u_1 \tag{5.29}$$

and

$$\dot{x}_3 = x_4 \tag{5.30}$$

$$\dot{x}_4 = \frac{b}{c} + \frac{\eta}{c}u_2 \tag{5.31}$$

for pendulum subsystem.

The new state is $y = [x_1 \quad x_2]^T$ for cart subsystem and $y = [x_3 \quad x_4]^T$ for pendulum subsystem. Then applying the concept explained in chapter 3 section 3.6 using feedback gain $F = [k_1, k_2]$ designed for linearized part. Which can is designed using linear Quadratic regulator (LQR). A design parameter Γ is 4 by 4 diagonal matrix, P_a and Q_a are 2 by 2 positive definite matrices. As indicated on [7] γ (diagonal elements of Γ matrix) can be any positive number that satisfy the criteria stated in section 3.6.
The reference model for both subsystem is same with

$$A = \begin{bmatrix} 0 & 1 \\ 0 & 0 \end{bmatrix} \quad B = \begin{bmatrix} 0 \\ 1 \end{bmatrix} \quad C = \begin{bmatrix} 1 & 0 \end{bmatrix}$$

$$\alpha_1(x) = \frac{\xi}{c} \quad \alpha_2(x) = \frac{\eta}{c}$$

$$\beta_1(x) = \frac{a}{c} \quad \beta_2(x) = \frac{b}{c}$$

For cart subsystem, feedback linearizing control signal is

$$\begin{aligned} u_1 &= \alpha_1^{-1}(x)(w_1 + \beta_1(x)) + u_{n1} \\ &= \frac{w_1((m_p + m_c)\xi) - (m_p l \cos x_3)^2 - \xi m_p l x_4^2 \sin x_3 + (m_p l)^2 g \sin x_3 \cos x_3}{\xi} \end{aligned} \tag{5.32}$$

and for pendulum subsystem, feedback linearizing control signal is

$$\begin{aligned} u_2 &= \alpha_2^{-1}(x)(w_2 + \beta_2(x)) + u_{n2} \\ &= \frac{w_2((m_p + m_c)\xi) - (m_p l \cos x_3)^2 - \xi m_p l x_4^2 \sin x_3 \cos x_3 + (m_p + m_c)(m_p l) g \sin x_3}{m_p l \cos x_3} \end{aligned} \tag{5.33}$$

where

$$w_1 = -Fy + r_{poss} \tag{5.34}$$

$$w_2 = -Fy + r_{ang} \tag{5.35}$$

are control signals for linearized subsystems with state matrix A and input matrix B. With this feedback linearization inputs signals the dynamic equation of each subsystem becomes,

$$\dot{y}_1 = y_2 \tag{5.36}$$
$$\dot{y}_2 = w_1 \tag{5.37}$$

for cart subsystem and

$$\dot{y}_1 = y_2 \tag{5.38}$$
$$\dot{y}_2 = w_2 \tag{5.39}$$

for pendulum subsystem.
Considering $\omega(t) = \omega^*(t)$,from (5.33) and (5.34)

$$\omega_1(t) = \begin{bmatrix} w_1 \\ -w_1 \cos^2 x_3 \\ -x_4^2 \sin x_3 \\ \sin x_3 \cos x_3 \end{bmatrix} \quad \omega_2(t) = \begin{bmatrix} w_2 \sec x_3 \\ -w_2 \cos x_3 \\ x_4^2 \sin x_3 \\ \tan x_3 \end{bmatrix} \tag{5.40}$$

The the estimate of system parameters are,

$$\theta_1(t) = \begin{bmatrix} m_p + m_c \\ \dfrac{(m_p l)^2}{\xi} \\ m_p l \\ \dfrac{(m_p l)^2}{\xi} g \end{bmatrix}^T = \begin{bmatrix} \theta_{11} \\ \theta_{12} \\ \theta_{13} \\ \theta_{14} \end{bmatrix}^T \quad \theta_2(t) = \begin{bmatrix} \dfrac{m_p + m_c}{m_p l} \\ m_p l \\ m_p l \\ (m_p + m_c) g \end{bmatrix}^T = \begin{bmatrix} \theta_{21} \\ \theta_{22} \\ \theta_{23} \\ \theta_{24} \end{bmatrix}^T \tag{5.41}$$

parametrizing a, b, c with estimate of system parameters,

$$a = \frac{\theta_{13}^2}{\theta_{12}} (\theta_{13} x_4^2 \sin x_3 - \theta_{14} \sin x_3 \cos x_3) \tag{5.42}$$
$$b = \theta_{23} (-\theta_{23} x_4^2 \sin x_3 \cos x_3 - \theta_{24} \sin x_3) \tag{5.43}$$
$$c = \theta_{13}^2 \left(\frac{\theta_{11}}{\theta_{12}} - \cos^2 x_3 \right) = \theta_{22} (\theta_{21} - \theta_{22} \cos^2 x_3) \tag{5.44}$$

and overall system control signal is

$$u(t) = \sigma(u_1 + u_2) \tag{5.45}$$

where σ is any positive number that adjust the gain of combined control signals. MATLAB script used to derive this control signal is shown on appendix B.
To design LQR controller for linearized system with state matrix A, input matrix B and output matrix C, Q matrix is selected as $C^T C$ and $R = 1$. The selection of Q and R has no effect on this system, since the reference model output is zero for very every state and LQR controller gain is used to multiply the state feedback of the reference model to determine the desired control signal w_1 and w_2 with are always zero(considering the reference angle of the pendulum and reference position of a cart to be zero). The effect can only seen on tracking problem[1](which is not the focus of this research)

[1]Tracking problem for IPC using AFLSC have not been done yet

Chapter 6

Simulation Results

6.1 Model validation and Natural dynamics of IPC

Simulation is performed using MATLAB/SIMULINK. An inverted pendulum system model shown on figure 6.1 is designed using SOLIDWORK software in order to incorporate the real features. The model is then exported to MATLAB/SIMULINK. Where it's is is checked before testing the performance of the controllers.

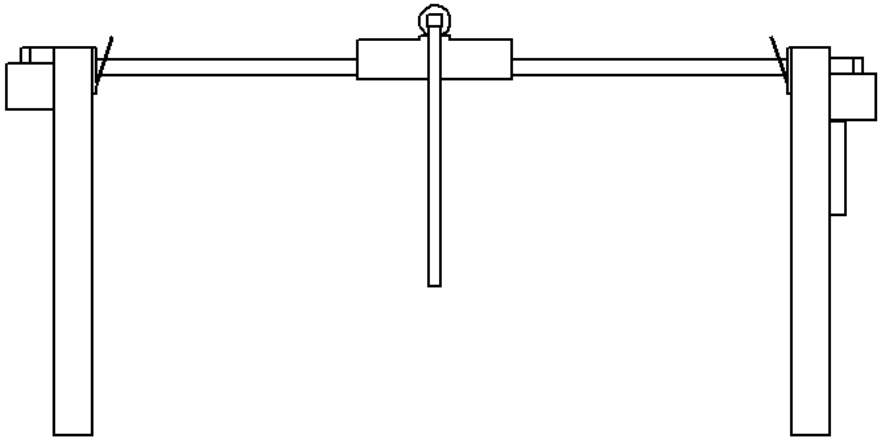

Figure 6.1: MATLAB/SIMULINK multibody imported from SOLIDWORKS

To test the validity of the model an impulse of 15 deg is applied to angle of the pendulum as disturbance when it is at it's upright position and allowed to naturally evolve over time. From figure 6.2 and 6.3, it is observed that the pendulum and the cart, start from an initial angle of 0 deg and 0 m respectively. The cart moves back and forth within a small displacement from origin until it comes to rest. The pendulum falls off from the upright position and keeps swinging back and forth about vertical line connecting the stable equilibrium point and unstable equilibrium point with decreasing amplitude until it comes to rest at it's pendant position. The pendulum is unstable in the upright position as it moves away from it. While it is stable at pendant position as it converges to it. This behavior is expected from a physical inverted pendulum plant with friction. Therefore this validates the model of the system.

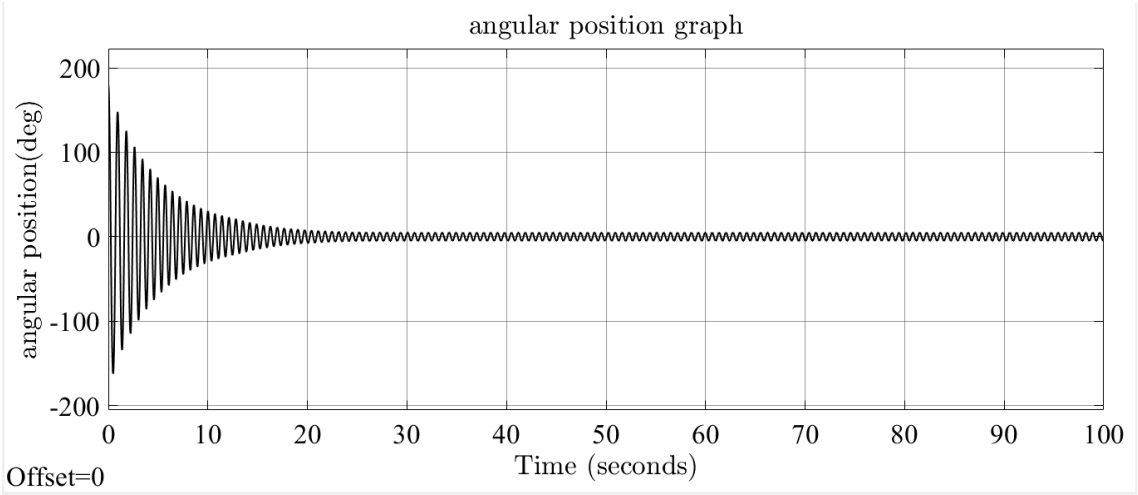

Figure 6.2: IPC pendulum angular position natural dynamics

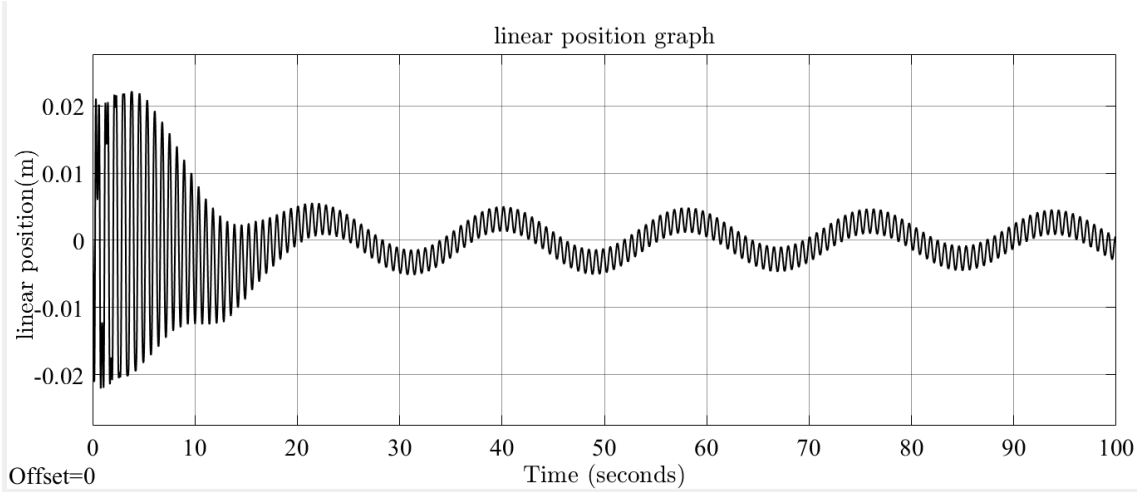

Figure 6.3: IPC cart linear position natural dynamics

6.1.1 Phase Portraits of IPC Natural Dynamics

Phase plane analysis is powerful tool in analysis of non linear system behavior [6]. Figure 6.4 and 6.5 shows phase portrait of an inverted pendulum system. The position subsystem has stable focus at $(x, 0)$. Linear position is a free variable i.e the equilibrium point of linear position can be anywhere as seen from figure 6.4. For simplicity in this case x_{eq} is taken to be 0. Similarly the angle subsystem has stable focus at $(\pi, 0)$ as indicated on figure 6.5.

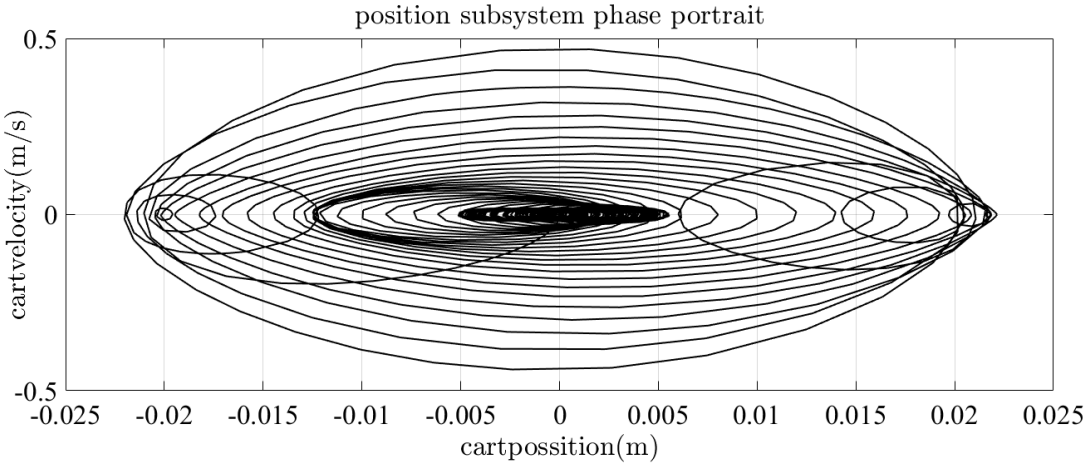

Figure 6.4: Cart subsystem natural dynamics phase portrait

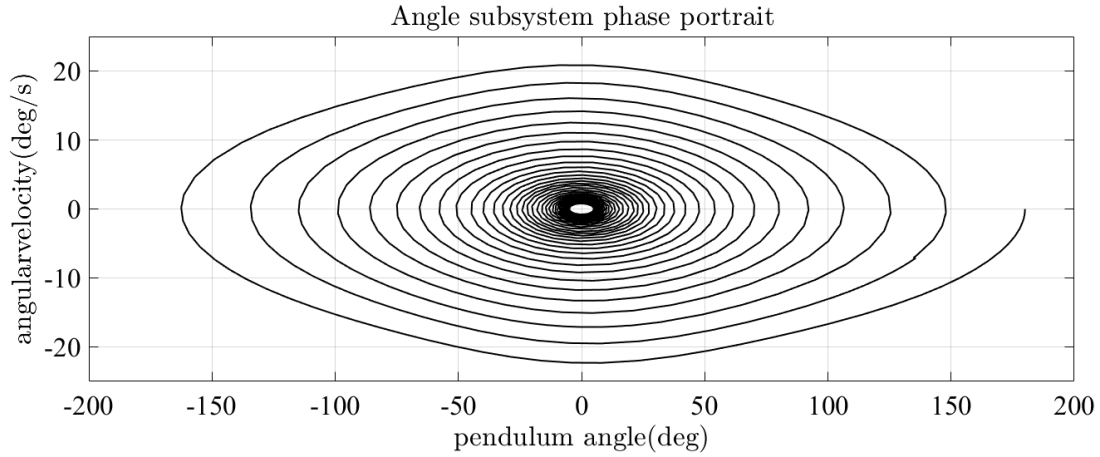

Figure 6.5: Pendulum subsystem natural dynamics phase portrait

6.2 Response of the System with AFLSC

The dynamics of overall system response with an adaptive feedback linearization based stabilizing controller depends on design parameters as indicated in chapter 4. The value of this design parameters have significant effect on system overall system. For some design parameters the dynamics may not converge i.e the dynamics of IPC are uncontrollable. Tuning of this parameters is very important in designing adaptive inverse control based on feedback linearization.

In this thesis the design parameters are tuned manually by looking at the response of the IPC system. From tuning of these parameters; Very large or very small values for matrix Q_a drives the system to instability range. Thus observing the response of the system the element wise selection range of matrix Q_a is summarized in table 6.1.

Table 6.1: Q_a matrix selection range

values	cart subsystem response	pendulum subsystem response
< 0.001	position out of range$[0-15]m$	smaller settling time
≥ 0.001 and < 0.1	position in range $[0-1]m$	small settling time
≥ 0.01	uncontrollable	uncontrollable

For this thesis the value of Q_a is

$$Q_a = \begin{bmatrix} 0.0045 & 0.0030 \\ 0.0030 & 0.0045 \end{bmatrix}$$

with eigenvalue

$$eig(Q_a) = \begin{bmatrix} 0.0010 \\ 0.0080 \end{bmatrix}$$

Solving lyapunov equation on 3.88, The value of P_a is

$$P_a = \begin{bmatrix} 0.0057 & 0.0045 \\ 0.0045 & 0.0064 \end{bmatrix}$$

with eigenvalue

$$eig(P_a) = \begin{bmatrix} 0.0015 \\ 0.0106 \end{bmatrix}$$

Other design parameters are selected in similar way, $\gamma = 240$ for cart subsystem and $\gamma = 12$ for pendulum subsystem. The elements of Γ matrix are also selected to be in range indicated on 3.6

$$\Gamma = \begin{bmatrix} 0.5 & 0 & 0 & 0 \\ 0 & 0.5 & 0 & 0 \\ 0 & 0 & 0.5 & 0 \\ 0 & 0 & 0 & 0.5 \end{bmatrix}$$

The value of σ greater than 25 will result in good response. For this thesis $\sigma = 250$. The initial condition and parameter projection function maximum and minimum range considered in this simulation are stated on table 6.2.

Table 6.2: Design parameters

parameter	initial condition	minimum value	maximum value
mass of cart	0.1 kg	0.02 kg	4 kg
mass of pendulum	0.01 kg	0.002 kg	4 kg
length of pendulum	0.1 m	0.1 m	0.7 m

Table 6.3: Physical constraints

parameter	value
linear friction coefficient	0.1 N/m
angular friction coefficient	0 rad/s
linear damping coefficient	0.01 N/(m/s)
angular damping coefficient	0.00025 rad/(m/s)
gravitational acceleration	9.81 m/s^2

The physical constraints used for simulation are stated in table 6.3.

Using these parameters; the performance of the controller is tested usig different pendulum mass and cart mass for standard $0.3m - 0.4m$ pendulum rod. For pulse signal having amplitude of 15 $deg = 0.2618$ rad added to angle of the system at $t = 1sec$ as shown on figure 6.6.

The results under this disturbance are shown below. Figures 6.7 shows the result

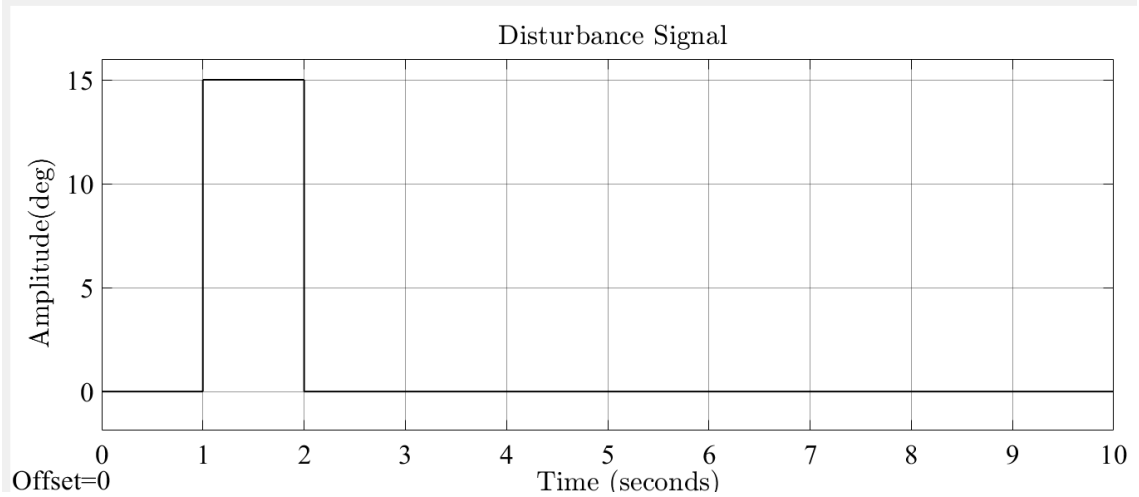

Figure 6.6: Disturbance signal

of cart positions under different values of pendulum mass, with constant value of cart mass and figure 6.10 shows responses of the cart position under different values of cart mass with constant value of pendulum mass. While figure 6.8 shows angular position responses of a pendulum with constant value of cart mass with different values of pendulum mass. Figure 6.11 shows responses of angular position of a pendulum for constant value of pendulum mass with different values of cart mass. The control signal generated by AFLSC is feed as voltage source to DC motor

which generate a required force to drive the cart. The force signals generated under different values of cart mass and constant value of pendulum mass are shown on figure 6.12 and those signals generated for different values of pendulum mass with constant value of cart mass are shown on figure 6.9.

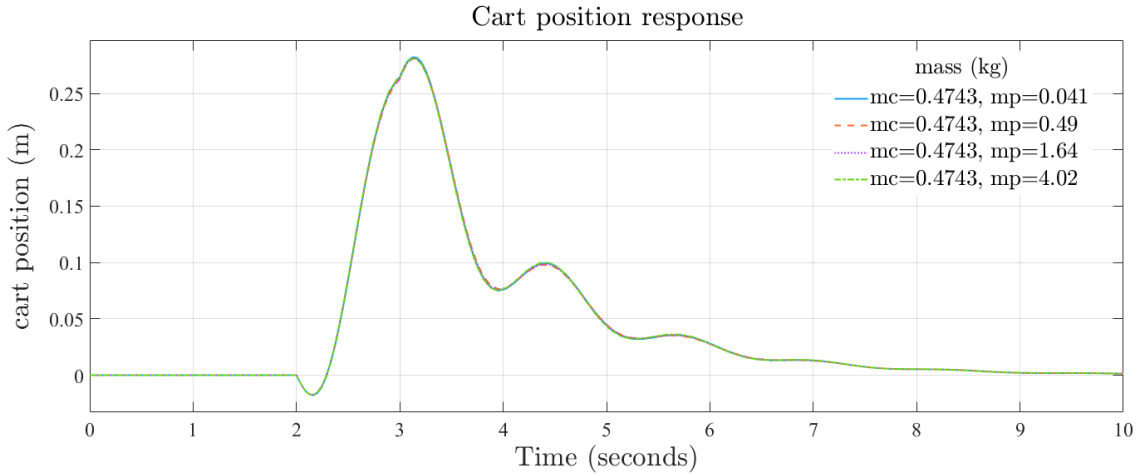

Figure 6.7: Cart position response with different values of m_p

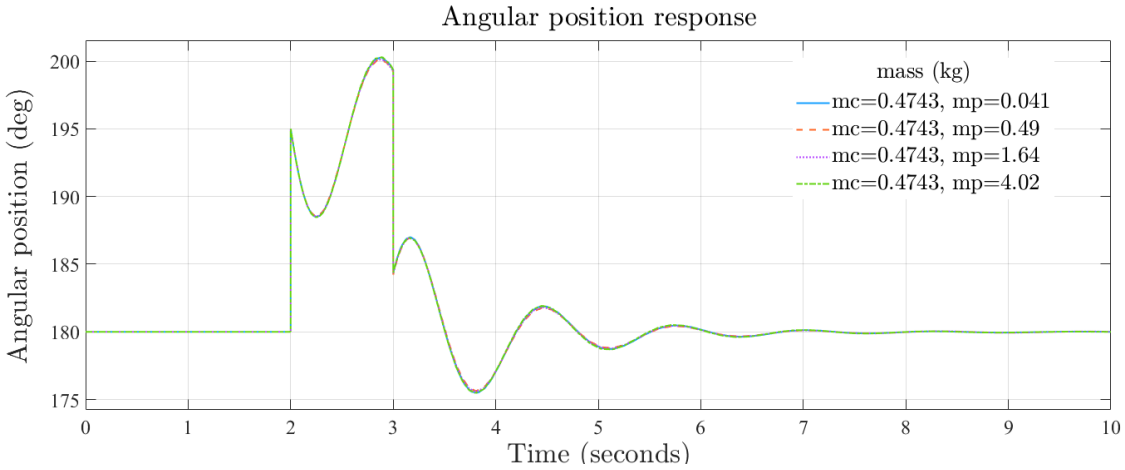

Figure 6.8: Pendulum position response with different values of m_p

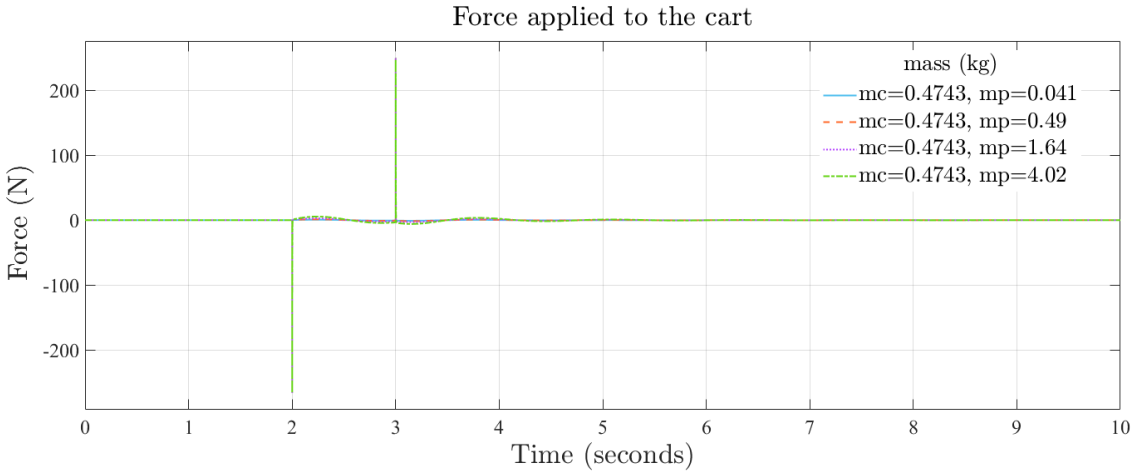

Figure 6.9: Force applied to a cart with different values of m_p

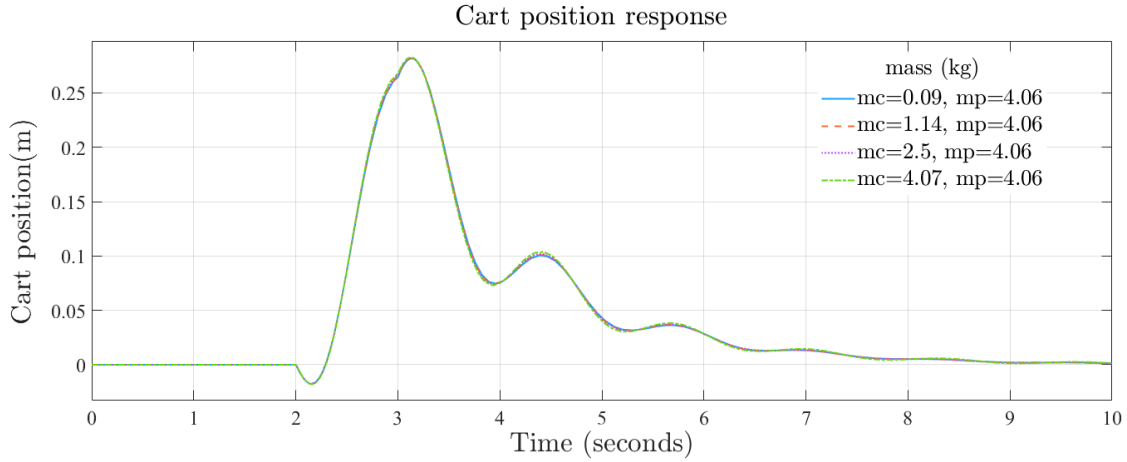

Figure 6.10: Cart position response with different values of m_c

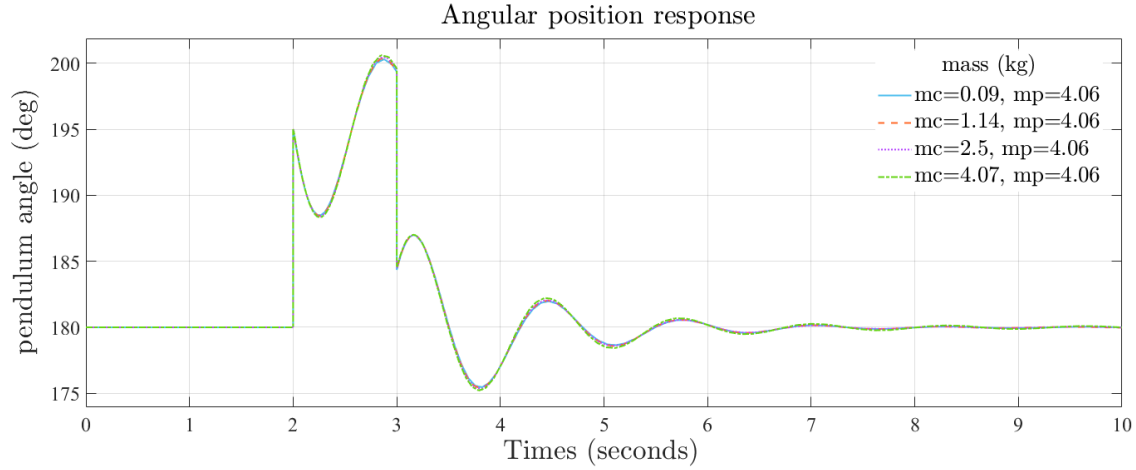

Figure 6.11: Pendulum position response with different values of m_c

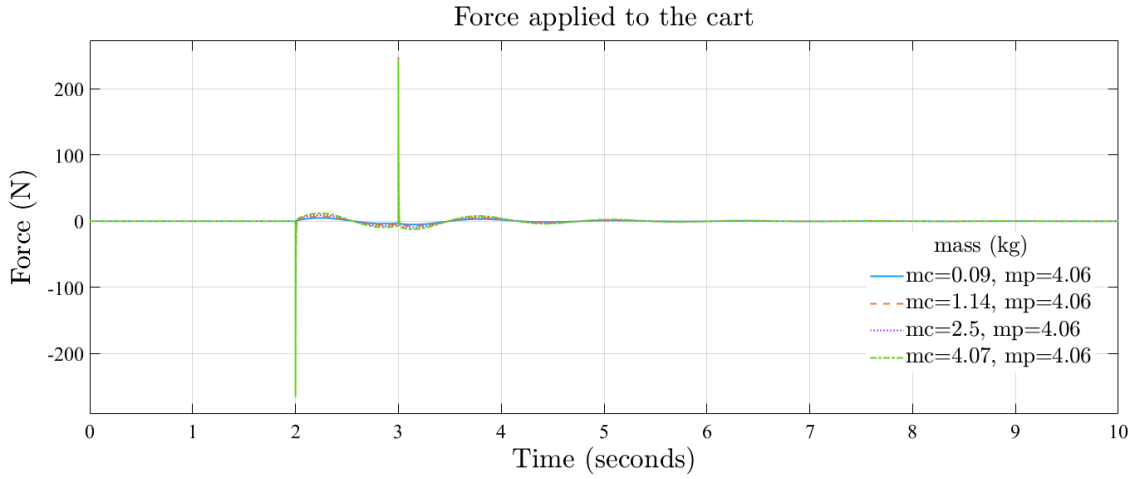

Figure 6.12: Force applied to a cart with different values of m_c

6.2.1 IPC Phase Portraits with AFLSC

The phase portraits of the overall system are shown on figure 6.13 for cart subsystem for different values of pendulum mass with constant value of cart mass and figure 6.15 cart subsystem for different values of cart mass with constant value of pendulum mass. Figure 6.14 shows phase portraits of pendulum subsystem for different values of pendulum mass with constant value of cart mass, where figure 6.16 shows phase portraits of pendulum subsystem for different values of cart mass with constant value of pendulum mass. From this results, it can be concluded that the controller changes the unstable saddle equilibrium point $(0, 0, \pi, 0)$ to stable focus for different values of cart mass and pendulum mass in the range shown on table 6.2.

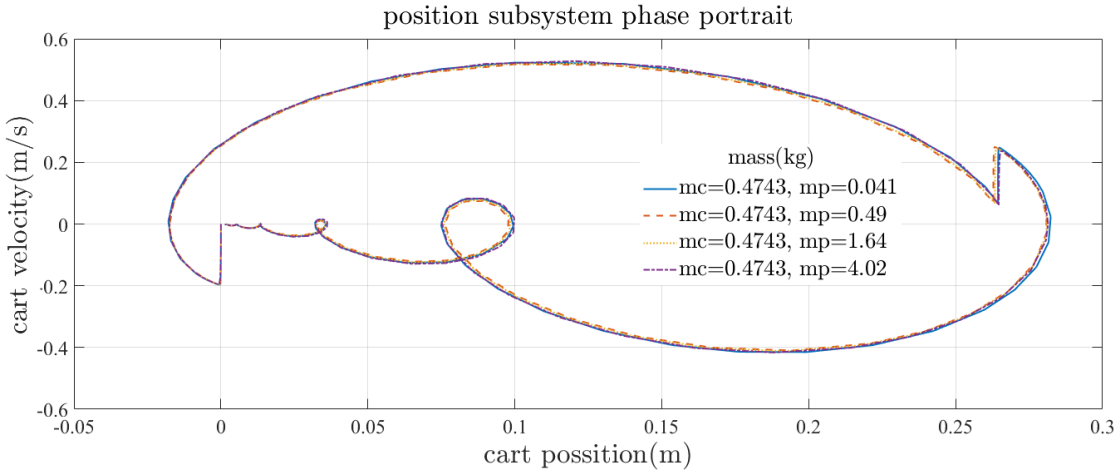

Figure 6.13: Cart subsystem phase portraits with different values of m_p

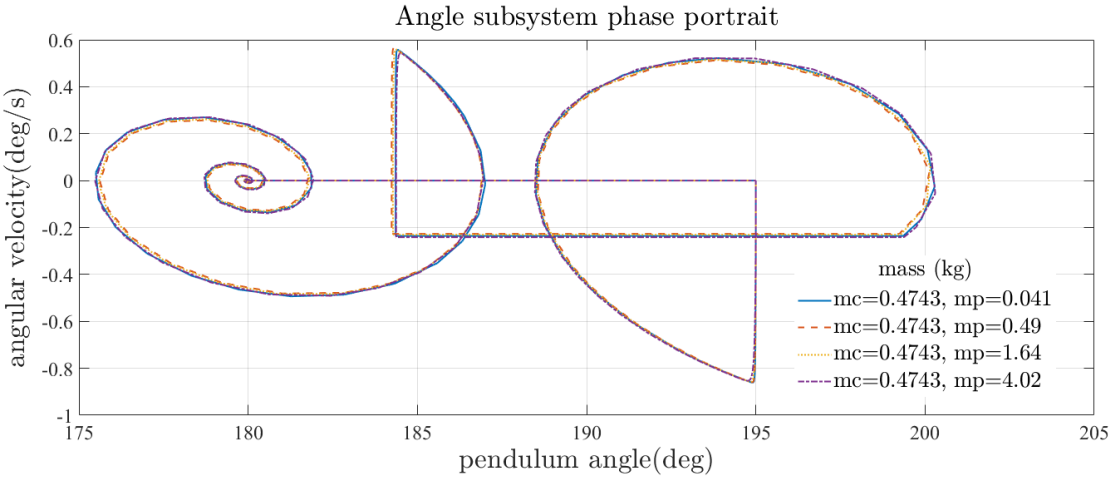

Figure 6.14: Pendulum subsystem phase portraits with different values of m_p

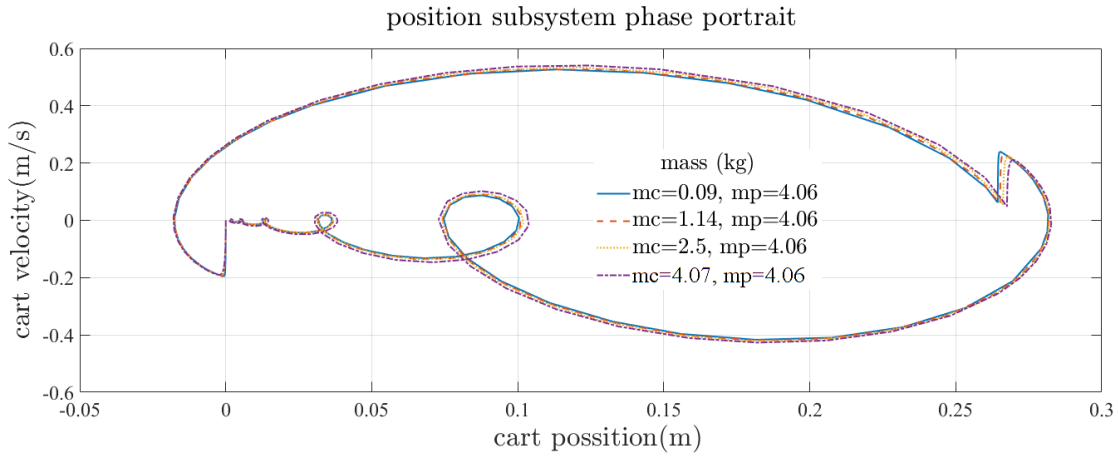

Figure 6.15: Cart subsystem phase portraits with different values of m_c

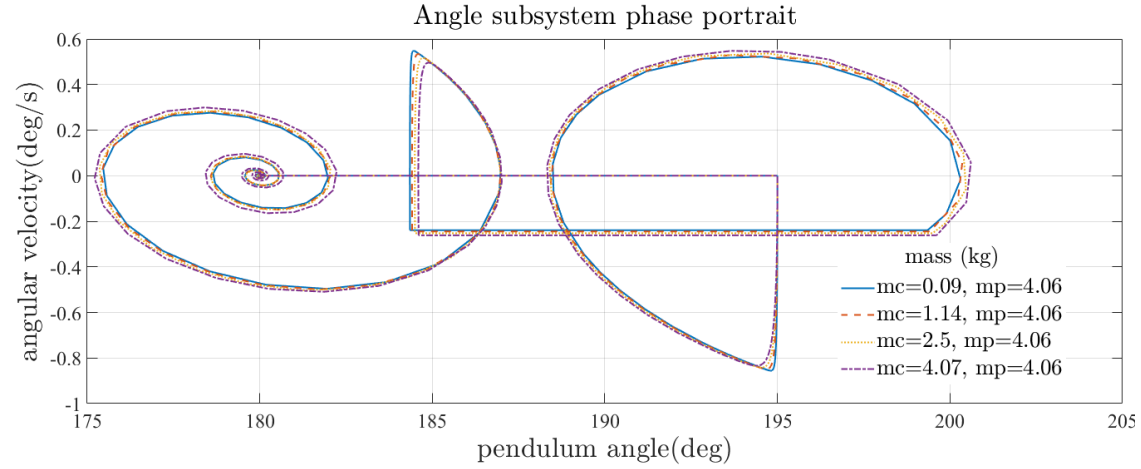

Figure 6.16: Pendulum subsystem phase portraits with different values of m_c

6.3 Response of the System with AFLSC and AFLSUC

Using the same system parameters and the same constraints, The performance of AFLSC with AFLSUC is evaluated using MATLAB/SIMULINK simulation. Even-though controllers adapt for standard pendulum for mass of pendulum between $0.01kg$ up to $4kg$ and $0.1kg$ up to $4kg$ mass of a cart. The output gain of AFLSUC control signal should be selected properly. The designer can select this gain trivially by looking at the cart. If it is big select big value, if it is small select small value. In this thesis output gain $k = 6$ is selected for small cart and output gain $k = 12$ is selected for big cart. After selecting the output gain the controller adapt to mass of the cart up to 4 times its initial mass and 10 times initial mass of the pendulum.

Figures 6.17 and 6.20 shows the response of the cart position for the overall system with different values of pendulum mass having constant value of cart mass. While figure 6.18 and 6.21 shows the response of pendulum angle with same case with fuzzy logic controller output gain $k = 6$ and $k = 12$ respectively. For constant value of pendulum mass with different cart mass responses of the cart position are shown on figure 6.23 and 6.26, where figure 6.24 and figure 6.27 shows responses of pendulum angular position with fuzzy logic controller output gain $k = 6$ and $k = 12$ respectively.

The force applied to the cart are shown on figure 6.19 and figure 6.25 for $k = 6$. For $k = 12$ the force applied to the cart are shown on figure 6.22 and figure 6.28.

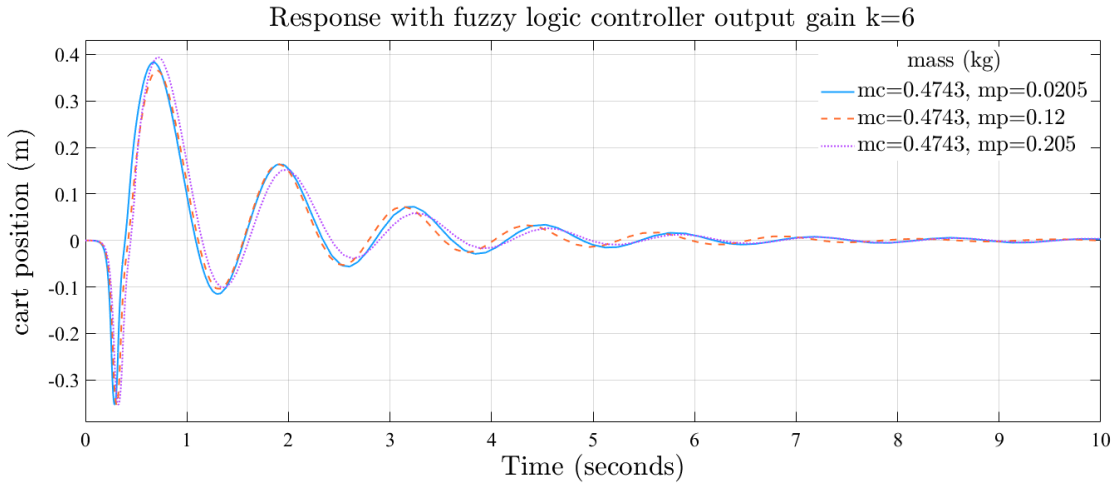

Figure 6.17: Cart position response with different values of m_p for $k = 6$

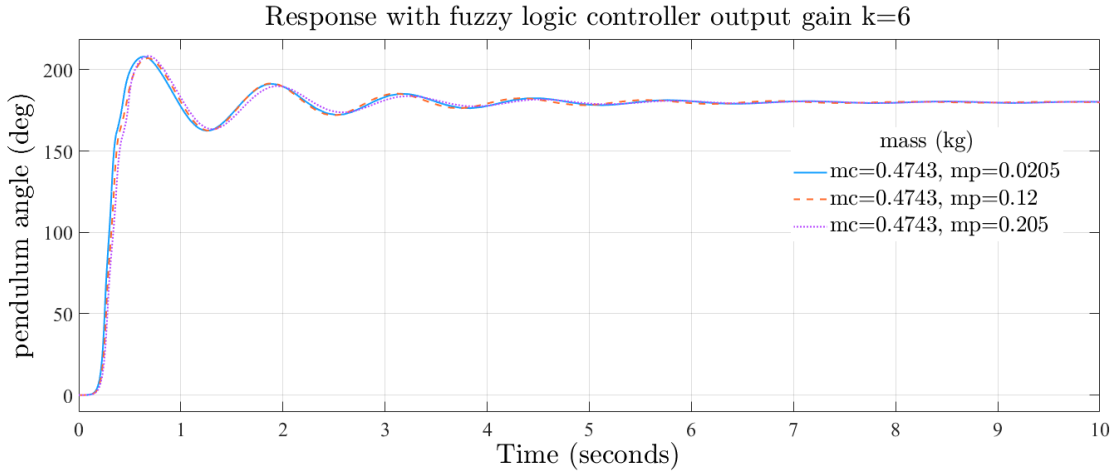

Figure 6.18: Pendulum position response with different values of m_p for $k = 6$

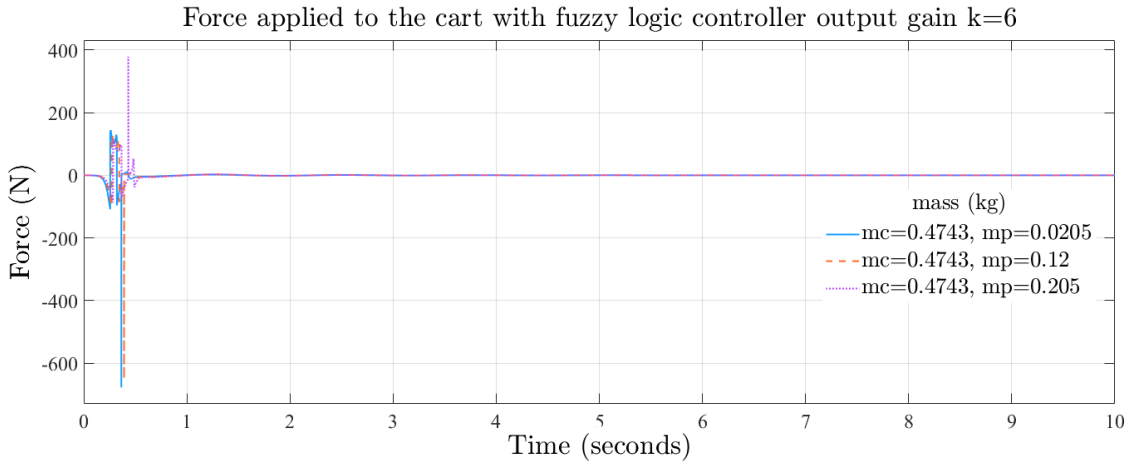

Figure 6.19: Force applied to a cart with different values of m_p for $k = 6$

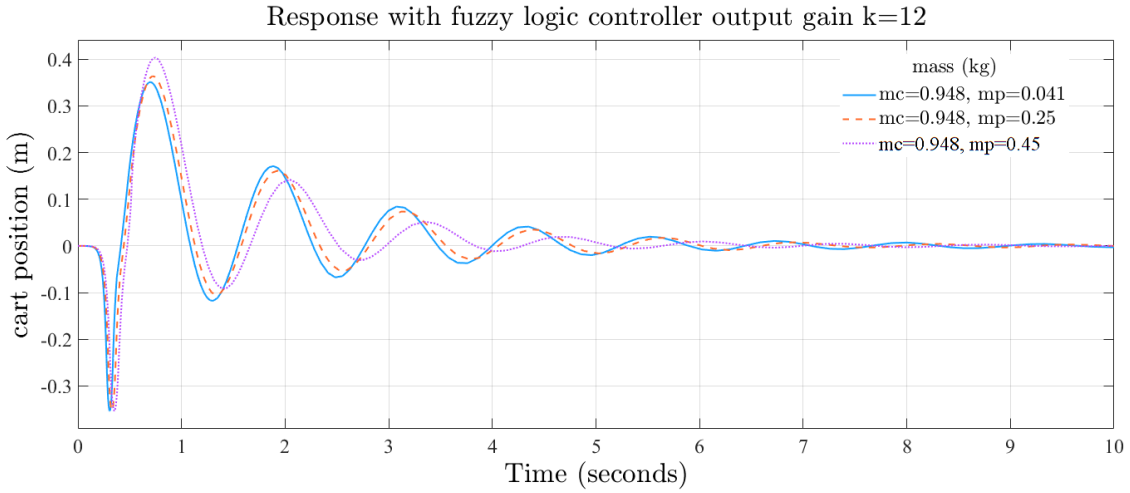

Figure 6.20: Cart position response with different values of m_p for $k = 12$

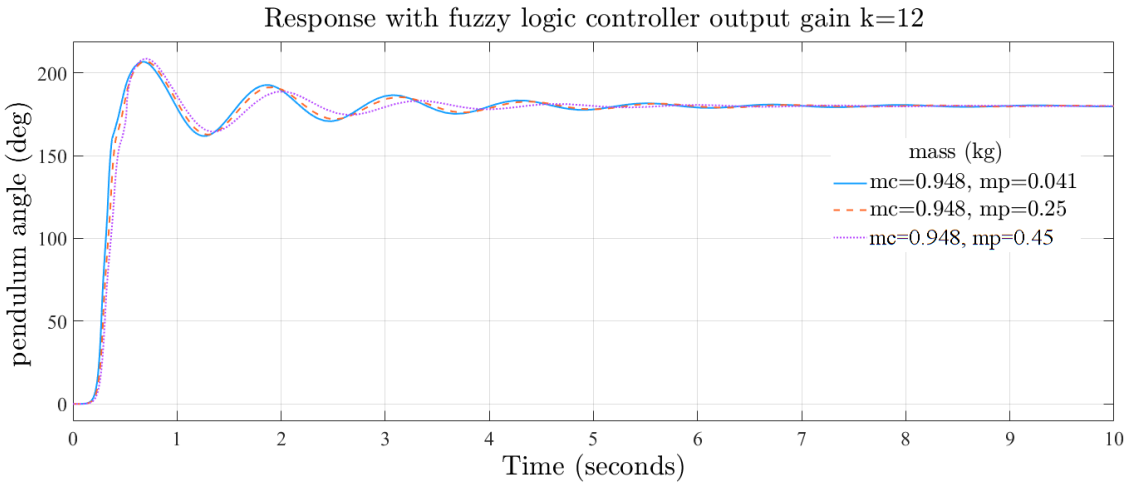

Figure 6.21: Pendulum position response with different values of m_p for $k = 12$

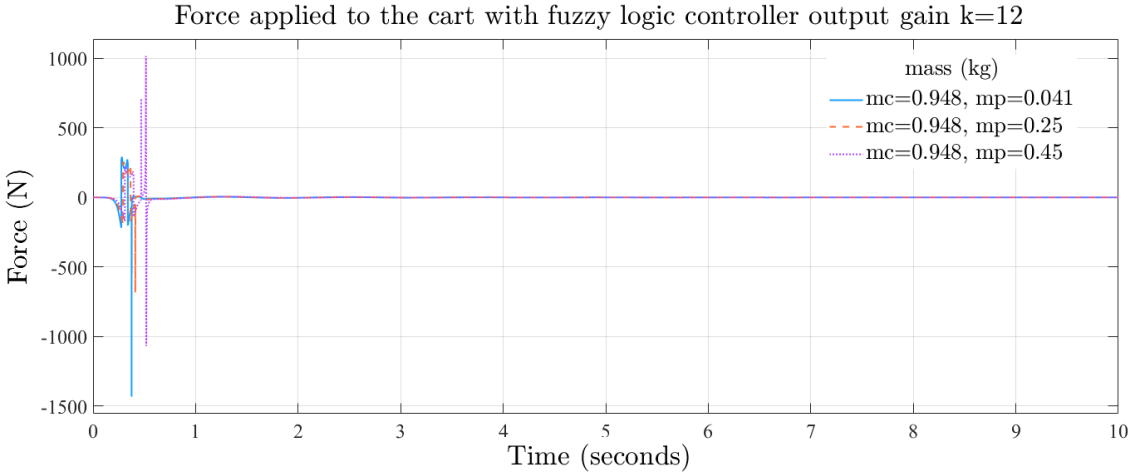

Figure 6.22: Force applied to a cart with different values of m_p for $k = 12$

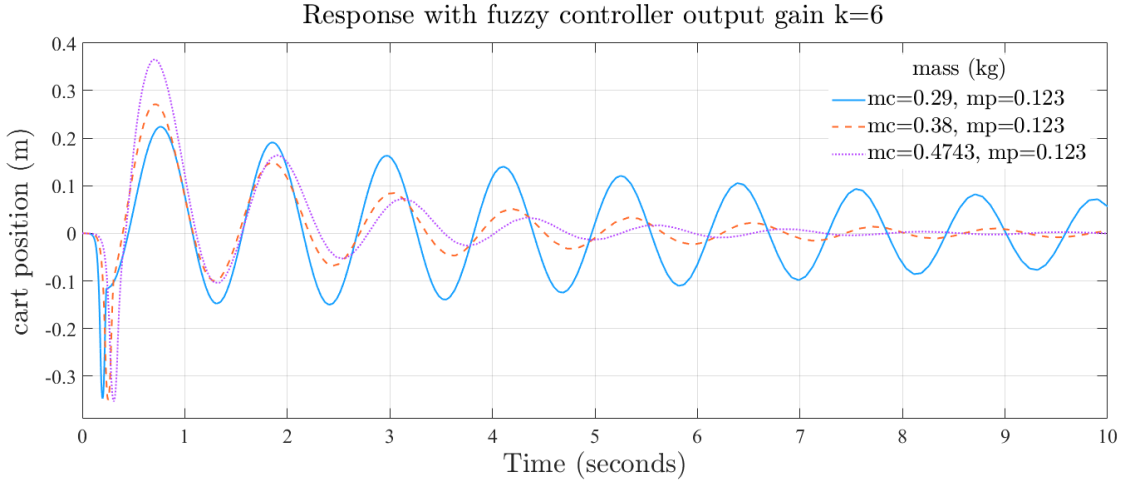

Figure 6.23: Cart position response with different values of m_c for $k = 6$

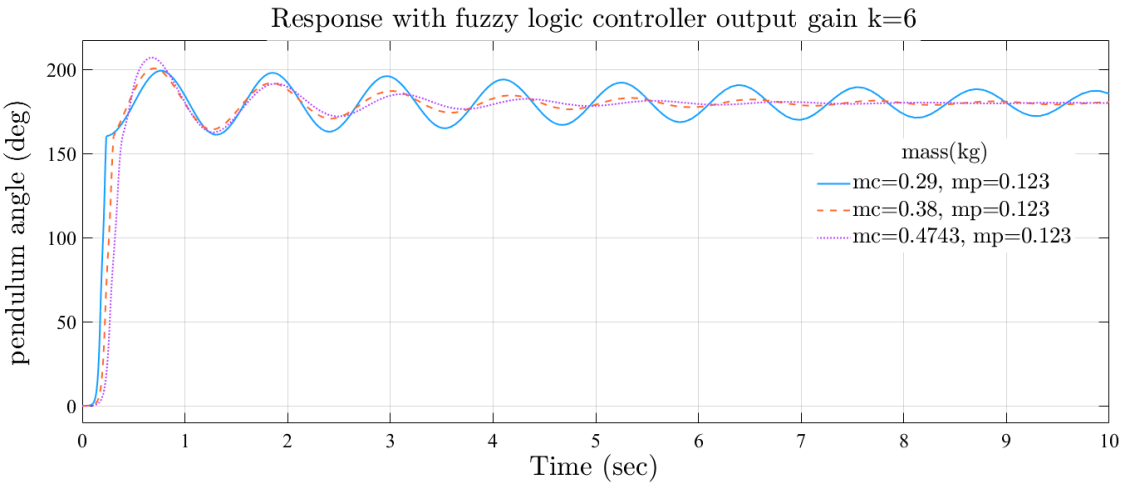

Figure 6.24: Pendulum position response with different values of m_c for $k = 6$

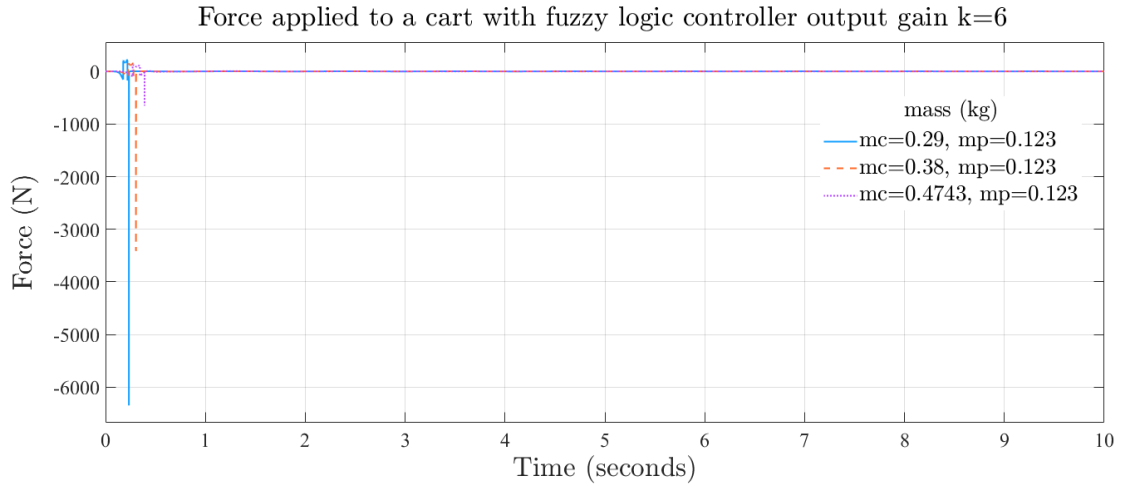

Figure 6.25: Force applied to a cart with different values of m_c for $k = 6$

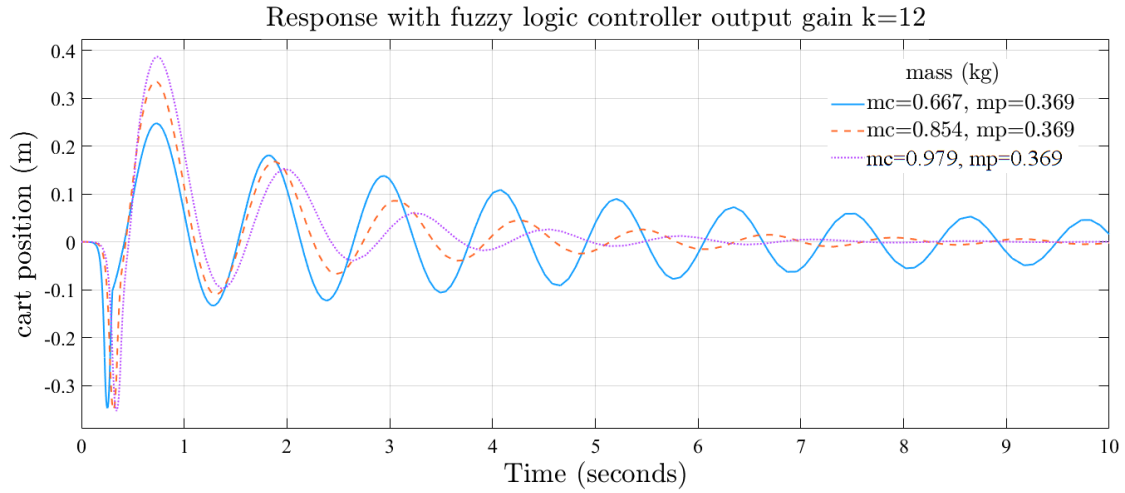

Figure 6.26: Cart position response with different values of m_c for $k = 12$

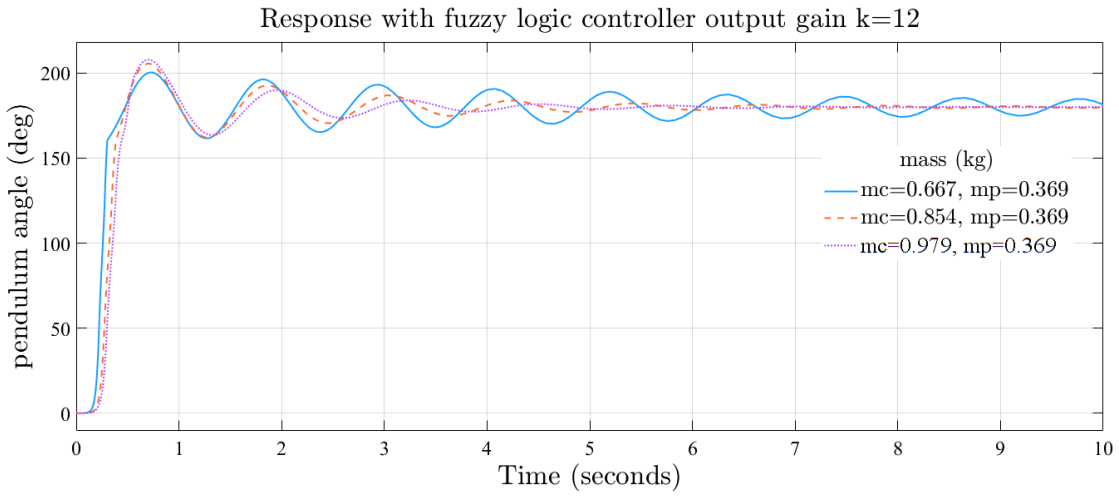

Figure 6.27: Pendulum position response with different values of m_c for $k = 12$

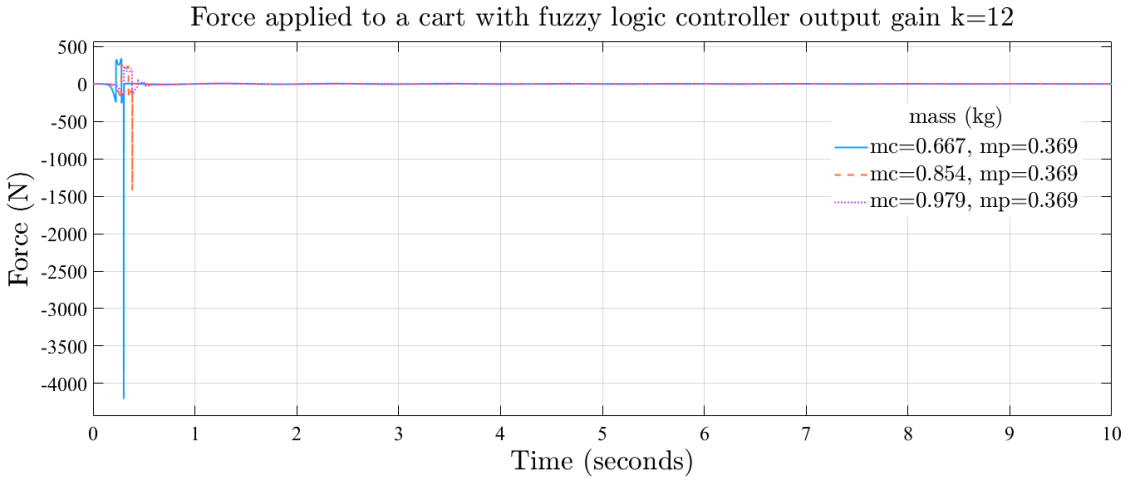

Figure 6.28: Force applied to a cart with different values of m_c for $k = 12$

6.3.1 IP Phase Portraits with AFLSC and AFLSUC

The cart subsystem phase portraits of the combined controller for different value of pendulum mass are shown on figure 6.29 for fuzzy logic controller output gain $k = 6$ and 6.31 for $k = 12$. The respective pendulum subsystem phase portraits are shown on figure 6.30 for $k = 6$ and figure 6.32. For the case of different value of cart mass the cart subsystem phase portraits are shown on figure 6.33 for $k = 6$ and figure 6.35. While their respective pendulum subsystem phase portraits are shown on figure 6.34 for $k = 6$ and figure 6.36.

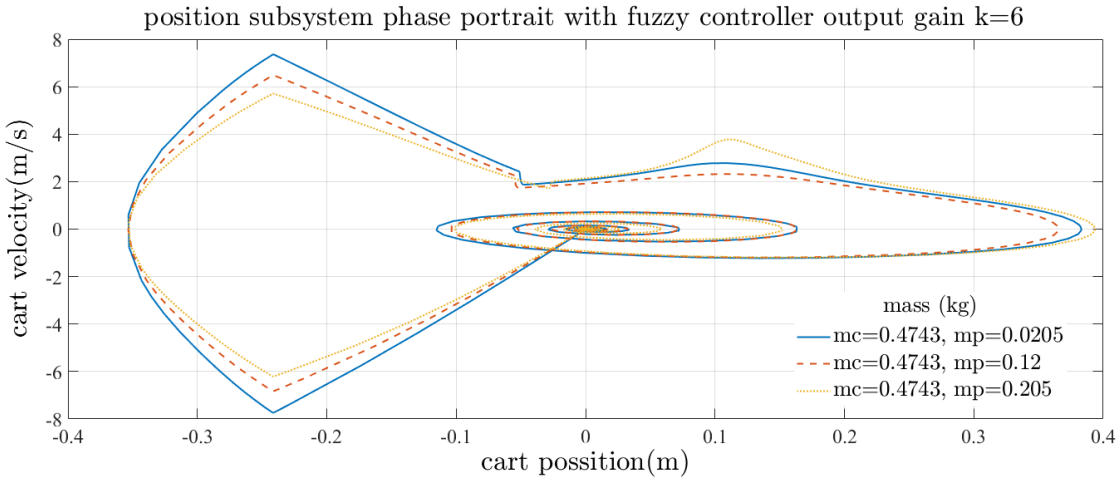

Figure 6.29: Cart subsystem phase portraits with different values of m_p for $k = 6$

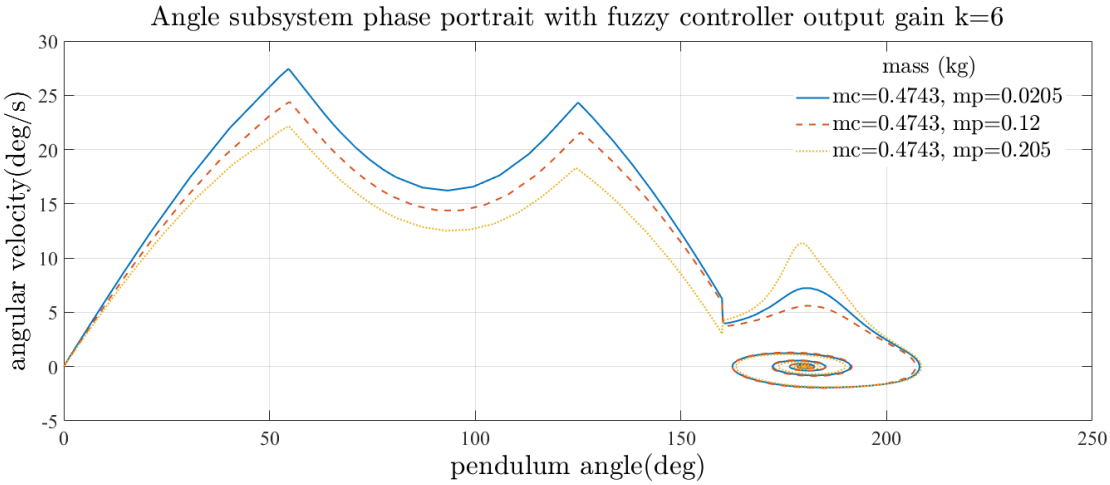

Figure 6.30: Pendulum subsystem phase portraits with different values of m_p for $k = 6$

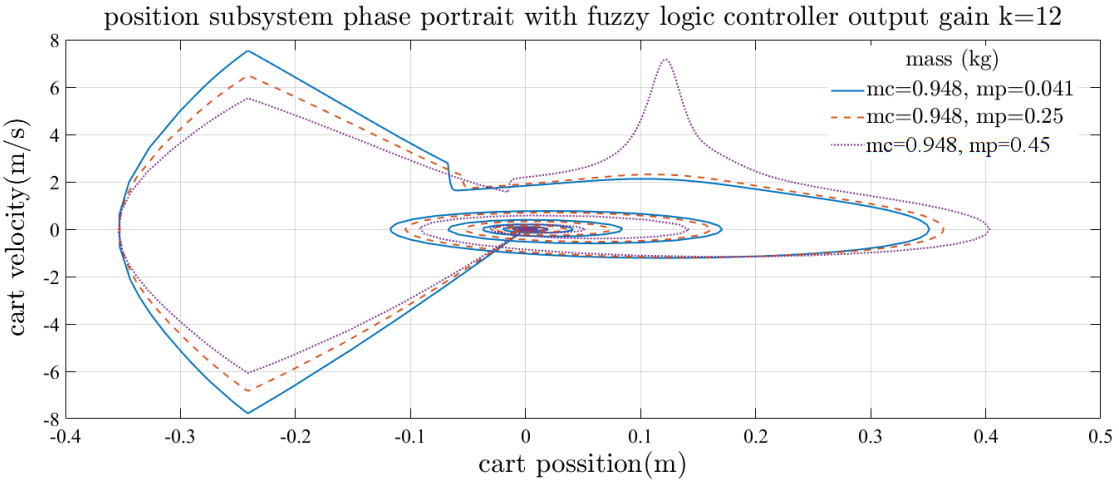

Figure 6.31: Cart subsystem phase portraits with different values of m_p for $k = 12$

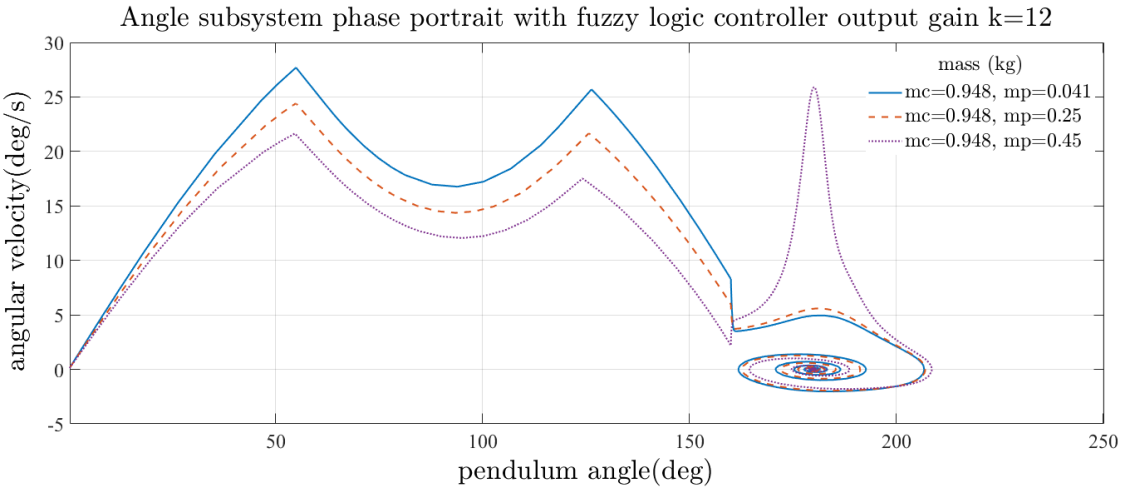

Figure 6.32: Pendulum subsystem phase portraits with different values of m_p for $k = 12$

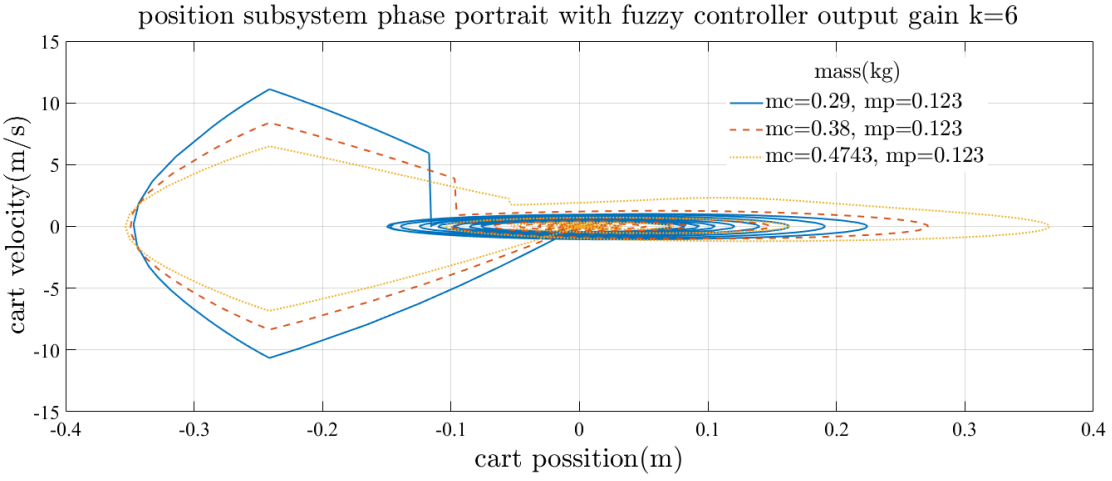

Figure 6.33: Cart subsystem phase portraits with different values of m_c for $k = 6$

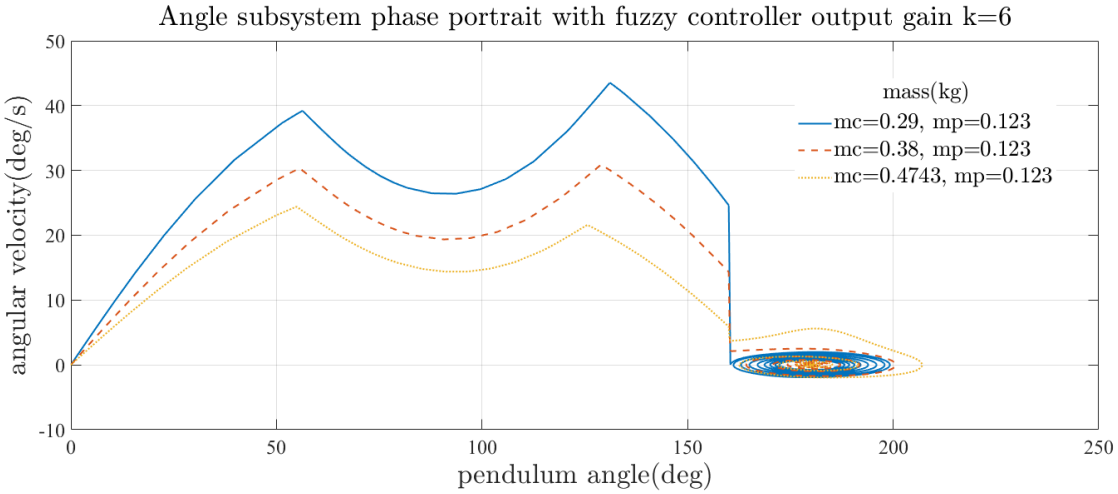

Figure 6.34: Pendulum subsystem phase portraits with different values of m_c for $k = 6$

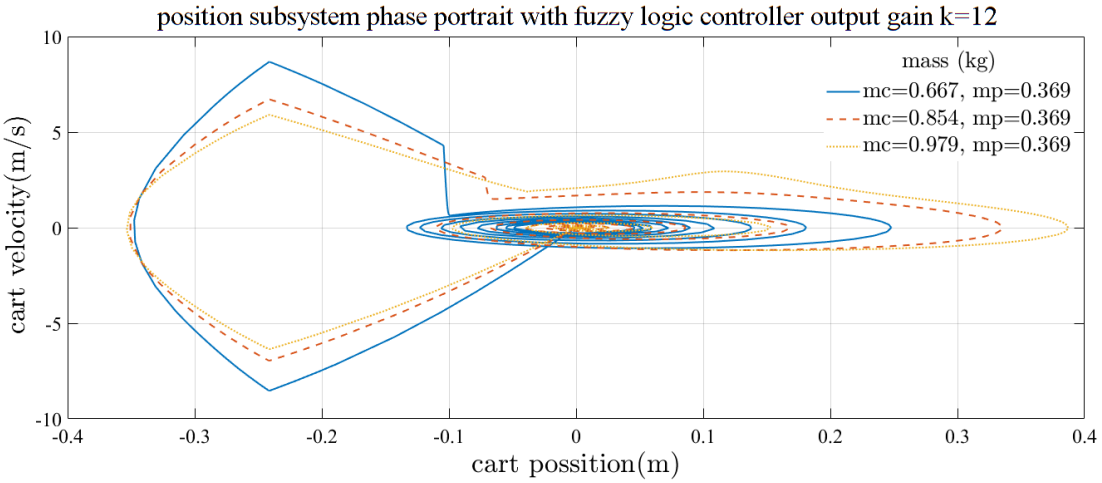

Figure 6.35: Cart subsystem phase portraits with different values of m_c for $k = 12$

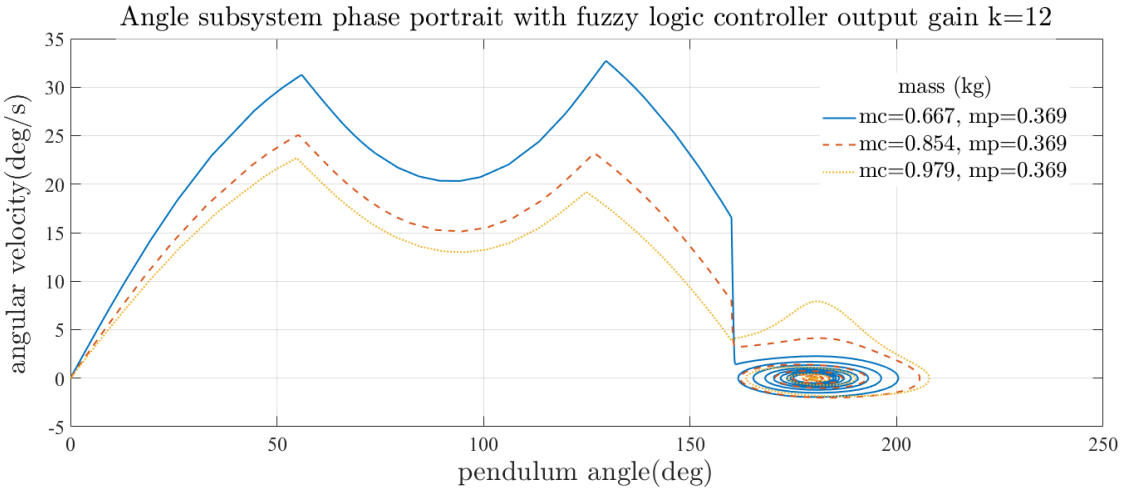

Figure 6.36: Pendulum subsystem phase portraits with different values of m_c for $k = 12$

These phase portraits shows that the controllers changes the unstable equilibrium point$(0, 0, \pi, 0)$ to stable focus. The peaks that appear near $(0, 0, \pi, 0)$ on the phase portraits shows incapability of AFLSUC in driving the pendulum from pendant position to vicinity of its inverted position without changing the controller's output multiplier gain k. This due to the reason that AFLSUC is unable to adapt to the whole range of system parameters shown on table 6.2.

Chapter 7

Hardware Setup and Experimentation Results

7.1 Integrated Hardware Setup Description

The setup is located in the control laboratory at Addis Ababa Institute of Technology, Addis Ababa University and is depicted in figure 7.1. The laboratory setup is prepared from printing machine abandoned by the university for long time. It is arranged and developed in such a way that it suits for this application with the help of Mechanical and Industrial engineering department of laboratory.

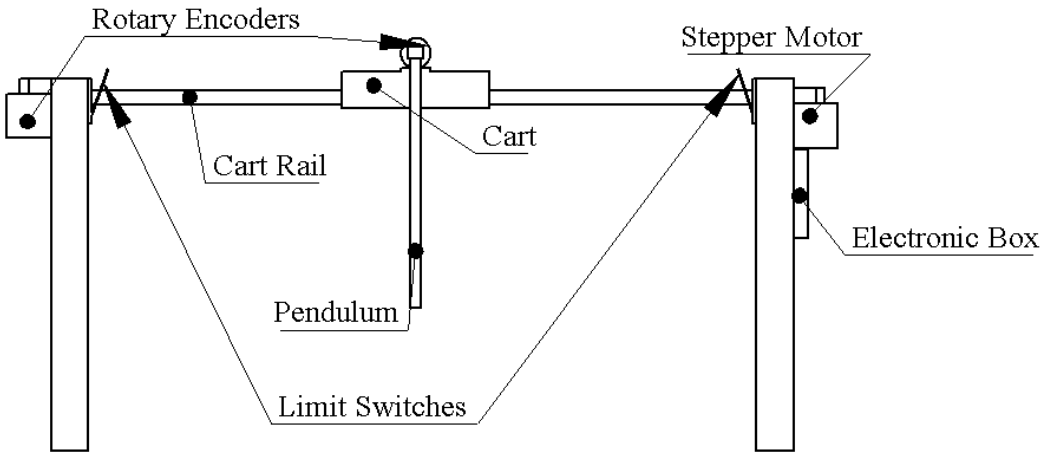

Figure 7.1: Integrated system hardware setup description

The hardware setup consists of a pendulum attached to a cart. The cart is attached to the rail, and is able to move horizontally. A belt connects the cart to the pulleys at each end of the rail. The pulley at the right side is mounted on shaft of stepper motor, which effectively drives the cart. The pulley on the other end is mounted on shaft of incremental rotary encoder. This incremental rotary encoder measure the cart position.
The incremental rotary encoder used in this thesis hardware experimentation has a resolution of 400 pulse per revolution(PPR). Which shows that the total pulse

generated for both channel of the encoder is 1600 pulses(for detail operation of Incremental rotary encoder see [39]).
To determine the linear position of the cart the number of pulses generated over maximum rail length is counted first. The maximum rail length is $0.85m$ then for any count the conversion to rail length in meters m is

$$x_1 = \frac{Number\ of\ pulse\ counted}{number\ of\ pulse\ counted\ for\ maximum\ rail\ length} maximum\ rail\ length$$

The pendulum consists of a light metal rod attached to incremental optical rotary encoder,which is used to measure the angular displacement of the pendulum and angular velocity of the pendulum. The angular position of the pendulum is determined as,

$$x_3 = 2\pi \frac{Number\ of\ pulse\ counted}{1600}$$

Linear velocity of the cart and angular velocity of the pendulum are taken as time derivative of cart position and angular position of the pendulum respectively as shown in code used for hardware experimentation on appendix E.

The Electronic box on 7.1 symbolises the electronics of the setup, which includes stepper motor, motor driver IC(L298N motor drive), an Arduino and power supply unit. The two incremental rotary encoder are connected to arduino hardware interrupt pins. Arduino Mega2560 is suitable for this hardware experimentation, as it has six pins to read external interrupts.

The code for AFLSC is changed in a way that it is suitable for implementation on arduino to test the performance of the controller. Thus arduino can process the computation standalone. But since the result of the hardware experimentation is required the data is sent to laptop to analyze it using virtual oscilloscope. The virtual oscilloscope is called Serialplot[1]. Regarding AFLSUC the computation on MATLAB/SIMULINK is possible. Adapting the controller code to arduino code was unsuccessful. The reasons are stated in chapter 8 section 8.2.

A DC voltage source of magnitude $12V$ is applied to the stepper motor. There are two mechanical toggle switches at each end of the rail, when the cart reaches at these positions it switch off the voltage source. It is possible to monitor it using soft-computation but, if the cart it at high speed it is not possible to stop it. The encoder need a DC voltage source of magnitude $5V$ to operate, which voltage applied to them from arduino Mega2560 board. To read the count of the encoders, encoder library (Encoder.h[2]) is used. While for stepper motor control internal arduino library is used. The overall block diagram representation of the system is shown on figure 7.3. As indicated in the code on appendix E, the control command applied to the stepper motor is position. The pendulum is driven to it's inverted position manually. When the pendulum reaches in the range $(\pi - \frac{\pi}{9}, \pi + \frac{\pi}{9})$ AFLSC will be switched on to stabilize the pendulum at its unstable point.

[1]Serialplot is a free software to plot and analyze data from serial port, which can be downloaded from https://hackaday.io/project/5334-serialplot-realtime-plotting-software

[2]Encoder.h library is downloaded from https://www.arduinolibraries.info/libraries/encoder

Figure 7.2: Hardware setup for Experimentation

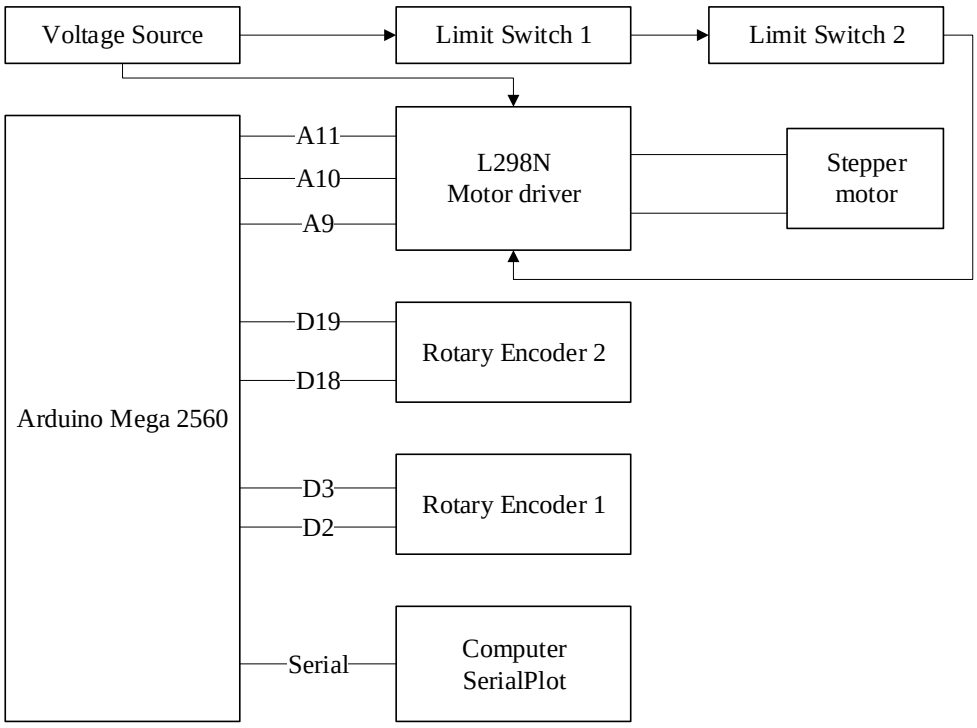

Figure 7.3: Electrical circuit block diagram representation

7.2 Experimentation Result

7.2.1 Hardware setup validation

Before testing AFLSC the validation of the developed hardware is tested. The result of the angular position of the pendulum under no control action is shown on figure 7.4 and response of the cart position is shown on figure 7.5. The angular friction of rotary encoder is negligible, which can be inferred from the figure. This validates the assumption used used during mathematical model development in chapter 3 section 3.3. Linear bearing is used to minimize the friction between the cart and the

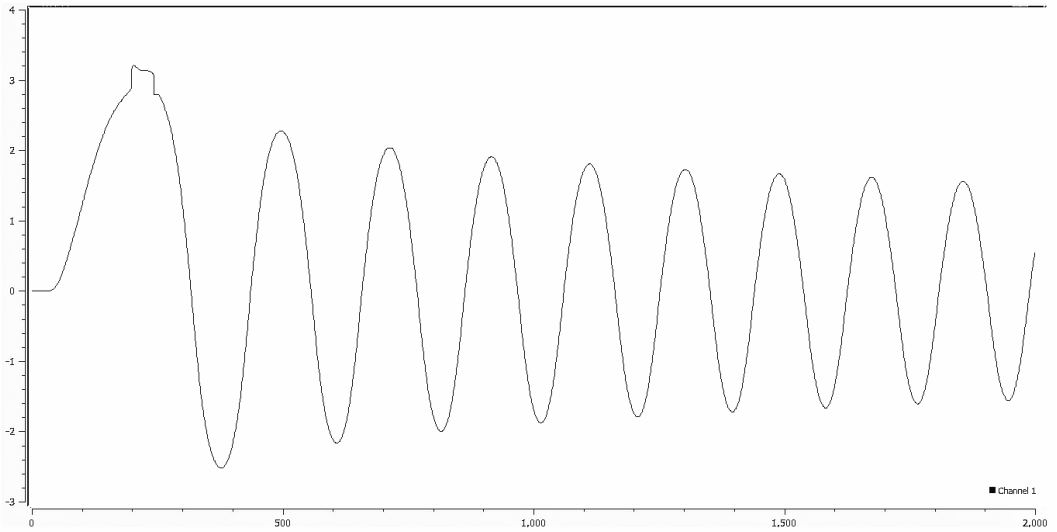

Figure 7.4: Pendulum angular position natural dynamics

rail. But still the friction is significant. This can be understood from the position response of the cart. If it was small the cart angular position response will look like sinusoidal wave form as on on figure 6.2. Since the controller is adaptive it should have overcome this problem, and it does. Hence the hardware setup is valid for testing the stabilizing controller.

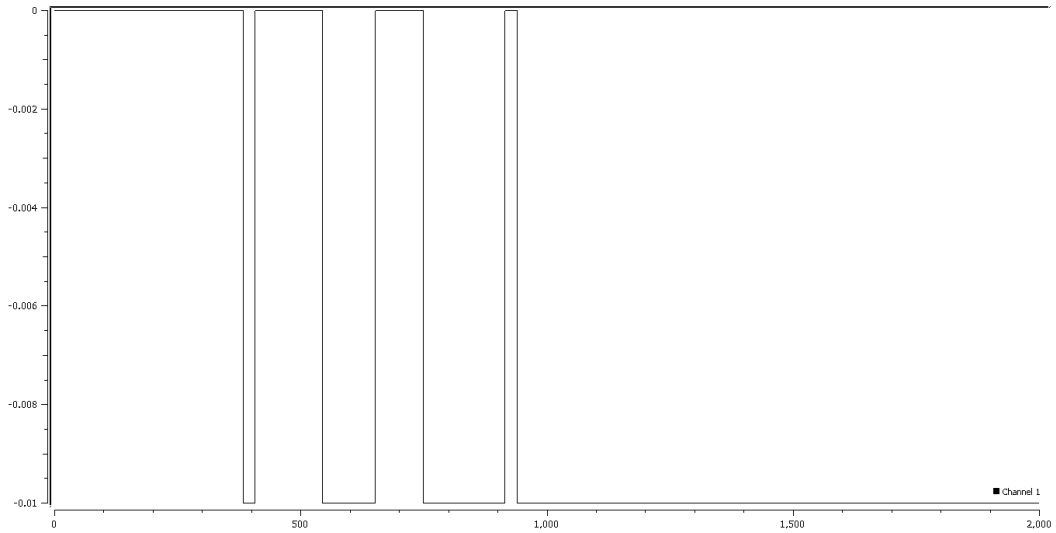

Figure 7.5: Cart position natural dynamics

7.2.2 Response of the hardware setup with AFLSC

The response of the angular position of the pendulum with AFLSC is shown on figure 7.6. The controller stabilize the pendulum. But as time goes on the defect in mechanical design force the pendulum to fall. This defect is caused by the misalignment of the pendulum center of mass and the cart center of mass. Thus when the pendulum moves large angel in one direction the controller is unable to respond at required rate, because the pendulum falls at high rate. The picture 7.6 shows the same result.

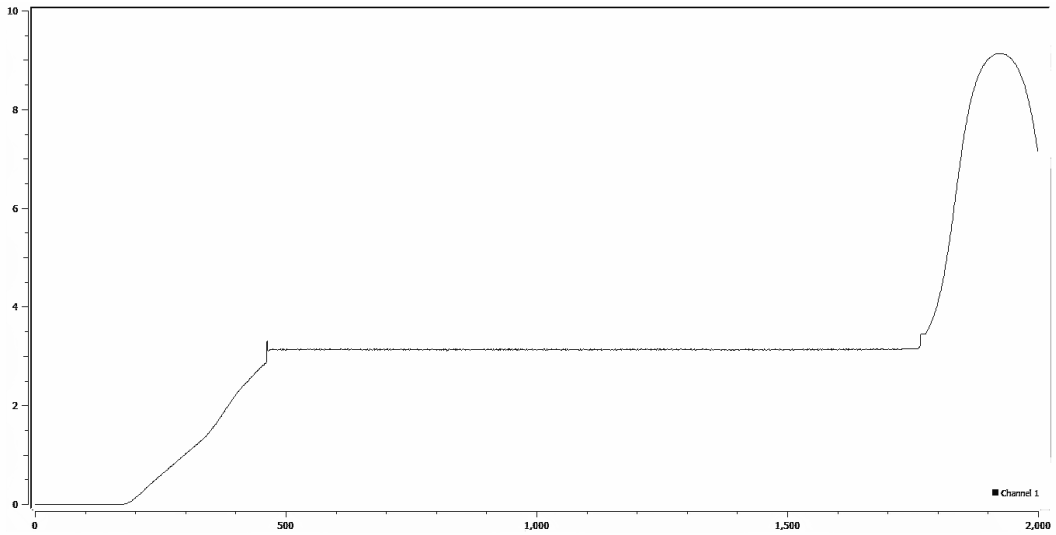

Figure 7.6: Pendulum angular position response with AFLSC

The position of the cart with AFLSC is shown on figure 7.7. This result depict the same scenario.
The control signal generated by AFLSC is shown on figure 7.8. As shown on the figure the controller losses its ability due to hardware setup limitations.

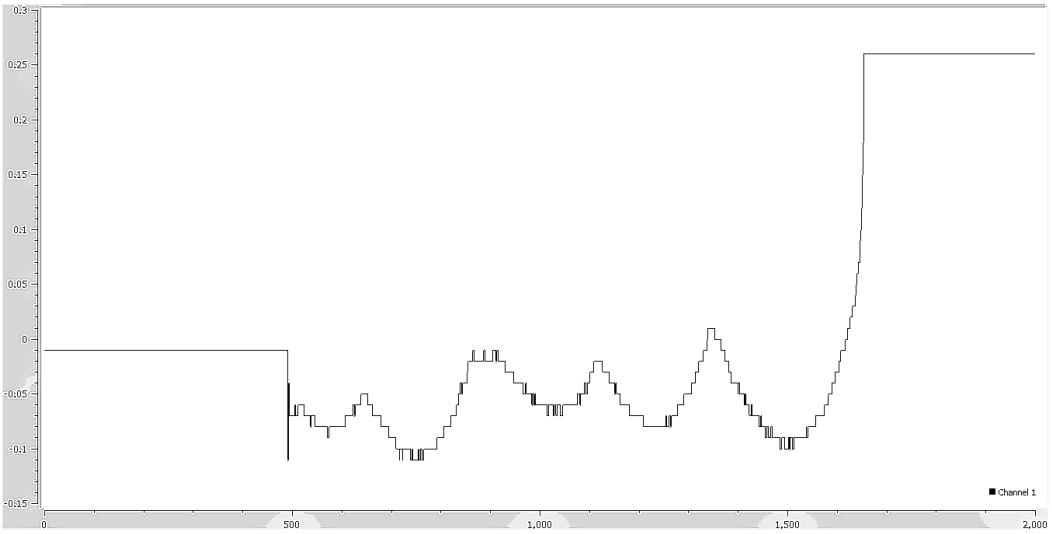

Figure 7.7: Cart position response with AFLSC

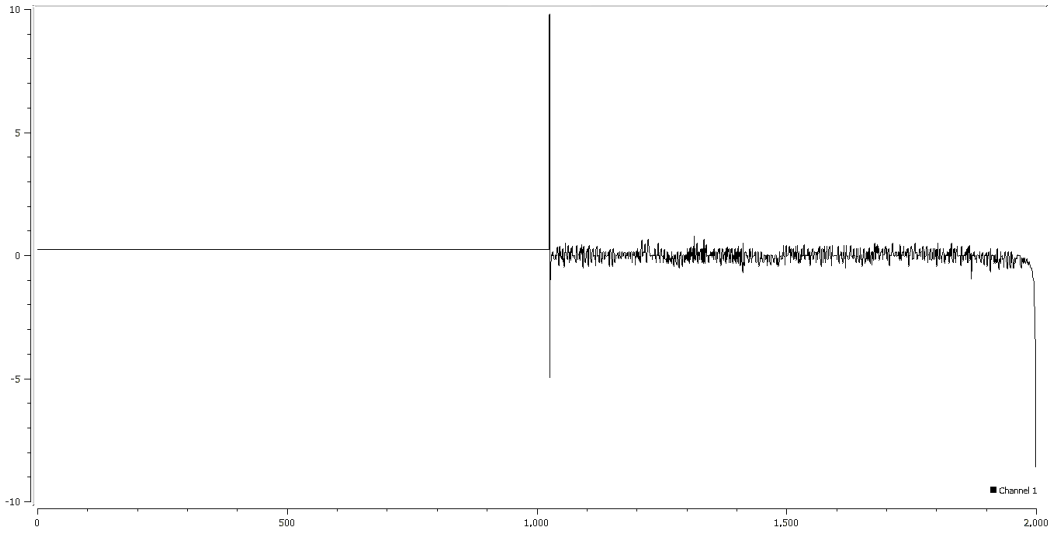

Figure 7.8: Control signal generated by AFLSC

Chapter 8

Conclusion, Recommendation and Limitations

8.1 Conclusion

This thesis introduced application of feedback linearization to inverted pendulum on a cart stabilization problem and adaptive fuzzy swing up to swing up problem of a pendulum. By decomposing the system into cart subsystem and pendulum subsystem in combination with adaptive inverse control to stabilize a pendulum about upright position. While AFLSUC is used to swing up a pendulum from it's pendant position to inverted position. Simulation result shows promising result under different cart mass and pendulum mass for $0.3m - 0.4m$ arm length pendulum. For disturbance up to ± 15 degree an AFLSC stabilize the system with small deviation in the position of the cart from origin $(0, 0)$.

Combining AFLSC with AFLSUC maximum deviation of the cart position from origin $(0, 0)$ is $0.35m$. The combined controller have adapted to 4 initial mass of the cart and 10 times initial mass of the pendulum after selecting fuzzy logic controller output gain multiplier. Compared to Adaptive fuzzy logic based stabilizing controller [17] which approximate feedback linearization by fuzzy logic the response of AFLSC is better. The fuzzy logic approximated adaptive feedback linearization compensate for only ± 4 degree for inverted pendulum as indicated on the paper.

The hardware experimentation shows promising result under unknown cart mass and pendulum mass. Additionally the arm length of the pendulum used in hardware experimentation is unknown. Thus the simulation results and hardware experimentation results shows that an AFLSC is a solution to stability problem of an arbitrary inverted pendulum on a cart. While from simulation results it can be concluded that an AFLSUC is a solution for swing up problem of an arbitrary pendulum from it's pendant position.

8.2 Recommendation

The system parameters used in designing AFLSC are selected by observing the response of IPC as stated in section 6.2. And AFLSUC output control signal gain scalar multiplier is selected manually for particular initial mass of a cart in this thesis. The mass of the cart has significant effect in the energy requirement for swing up. For different range of cart mass the controller need different output gain. But after the selection of gain it will adapt for 4 times the initial mass of an cart and 10 times initial mass of a pendulum. The author recommend interested researchers to design a systematic way of selecting the gain and system parameters.

8.3 Limitations

The hardware setup is developed by the researcher from locally available material except for the sensors. Even though the researcher give high focus to the control problem as it is his field of study and he want to prove AFLSC is a solution to the stabilization problem of an inverted pendulum on a cart. The mechanical system hardware setup development is also given equivalent focus, as the setup may be used to test different controllers developed by AAiT students in the future.

The swing up was not included in the proposal of this research, the researcher communicated with his adviser to include the topic, which takes over two month to incorporate into simulation framework. But testing the response of AFLSUC on hardware experimentation was unsuccessful due to computation problem. The first idea of the researcher was to use DC motor as an actuator and perform computation on MATLAB by reading sensor data through arduino hardware. But the communication between arduino hardware and MATLAB software was very slow. So the researcher adapt the AFLSC code shown on appendix E to be computed on arduino. Additionally the researcher try to use ultrasonic sensor to minimize hardware setup cost, but the time derivative of the position read by the ultrasonic sensor was not consistent, hence additional incremental rotary encoder is used. The hardware setup was redesigned more than 10 times to make is worthy of future use which was successful.

References

[1] K. Ogata and Y. Yang, *Modern control engineering*. Prentice-Hall, 2002, vol. 4.

[2] A. A. J, "Feedback linearization, sliding mode and swing up control for the inverted pendulum on a cart," Master's thesis, University of Manchester,Faculty of Engineering and Physical Sciences, 2015.

[3] R. Olfati-Saber, "Nonlinear control of underactuated mechanical systems with application to robotics," PhD thesis, MIT, 2001.

[4] Y. L. Sachkov, "Control theory on lie groups," *Journal of Mathematical Sciences*, vol. 156, no. 3, p. 381, 2009.

[5] J. Cariñena, J. Clemente-Gallardo, and A. Ramos, "Motion on lie groups and its applications in control theory," *Reports on Mathematical Physics*, vol. 51, no. 2-3, pp. 159–170, 2003.

[6] J.-J. E. Slotine, W. Li, *et al.*, *Applied nonlinear control*, 1. Prentice hall Englewood Cliffs, NJ, 1991, vol. 199.

[7] G. Tao, "Adaptive control design and analysis," in. John Wiley & Sons, 2003, vol. 37.

[8] S. Ghosh, *Control Systems*, 2nd Edition. Pearson Education, 2009.

[9] H. K. Khalil and J. W. Grizzle, *Nonlinear systems*. Prentice hall Upper Saddle River, NJ, 2002, vol. 3.

[10] J.-J. E.Slotine. (2019). A slotine lectures on nonlinear systems mit, [Online]. Available: `https://www.youtube.com`.

[11] K. H. Lundberg and T. W. Barton, "History of inverted-pendulum systems," *IFAC Proceedings Volumes*, vol. 42, no. 24, pp. 131–135, 2010.

[12] C.-S. Chen and W.-L. Chen, "Robust adaptive sliding-mode control using fuzzy modeling for an inverted-pendulum system," *IEEE Transactions on Industrial Electronics*, vol. 45, no. 2, pp. 297–306, 1998.

[13] M.-S. Park and D. Chwa, "Swing-up and stabilization control of inverted-pendulum systems via coupled sliding-mode control method," *IEEE transactions on industrial electronics*, vol. 56, no. 9, pp. 3541–3555, 2009.

[14] V. Mladenov, G. Tsenov, L. Ekonomou, N. Harkiolakis, and P. Karampelas, "Neural network control of an inverted pendulum on a cart," in *WSEAS International Conference. Proceedings. Mathematics and Computers in Science and Engineering*, World Scientific, Engineering Academy, and Society, 2009.

[15] C.-W. Tao, J. S. Taur, T. W. Hsieh, and C. Tsai, "Design of a fuzzy controller with fuzzy swing-up and parallel distributed pole assignment schemes for an inverted pendulum and cart system," *IEEE Transactions on Control Systems Technology*, vol. 16, no. 6, pp. 1277–1288, 2008.

[16] J. Wu and Z. Wang, "Research on fuzzy control of inverted pendulum," in *2011 First International Conference on Instrumentation, Measurement, Computer, Communication and Control*, IEEE, 2011, pp. 868–871.

[17] H. M. E. Mohamed I. El-Hawwary A. L. Elshafei and H. A. A. Fattah, "Adaptive fuzzy control of the inverted pendulum problem," *IEEE Transactions on Control Systems Technology*, November 2006.

[18] A. Casavola, E. Mosca, and M. Papini, "Control under constraints: An application of the command governor approach to an inverted pendulum," *IEEE Transactions on control systems technology*, vol. 12, no. 1, pp. 193–204, 2004.

[19] G Garcia-Chavez and E Munoz-Panduro, "Global control for the furuta pendulum based on partial feedback linearization and stabilization of the zero dynamics," in *2017 13th IEEE Conference on Automation Science and Engineering (CASE)*, IEEE, 2017, pp. 334–339.

[20] J. F. Kaustubh Pathak and S. K. Agrawal, "Velocity and position control of a wheeled inverted pendulum by partial feedback linearization," *IEEE Transactions On Robotics*, June 2005.

[21] S. Renou and L. Saydy, "Real time control of an inverted pendulum based on approximate linearization," in *Proceedings of 1996 Canadian Conference on Electrical and Computer Engineering*, Ieee, vol. 2, 1996, pp. 502–504.

[22] R. Chanchareon, V. Sangveraphunsiri, and S. Chantranuwathana, "Tracking control of an inverted pendulum using computed feedback linearization technique," in *2006 IEEE Conference on Robotics, Automation and Mechatronics*, IEEE, 2006, pp. 1–6.

[23] Z. Yakoub, M. Charfeddine, K. Jouili, and N. B. Braiek, "A combination of backstepping and the feedback linearization for the controller of inverted pendulum," in *10th International Multi-Conferences on Systems, Signals & Devices 2013 (SSD13)*, IEEE, 2013, pp. 1–6.

[24] L. H. Torres, L. Schnitman, C. Junior, and J. F. de Souza, "Feedback linearization and model reference adaptive control of a magnetic levitation system," *Studies in Informatics and Control*, vol. 21, no. 1, pp. 67–74, 2012.

[25] S. H. Jeon and J. Y. Choi, "Adaptive feedback linearization control based on stator flux model for induction motors," in *Proceedings of the 2000 IEEE International Symposium on Intelligent Control. Held jointly with the 8th IEEE Mediterranean Conference on Control and Automation (Cat. No. 00CH37147)*, IEEE, 2000, pp. 273–278.

[26] E. Shameli, M. B. Khamesee, and J. P. Huissoon, "Application of a model reference adaptive feedback linearization controller to a magnetic telemanipulation system," in *2008 IEEE International Conference on Mechatronics and Automation*, IEEE, 2008, pp. 219–223.

[27] K. Yoshida, "Swing-up control of an inverted pendulum by energy-based methods," in *Proceedings of the 1999 American Control Conference (Cat. No. 99CH36251)*, IEEE, vol. 6, 1999, pp. 4045–4047.

[28] K. J. Åström and K. Furuta, "Swinging up a pendulum by energy control," *Automatica*, vol. 36, no. 2, pp. 287–295, 2000.

[29] S. V. Radhamohan, M. Subramaniam, M. Nigam, *et al.*, "Fuzzy swing-up and stabilization of real inverted pendulum using single rulebase," *Journal of Theoretical and Applied Information Technology*, vol. 14, no. 1/2, pp. 43–49, 2010.

[30] N. Kouda, N. Matsui, and H. Nishimura, "Control for swing-up of an inverted pendulum using qubit neural network," in *Proceedings of the 41st SICE Annual Conference. SICE 2002.*, IEEE, vol. 2, 2002, pp. 765–770.

[31] T. A. Albahkali, "An impulse-momentum approach to swing-up control of double inverted pendulum on a cart," *World Academy of Science, Engineering and Technology*, vol. 54, 2011.

[32] Y. Wang, "Optimal swing-up control of an inverted pendulum," 2016.

[33] J. H. Christensen and C. Rasmus, "Swing up and stabilisation of an inverted pendulum on a cart using nonlinear methods," Master's thesis, Aalborg University, 2017.

[34] P. Donner, F. Christange, and M. Buss, "Adaptive simple pendulum swing-up controller based on the closed-loop fundamental dynamics," in *2015 European Control Conference (ECC)*, IEEE, 2015, pp. 2798–2805.

[35] *Nonlinear Proccess control*. Prentice Hall, ch. 4.

[36] G. Meurant, *Introduction to Lie groups and Lie algebras*. Academic Press, 1973, vol. 51.

[37] C. Arrezo. (2013). Math - differential geometry - ictp, [Online]. Available: `https://www.youtube.com`.

[38] G. S. Cardoso and L. Schnitman, "Analysis of exact linearization and aproximate feedback linearization techniques," *Mathematical Problems in Engineering*, vol. 2011, 2011.

[39] D. COLLINS. (2015). What do x1, x2, and x4 position encoding mean for incremental encoders? [Online]. Available: `https://www.motioncontroltips.com/faq-what-do-x1-x2-and-x4-position-encoding-mean-for-incremental-encoders/`.

Appendices

A MATLAB script to check for feedback linearizability

Matlab script for checking of necessary and sufficient condition

$m_p = sym('m_p');$
$m_c = sym('m_c');$
$l = sym('l');$
$g = sym('g');$
$I = sym('I');$
$u = sym('u');$
$syms\ x_1\ x_2\ x_3\ x_4\ 'real'$
$syms\ x_{1dot}\ x_{2dot}\ x_{3dot}\ x_{4dot}\ 'real'$
$A = [m_p + m_c\ m_p * l * cos(x_3);\ m_p * l * cos(x_3),\ m_p * l^2 + I];$
$B_1 = [m_p * l * (x_4^2) * sin(x_3)\ ; m_p * l * g * sin(x_3)];$
$B_2 = [1; 0];$
$x_{dot} = [x_{1dot}; x_{2dot}; x_{3dot}; x_{4dot}];$
$c = det(A);$
$f_1 = c * inv(A) * B_1;$
$g_1 = c * inv(A) * B_2;$
$f_2 = [x_2; f_1(1,1)/c; x_4; f_1(2,1)/c];$
$g_2 = [0; g_1(1,1)/c; 0; g_1(2,1)/c];$
$ad_{fg1} = simplify((jacobian(g_2, [x_1, x_2, x_3, x_4])) * f_2 - (jacobian(f_2, [x_1, x_2, x_3, x_4])) * g_2);$
$ad_{fg2} = simplify((jacobian(ad_{fg1}, [x_1, x_2, x_3, x_4])) * f_2 - (jacobian(f_2, [x_1, x_2, x_3, x_4])) * ad_{fg1});$
$ad_{fg3} = simplify((jacobian(ad_{fg2}, [x_1, x_2, x_3, x_4])) * f_2 - (jacobian(f_2, [x_1, x_2, x_3, x_4])) * ad_{fg2});$
$cont = simplify([g, ad_{fg1}, ad_{fg2}, ad_{fg3}]);$
$rank(cont)$

B MATLAB script for AFLSC design

Matlab script for Adaptive Feedback Linearization based Stabilizing controller design

$function[u, alpha_x, betha_x, theta_{dot}] = adaptive(K_1, P, x_1, x_2, x_3, x_4, x_{1r}, x_{2r}, x_{3r}, x_{4r}, theta_{up})$
$theta = theta_{up};$
$x_{1tel} = x_{1r} - x_1;\ x_{2tel} = x_{2r} - x_2;\ x_{3tel} = x_{3r} - x_3;\ x_{4tel} = x_{4r} - x_4;$
$y_{1tel} = [x_{1tel}; x_{2tel}];\ y_{2tel} = [x_{3tel}; x_{4tel}];$
$m_{cmax} = 4;\ m_{pmax} = 4;\ m_{cmin} = 0.02;\ m_{pmin} = 0.002;\ l_{max} = 1;\ l_{min} = 0.1;$
$v_1 = -K_1' * [x_{1r}; x_{2r}];\ v_2 = -K_1' * [x_{3r}; x_{4r}];\ B_1 = [0; 1];$
$w_1 = [v_1; -v_1 * cos(x_3) * cos(x_3); -(x_4^2) * sin(x_3); sin(x_3) * cos(x_3)];$
$w_2 = [v_2 * sec(x_3); -v_2 * cos(x_3); (x_4^2) * sin(x_3); tan(x_3)];$
$gm_1 = 0.5 * eye(4);\ gm_2 = 0.5 * eye(4);\ gama_1 = 240;\ gama_2 = 16;$
$g_1 = -gm_1 * w_1 * y_{1tel}' * P * B_1;\ g_2 = -gm_2 * w_2 * y_{2tel}' * P * B_1;$
$[theta_{max}, theta_{min}] = determine_{minmax}(m_{cmax}, m_{cmin}, m_{pmax}, m_{pmin}, l_{max}, l_{min});$
$f_{theta} = determine_{projection}(theta_{max}, theta_{min}, theta, g_1, g_2);$
$etha = (theta(3,1)^2)/theta(2,1);$
$a = etha * (theta(3,1) * (x_4^2) * sin(x_3) - theta(4,1) * sin(x_3) * cos(x_3));$
$b = theta(7,1) * (-theta(7,1) * (x_4^2) * sin(x_3) * cos(x_3) + theta(8,1) * sin(x_3));$
$c = etha * (theta(1,1) - theta(4,1) * cos(x_3) * cos(x_3));$
$alpha_{1x} = etha/c;\ alpha_{2x} = -theta(6,1) * cos(x_3)/c;\ betha_{1x} = a/c;\ betha_{2x} = b/c;$
$alpha_x = [alpha_{1x}; alpha_{2x}];\ betha_x = [betha_{1x}; betha_{2x}];$
$theta_{1dot} = -alpha_{1x} * gm_1 * w_1 * y_{1tel}' * P * B_1;$
$theta_{2dot} = -alpha_{2x} * gm_2 * w_2 * y_{2tel}' * P * B_1;$
$theta_{dot} = [theta_{1dot}; theta_{2dot}] + f_{theta};$
$u_{n1} = -gama_1 * alpha_{1x} * y_{1tel}' * P * B_1;\ u_{n2} = -gama_2 * alpha_{2x} * y_{2tel}' * P * B_1;$
$u_1 = ((v_1 - betha_{1x})/alpha_{1x}) + u_{n1};\ u_2 = ((v_2 - betha_{2x})/alpha_{2x}) + u_{n2};$
$u = 250 * (u_1 + u_2);\ end$
$function f_{theta} = determine_{projection}(theta_{max}, theta_{min}, theta, g_1, g_2)$
$if\ theta(1,1) > theta_{min(1,1)}\ \&\&\ theta(1,1) < theta_{max(1,1)}\ f_{theta11} = 0;$
$elseif\ theta(1,1) == theta_{min(1,1)}\ \&\&\ g_1(1,1) >= 0\ f_{theta11} = 0;$
$elseif\ theta(1,1) == theta_{max(1,1)}\ \&\& g_1(1,1) <= 0\ f_{theta11} = 0;$
$else\ f_{theta11} = -g_1(1,1);\ end$
$if\ theta(2,1) > theta_{min(2,1)}\ \&\&\ theta(2,1) < theta_{max(2,1)}\ f_{theta12} = 0;$
$elseif\ theta(2,1) == theta_{min(2,1)}\ \&\&\ g_1(2,1) >= 0\ f_{theta12} = 0;$
$elseif\ theta(1,1) == theta_{max(2,1)}\ \&\&\ g_1(2,1) <= 0\ f_{theta12} = 0;$
$else\ f_{theta12} = -g_1(2,1);\ end$
$if\ theta(3,1) > theta_{min(3,1)}\ \&\&\ theta(3,1) < theta_{max(3,1)}\ f_{theta13} = 0;$
$elseif\ theta(3,1) == theta_{min(3,1)}\ \&\&\ g_1(3,1) >= 0\ f_{theta13=0};$
$elseif\ theta(3,1) == theta_{max(3,1)}\ \&\&\ g_1(3,1) <= 0\ f_{theta13} = 0;$
$else\ f_{theta13} = -g_1(3,1);\ end$

$if\ theta(4,1) > theta_{min(4,1)}\ \&\&\ theta(4,1) < theta_{max(4,1)}\ f_{theta14} = 0;$
$elseif\ theta(4,1) == theta_{min(4,1)}\ \&\&\ g_1(4,1) >= 0\ f_{theta14} = 0;$
$elseif\ theta(4,1) == theta_{max(4,1)}\ \&\&\ g_1(4,1) <= 0\ f_{theta14} = 0;$
$else\ f_{theta14} = -g_1(4,1);\ end$
$if\ theta(5,1) > theta_{min(5,1)}\ \&\&\ theta(5,1) < theta_{max(5,1)}\ f_{theta21} = 0;$
$elseif\ theta(5,1) == theta_{min(5,1)}\ \&\&\ g_2(1,1) >= 0\ f_{theta21} = 0;$
$elseif\ theta(5,1) == theta_{max(5,1)}\ \&\&\ g_2(1,1) <= 0\ f_{theta21} = 0;$
$else\ f_{theta21} = -g_2(1,1);\ end$
$if\ theta(6,1) > theta_{min(6,1)}\ \&\&\ theta(6,1) < theta_{max(6,1)}\ f_{theta22} = 0;$
$elseif\ theta(6,1) == theta_{min(6,1)}\ \&\&\ g_1(2,1) >= 0\ f_{theta22} = 0;$
$elseif\ theta(6,1) == theta_{max(6,1)}\ \&\&\ g_2(2,1) <= 0\ f_{theta22} = 0;$
$else\ f_{theta22} = -g_2(2,1);\ end$
$if\ theta(7,1) > theta_{min(7,1)}\ \&\&\ theta(7,1) < theta_{max(7,1)}\ f_{theta23} = 0;$
$elseif\ theta(7,1) == theta_{min(7,1)}\ \&\&\ g_2(3,1) >= 0\ f_{theta23} = 0;$
$elseif\ theta(7,1) == theta_{max(7,1)}\ \&\&\ g_2(3,1) <= 0\ f_{theta23} = 0;$
$else\ f_{theta23} = -g_2(3,1);\ end$
$if\ theta(8,1) > theta_{min(8,1)}\ \&\&\ theta(8,1) < theta_{max(8,1)}\ f_{theta24} = 0;$
$elseif\ theta(8,1) == theta_{min(8,1)}\ \&\&\ g_2(4,1) >= 0\ f_{theta24} = 0;$
$elseif\ theta(8,1) == theta_{max(8,1)}\ \&\&\ g_2(4,1) <= 0\ f_{theta24} = 0;$
$else\ f_{theta24} = -g_2(4,1);\ end$
$f_{theta1} = [f_{theta11}; f_{theta12}; f_{theta13}; f_{theta14}];\ f_{theta2} = [f_{theta21}; f_{theta22}; f_{theta23}; f_{theta24}];$
$f_{theta} = [f_{theta1}; f_{theta2}];\ end$
$function[theta_{max}, theta_{min}] = determine_{minmax}(m_{cmax}, m_{cmin}, m_{pmax}, m_{pmin}, l_{max}, l_{min})$
$g = -9.81;\ I_{min} = 0.5 * m_{pmin} * l_{min}^2;\ I_{max} = 0.5 * m_{pmax} * l_{max}^2;$
$etha_{min} = I_{min} + m_{pmin} * l_{min}^2;\ etha_{max} = I_{max} + m_{pmax} * l_{max}^2;$
$theta_{11min} = m_{cmin} + m_{pmin};\ theta_{11max} = m_{cmax} + m_{pmax};$
$theta_{12min} = ((m_{pmin} * l_{min})^2)/(etha_{min});\ theta_{12max} = ((m_{pmax} * l_{max})^2)/(etha_{max});$
$theta_{13min} = m_{pmin} * l_{min};\ theta_{13max} = m_{pmax} * l_{max};$
$theta_{14min} = theta_{12min} * g;\ theta_{14max} = theta_{12max} * g;$
$theta_{21min} = ((m_{cmin} + m_{pmin}) * etha_{min})/(m_{pmin} * l_{min});$
$theta_{21max} = ((m_{cmax} + m_{pmax}) * etha_{max})/(m_{pmax} * l_{max});$
$theta_{22min} = m_{pmin} * l_{min};\ theta_{22max} = m_{pmax} * l_{max};$
$theta_{23min} = m_{pmin} * l_{min};\ theta_{23max} = m_{pmax} * l_{max};$
$theta_{24min} = (m_{cmin} + m_{pmin}) * g;\ theta_{24max} = (m_{cmax} + m_{pmax}) * g;$
$theta_{1min} = [theta_{11min}; theta_{12min}; theta_{13min}; theta_{14max}];$
$theta_{1max} = [theta_{11max}; theta_{12max}; theta_{13max}; theta_{14min}];$
$theta_{2min} = [theta_{21min}; theta_{22min}; theta_{23min}; theta_{24max}];$
$theta_{2max} = [theta_{21max}; theta_{22max}; theta_{23max}; theta_{24min}];$
$theta_{min} = [theta_{1min}; theta_{2min}];\ theta_{max} = [theta_{1max}; theta_{2max}];\ end$

C MATLAB script to determine design parameters and initial value of system parameters

Matlab script for calculating design parameters:

$syms\ p_{11}\ p_{12}\ p_{21}\ p_{22}\ 'real'$
$A_1 = [0\ 1; 0\ 0];\ B_1 = [0; 1];\ C_1 = [1\ 0];\ Q_1 = C_1' * C_1;\ R_1 = 1;$
$q_{11} = 0.0025;\ q_{12} = 0.001;\ q_{22} = 0.0085;\ q_{21} = q_{12};$
$Q = [q_{11}\ q_{12}; q_{21}\ q_{22}];\ P = [p_{11}\ p_{12}; p_{21}\ p_{22}];$
$eigen_{valuesofq} = eig(Q)\ q_{21} = q_{12};$
$K_1 = lqr(A_1, B_1, Q_1, R_1);$
$eqn = simplify(P * (A_1 - B_1 * K_1) + ((A_1 - B_1 * K_1)') * P + 2 * Q)$
$eqn_1 = eqn(1,1);\ eqn_2 = eqn(1,2);\ eqn_3 = eqn(2,1);\ eqn_4 = eqn(2,2);$
$vars = [p_{11}\ p_{12}\ p_{21}\ p_{22}];$
$[p_{11}\ p_{12}\ p_{21}\ p_{22}] = solve(eqn_1 == 0, eqn_2 == 0, eqn_3 == 0, eqn_4 == 0, vars);$
$P = double(simplify([p_{11}\ p_{12}; p_{21}\ p_{22}]))$
$eigen_{valuesofp} = eig(P)$

Matlab script for calculating initial value of system parameters

$m_c = 0.5;\ m_p = 0.1;\ l = 0.3;$
$m_{cin} = 0.1;\ m_{pin} = 0.1;\ l_{in} = 0.1;\ I_{in} = 0.5 * m_{pin} * l_{in}^2;$
$etha_{in} = I_{in} + m_{pin} * l_{in}^2;$
$theta_{11in} = m_{cin} + m_{cin};$
$theta_{12in} = ((m_{pin} * l_{in})^2)/(etha_{in});$
$theta_{13in} = m_{pin} * l_{in};$
$theta_{14in} = theta_{12in} * g;$
$theta_{21in} = ((m_{cin} + m_{pin}) * etha_{in})/(m_{pin} * l_{in});$
$theta_{22in} = m_{pin} * l_{in};$
$theta_{23in} = m_{pin} * l_{in};$
$theta_{24in} = (m_{cin} + m_{pin}) * g;$
$theta_{1in} = [theta_{11in}; theta_{12in}; theta_{13in}; theta_{14in}];$
$theta_{2in} = [theta_{21in}; theta_{22in}; theta_{23in}; theta_{24in}];$
$theta_{in} = [theta_{1in}; theta_{2in}];$
$g = -9.81;$

D MATLAB/SIMULINK Block Diagrams

Matlab/Simulink Block Diagrams

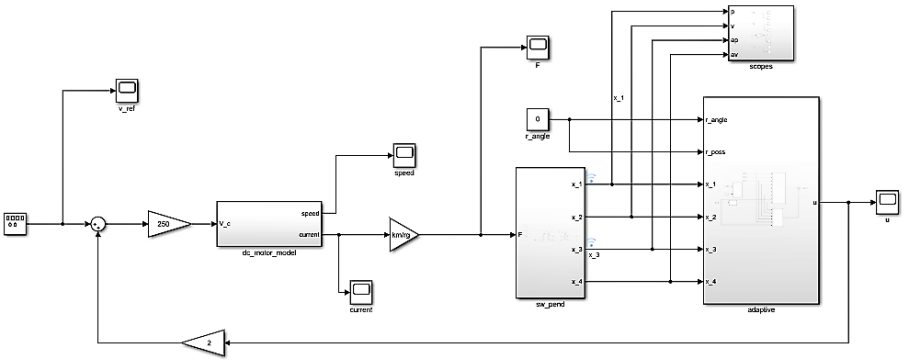

Figure D.1: Overall System

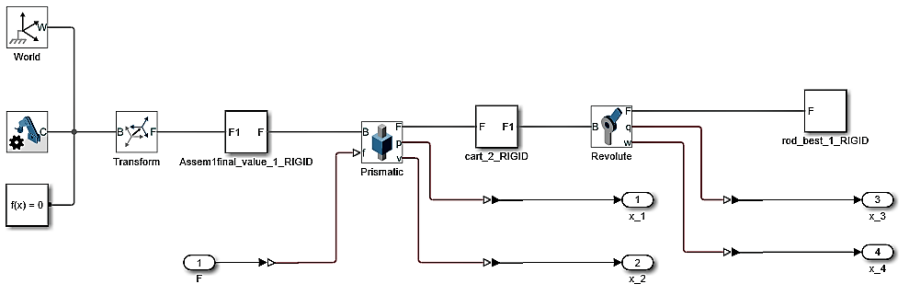

Figure D.2: Solidwork multibody

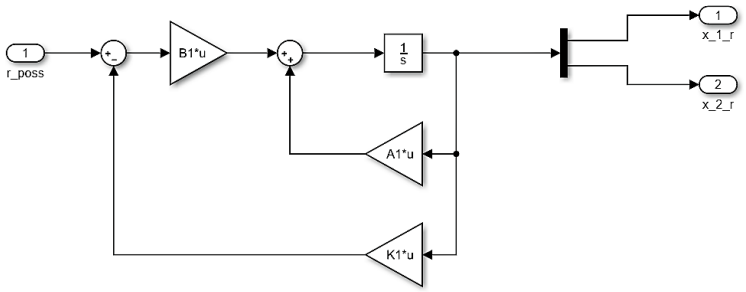

Figure D.3: Reference Model

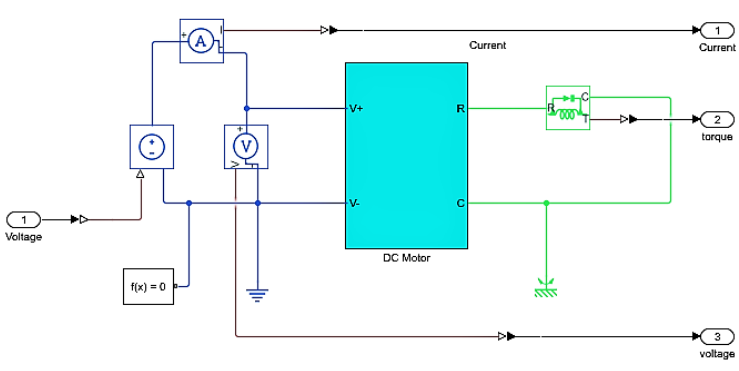

Figure D.4: DC motor model

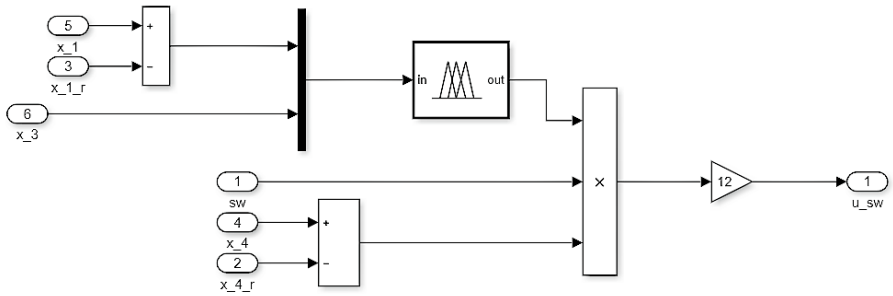

Figure D.5: Adaptive Fuzzy Logic based Swing up Controller

E Arduino Code for Hardware Experimentation

$\#\ include\ <Stepper.h>\ \#\ include\ <Encoder.h>$
$const\ int\ stepsPerRevolution = 200;\ Stepper\ myStepper(stepsPerRevolution, 4, 5, 6, 7);$
$Encoder\ angular(2, 3);\ Encoder\ linear(18, 19);$
$float\ x_{1k1} = 0;\ float\ x_{1k0} = 0;\ float\ x_{2k1} = 0;\ float\ x_{3k1} = 0;\ float\ x_{3k0} = 0;$
$float\ x_{4k1} = 0;\ float\ t_0 = 0;\ float\ t_1 = 0;\ float\ angle = 0;\ float\ poss = 0;\ float\ u = 0;$
$float\ f_{theta}[8] = \{0, 0, 0, 0, 0, 0, 0, 0\};$
$float\ thetak1[8] = \{0.02, 0.0133, 0.002, -0.1308, 0.003, 0.002, 0.002, -0.1962\};$
$float\ a, b, c, etha, u_{n1}, u_{n2}, u_1, u_2, alpha_{1x}, alpha_{2x}, betha_{1x}, betha_{2x};$
$float\ theta_{1c}[4];\ float\ theta_{2c}[4];\ float\ theta_c[8];\ float\ g_1[4];\ float\ g_2[4];$
$float\ sum = 0,\ x_{req} = 0;$
$voidsetup()\ \{\ Serial.begin(9600);\ myStepper.setSpeed(250);\ \}$
$void\ loop()\{\ t1 = millis();\ angle = angular.read();\ poss = linear.read();$
$x_{3k1} = 6.28 * (angle/1600);\ x_{1k1} = 0.85 * (poss/26158);$
$x_{4k1} = 1000 * (x_{3k1} - x_{3k0})/(t_1 - t_0);\ x_{2k1} = 1000 * (x_{1k1} - x_{1k0})/(t_1 - t_0);$
$x_{1k0} = x_{1k1};\ x_{3k0} = x_{3k1};\ t_0 = t_1;\ u = adaptive(x_{1k1}, x_{2k1}, x_{3k1}, x_{4k1});$
$myStepper.step(u * stepsPerRevolution);$
$float\ adaptive(float\ x_{1k1}, float\ x_{2k1}, float\ x_{3k1}, float\ x_{4k1})\ \{$
$float\ x_{1tel} = -x_{1k1};\ float\ x_{2tel} = -x_{2k1};\ float\ x_{3tel} = -x_{3k1};\ float\ x_{4tel} = -x_{4k1};$
$float\ v_1 = 0;\ float\ v_2 = 0;$
$float\ w_1[4] = \{0, -v_1 * cos(x_{3k1}) * cos(x_{3k1}), -pow(x_{4k1}, 2) * sin(x_{3k1}), sin(x_{3k1}) * cos(x_{3k1})\};$
$float\ w_2[4] = \{0, v_2 * cos(x_{3k1}), -pow(x_{4k1}, 2) * sin(x_{3k1}), tan(x_{3k1})\};$
$float\ gm_1 = 1;\ float\ gm_2 = 1;\ float\ gama_1 = 240e-5;\ float\ gama_2 = 12e-5;$
$for(inti = 0; i <= 3; i++)\ \{\ g_1[i] = -gm_1 * (-0.0045 * x_{1tel} - 0.0064 * x_{2tel}) * w_1[i];$
$g_2[i] = -gm_2 * (-0.0045 * x_{3tel} - 0.0064 * x_{4tel}) * w_2[i];\ \}$
$float\ theta_{max}[8] = \{8, 2.6667, 4, -26.16, 12, 4, 4, -78.48\};$
$float\ theta_{min}[8] = \{0.01, 0.0067, 0.001, -0.0654, 0.0015, 0.001, 0.001, -0.0981\};$
$if(thetak1[0] > theta_{min}[0]\&\&thetak1[0] < theta_{max}[0])\ \{\ f_{theta}[0] = 0;\ \}$
$elseif(thetak1[0] == theta_{min}[0]\&\&g_1[0] >= 0)\ \{\ f_{theta}[0] = 0;\ \}$
$elseif(thetak1[0] == theta_{max}[0]\&\&g_1[0] <= 0)\ \{\ f_{theta}[0] = 0;\ \}$
$else\ \{\ f_{theta}[0] = -g_1[0];\ \}$
$if(thetak1[1] > theta_{min}[1]\&\&thetak1[1] < theta_{max}[1])\ \{\ f_{theta}[1] = 0;\ \}$
$elseif(thetak1[1] == theta_{min}[1]\&\&g_1[1] >= 0)\ \{\ f_{theta}[1] = 0;\ \}$
$elseif(thetak1[1] == theta_{max}[2]\&\&g_1[1] <= 0)\ \{\ f_{theta}[1] = 0;\ \}$
$else\ \{\ f_{theta}[1] = -g_1[1];\ \}$
$if(thetak1[2] > theta_{min}[2]\&\&thetak1[2] < theta_{max}[2])\ \{\ f_{theta}[2] = 0;\ \}$
$elseif(thetak1[2] == theta_{min}[2]\&\&g_1[2] >= 0)\ \{\ f_{theta}[2] = 0;\ \}$
$elseif(thetak1[2] == theta_{max}[2]\&\&g_1[2] <= 0)\ \{\ f_{theta}[2] = 0;\ \}$
$else\ \{\ f_{theta}[2] = -g_1[2];\ \}$

$if(thetak1[3] > theta_{min}[3]\&\&thetak1[3] < theta_{max}[3])\ \{\ f_{theta}[3] = 0;\ \}$
$elseif(thetak1[3] == theta_{min}[3]\&\&g_1[3] >= 0)\ \{\ f_{theta}[3] = 0;\ \}$
$elseif(thetak1[3] == theta_{max}[3]\&\&g_1[3] <= 0)\ \{\ f_{theta}[3] = 0;\ \}$
$else\ \{\ f_{theta}[3] = -g_1[3];\ \}$
$if(thetak1[4] > theta_{min}[4]\&\&thetak1[4] < theta_{max}[4])\ \{\ f_{theta}[4] = 0;\ \}$
$elseif(thetak1[4] == theta_{min}[4]\&\&g_2[0] >= 0)\ \{\ f_{theta}[4] = 0;\ \}$
$elseif(thetak1[4] == theta_{max}[4]\&\&g_2[0] <= 0)\ \{\ f_{theta}[4] = 0;\ \}$
$else\ \{\ f_{theta}[4] = -g_2[0];\ \}$
$if(thetak1[5] > theta_{min}[5]\&\&thetak1[5] < theta_{max}[5])\ \{\ f_{theta}[5] = 0;\ \}$
$elseif(thetak1[5] == theta_{min}[5]\&\&g_1[1] >= 0)\ \{\ f_{theta}[5] = 0;\ \}$
$elseif(thetak1[5] == theta_{max}[5]\&\&g_2[1] <= 0)\ \{\ f_{theta}[5] = 0;\ \}$
$else\ \{\ f_{theta}[5] = -g_2[1];\ \}$
$if(thetak1[6] > theta_{min}[6]\&\&thetak1[6] < theta_{max}[6])\ \{\ f_{theta}[6] = 0;\ \}$
$elseif(thetak1[6] == theta_{min}[6]\&\&g_2[2] >= 0)\ \{\ f_{theta}[6] = 0;\ \}$
$elseif(thetak1[6] == theta_{max}[6]\&\&g_2[2] <= 0)\ \{\ f_{theta}[6] = 0;\ \}$
$else\ \{\ f_{theta}[6] = -g_2[2];\ \}$
$if(thetak1[7] > theta_{min}[7]\&\&thetak1[7] < theta_{max}[7])\ \{\ f_{theta}[7] = 0;\ \}$
$elseif(thetak1[7] == theta_{min}[7]\&\&g_2[3] >= 0)\ \{\ f_{theta}[7] = 0;\ \}$
$elseif(thetak1[7] == theta_{max}[7]\&\&g_2[3] <= 0)\ \{\ f_{theta}[7] = 0;\ \}$
$else\ \{\ f_{theta}[7] = -g_2[3];\ \}$
$etha = (pow(thetak1[2], 2))/thetak1[1];$
$a = etha * (thetak1[2] * pow(x_{4k1}, 2) * sin(x_3k1) - thetak1[3] * sin(x_{3k1}) * cos(x_{3k1}));$
$b = thetak1[6] * (-thetak1[6] * pow(x_{4k1}, 2) * sin(x_{3k1}) * cos(x_{3k1}) + thetak1[7] * sin(x_{3k1}));$
$c = etha * (thetak1[0] - thetak1[3] * cos(x_{3k1}) * cos(x_{3k1}));$
$alpha_{1x} = etha/c;\ alpha_{2x} = -thetak1[5] * cos(x_{3k1})/c;$
$betha_{1x} = a/c;\ betha_{2x} = b/c;\ for(int\ i = 0; i <= 3; i++)\ \{$
$theta_{1c}[i] = -alpha_{1x} * gm_1 * (-0.0045 * x_{1tel} - 0.0064 * x_{2tel}) * w_1[i];$
$theta_{2c}[i] = -alpha_{2x} * gm_2 * (-0.0045 * x_{3tel} - 0.0064 * x_{4tel}) * w_2[i];\ \}$
$for(int\ i = 0; i <= 7; i++)\ \{\ if(i <= 3)\ \{\ theta_c[i] = theta_{1c}[i] + f_{theta}[i];\ \}$
$if(i > 3\&\&i <= 7)\ \{\ theta_c[i] = theta_{2c}[i - 4] + f_{theta}[i];\ \}\ \}$
$u_{n1} = -gama_1 * alpha_{1x} * (-0.0045 * x_{1tel} - 0.0064 * x_{2tel});$
$u_{n2} = -gama_2 * alpha_{2x} * (-0.0045 * x_{3tel} - 0.0064 * x_{4tel});$
$u_1 = ((v_1 - betha_{1x})/alpha_{1x}) + u_{n1};\ u_2 = ((v_2 - betha_{2x})/alpha_{2x}) + u_{n2};$
$u = 25 * (u_1 + u_2);$
$for(inti = 0; i <= 0; i++)\ \{\ thetak1[i] = thetak1[i] + theta_c[i];\ \}$
$sum = sum + u/(0.075 * thetak1[1]);\ x_{req} = x_{req} + sum;\ returnx_{req};\ \}$